How integrated are credit and equity markets? Evidence from index options*

Pierre Collin-Dufresne[†] Benjamin Junge[‡] Anders B. Trolle[§]

Abstract

In recent years, a liquid market for credit index (CDX) options has developed. We study the extent to which these options are priced consistently with S&P 500 (SPX) equity index options. We derive analytical expressions for CDX and SPX options within a rich structural credit risk model. The model captures many aspects of the joint dynamics of CDX and SPX options; however, it cannot reconcile the relative levels of option prices, suggesting that credit and equity markets are not fully integrated. A strategy of selling CDX volatility yields significantly higher average excess returns and Sharpe ratios than selling SPX volatility.

JEL Classification: G12, G13

Keywords: Credit risk, CDX, CDX options, SPX, SPX options, structural models

This version: February 26, 2021

Contains Internet Appendix

*We thank David Lando, Hugues Langlois (discussant), Allan Mortensen, Yoshio Nozawa (discussant), Nicki Rasmussen, Martin Scheicher, and seminar participants at the 2020 European Finance Association conference, the CEPR Advanced Forum in Financial Economics, the Virtual Derivatives Workshop, Boston University, Erasmus University, HEC Paris, Tilburg University, Tinbergen Institute, and UCLA for comments and suggestions. Collin-Dufresne gratefully acknowledges research support from the Swiss Finance Institute. Trolle gratefully acknowledges support from the Danish Finance Institute and the Center for Financial Frictions (FRIC), grant no. DNRF102.

[†]EPFL and Swiss Finance Institute. E-mail: pierre.collin-dufresne@epfl.ch

[‡]Capital Fund Management.

[§]Copenhagen Business School. E-mail: abtr.fi@cbs.dk

1 Introduction

Classic financial theory views corporate debt and equity as contingent claims on the firm's underlying asset value (Merton (1974)). As a consequence, credit spreads and equity returns should be tightly connected. Early tests of *first-generation* structural models find that these models tend to underpredict the level of credit spreads, especially for investment-grade bonds (Jones, Mason, and Rosenfeld (1984), Huang and Huang (2012)).

Instead, more complex *second-generation* structural models, which allow for time-varying risk premia and/or richer asset dynamics, are more successful at explaining the level of credit spreads (Cremers, Driessen, and Maenhout (2008), Chen, Collin-Dufresne, and Goldstein (2009), Du, Elkamhi, and Ericsson (2019)). In particular, Cremers et al. (2008) demonstrate a close connection between credit spreads and prices of equity index options. More recently, Culp, Nozawa, and Veronesi (2018) propose to use equity options and contingent-claim pricing to construct "pseudo firms" whose derived credit spreads they find to be consistent with actual credit spreads, suggesting "a good deal of integration between corporate bond and options markets."[1]

In this paper we revisit the question of how integrated credit and equity markets are by investigating whether, in addition to credit spreads, structural models can also match prices of credit options. Such options contain unique information about the higher-order moments of credit spreads, thus adding a new dimension to the issue of market integration. Specifically, we use a novel data set of options on a broad credit index to infer implied credit volatilities across a range of moneyness and maturities. We characterize the dynamics of the resulting credit-implied volatility surface and its relation to the volatility surface obtained from equity index options, and we explore whether the two surfaces and their time variation are consistent when examined through the lens of a rich structural model.[2]

[1] See Culp et al. (2018, p. 458).

[2] Under the null hypothesis of a Merton-style contingent-claim pricing model, both stock and bond prices and the associated equity and credit derivatives should be driven by the same risk factors that drive the

Credit indexes constitute the most liquid component of the corporate credit derivative market.[3] We focus on the credit index for North American investment-grade firms—the CDX North American Investment Grade Index, henceforth denoted CDX. The years after the financial crisis saw the development of an active credit index options market, and our first contribution is to characterize trading activity in CDX options since trade reporting became mandatory at the end of 2012. Trades are generally large with about two-thirds of the trades having a notional that is at or above the level where the reported notional is capped (typically either USD 100 million or USD 110 million).[4] We estimate that the average daily trading volume during our sample period was USD 4.35 billion, but trading volume exhibits an upward trend and peaks at the height of the Covid-19 crisis in March 2020, where we estimate that it reached an average of USD 11.08 billion per day. In the vast majority of option trades, the underlying is the five-year on-the-run (i.e., most recently issued) CDX contract, and these options are the focus of the paper. Furthermore, we show that trading activity is concentrated in relatively short-term (up to three to four months) options, and that there is relatively more trading in high-strike options.

Next, we use composite dealer quotes to characterize the pricing of CDX options and the relation to S&P 500 (SPX) options.[5] CDX implied volatility smiles are consistently positively skewed, which is economically consistent with the well-known negative skew of SPX implied volatility smiles, once one accounts for the fact that CDX options are quoted in terms of implied credit-spread volatilities. Since high credit spreads typically coincide with low equity

underlying firm asset values. This is the, admittedly strongly restrictive, sense in which we use "integration" in this paper. A broader definition of integration might only require that all prices are compatible with a common pricing kernel (see, e.g., Chen and Knez (1995) and Sandulescu (2020)). Indeed, more sophisticated structural models, such as the one with stochastic bankruptcy costs that we develop below in Section 6.4, allow for credit-specific risk factors.

[3] See Collin-Dufresne, Junge, and Trolle (2020) for a detailed description of this market.

[4] Trading between clients and dealers almost exclusively takes place over the counter, while interdealer trading often takes place on dedicated trading platforms. For the subset of trades that are executed on the main interdealer trading platform we have additional data from which we can infer that the capped trades on that platform have an average trade size of USD 353 million.

[5] We follow standard market practice and express CDX option prices in terms of log-normal credit-spread implied volatilities using a reduced-form model.

values, the positive (negative) skew of credit (equity) implied volatilities are consistent with a higher premium for options that pay off in bad economic states, where equity values are low and credit spreads are high.

We also show that, much like CDX and SPX returns are highly (negatively) correlated, the smile dynamics are also correlated. In particular, at-the-money (ATM) CDX and SPX implied volatilities are highly positively correlated, while the skewness of the CDX and SPX volatility smiles are negatively correlated.

Since the model-independent analysis shows a strong connection between CDX and SPX options, we next investigate if they can be linked through a structural credit risk model. We consider a model in which the asset value of a representative index constituent follows a jump-diffusion process with idiosyncratic and systematic risks. The firm has both short-term and long-term debt which generates a term structure of credit spreads. We derive analytical expressions for credit and equity indexes as well as index options which facilitates our calibration exercise.[6]

On a weekly basis, we calibrate the model to the CDX term structure, the SPX level, and the SPX volatility surface (as well as short- and long-term index leverage ratios and the index dividend yield), and then infer the CDX volatility surface out of sample. Consistent with the data, the resulting CDX implied volatility smiles are positively skewed; indeed, the magnitude of the skewness generated by the model is similar to that observed in the data. Furthermore, the model captures many aspects of the joint dynamics of CDX and SPX options in the sense that parameter configurations that increase the ATM SPX volatility tend to increase the ATM CDX volatility, and those that make the SPX volatility smile more negatively skewed tend to make the CDX volatility smile more positively skewed. However, the level of CDX implied volatilities generated by the model is systematically lower than that

[6] We verify that the model is sufficiently flexible to match CDX and SPX implied volatility smiles individually (via the systematic jump component) as well as the CDX term structure (via the idiosyncratic jump component). An interesting observation is that the pure-diffusion version of the model generates a CDX implied volatility smile that is not only much too flat but also counterfactually negatively skewed.

observed in the data—a result that is robust across a range of model specifications. This suggests that credit and equity markets are not fully integrated.

We discuss several possible explanations for this valuation puzzle. First, the model makes some simplifying assumptions that could be relaxed. For example, instead of assuming that index constituents are ex-ante identical, we extend the model to accommodate heterogeneity in leverage across firms, but find that this only exacerbates the valuation puzzle.

Second, while our analysis does not require the two indexes to be identical in terms of constituents, it requires a high degree of similarity in terms of index risk characteristics. We compare the two indexes in terms of the distributions of rating, leverage, and total and systematic asset return volatility across constituents—four characteristics that are central to our structural model. We find the distributions to be very similar in terms of mean and median values, even though the SPX distributions display more dispersion. In particular, because index option prices are increasing in systematic asset volatility, one potential resolution of the valuation puzzle could be a higher average systematic asset volatility among CDX constituents, but in fact we find it to be marginally lower.

Third, the two option contracts could span distinct economic states. As a result, state prices implied from equity index options may not give sufficiently reliable information about the prices of credit index options.[7] However, we show that in the model, credit and equity index options actually span very similar economic states, which makes them very good substitutes in terms of their payoffs. Of course, this makes our findings even more surprising; if SPX puts and CDX calls are substitutable, why do their prices not line up and why would there be demand for both products?

There may be at least two reasons for this. First, there might be credit-specific factors

[7] As an example, Collin-Dufresne, Goldstein, and Yang (2012) find that equity index options do not span the same states as super-senior CDX tranches, since the latter pay off in economic states that correspond to strikes that are much further out of the money than what is commonly quoted on the equity side. Thus, pricing super-senior tranches based on state prices extracted from equity index options amounts to extrapolation far out in the tails, which is very model dependent.

that affect credit derivatives but not equity derivatives so that CDX and SPX options are complements rather than substitutes. A natural candidate is a factor driving systematic bankruptcy costs, and we extend the model to incorporate this feature. In a parsimonious calibration, we show that the valuation puzzle for ATM CDX options can be mostly eliminated, but that it requires a very high variance of systematic bankruptcy costs.

Second, even if CDX and SPX options are close substitutes, they are not treated as such by regulators in the context of credit-risk hedging by financial institutions. Indeed, anecdotal evidence suggests that there is a structural demand for CDX call options by banks, who use these options to hedge credit exposures to reduce their regulatory capital. Using regulatory filings, we quantify one source of this demand by banks and show that it can potentially account for a significant fraction of total trading volume in CDX options.

Finally, we show that a strategy of selling CDX volatility yields significantly higher average excess returns and Sharpe ratios than selling SPX volatility.[8] A short-long strategy of selling CDX volatility vs. buying SPX volatility also generates a high Sharpe ratio, although lower than what is attained by selling CDX volatility outright. On the other hand, its higher-order moments are more attractive, with the return distribution being roughly symmetric (instead of highly negatively skewed) and much less leptokurtic.

The paper is related to several strands of literature. The model framework is most closely related to Bai, Goldstein, and Yang (2019b) who focus on pricing equity index options. Relative to their paper, we also treat credit index options, allow option expiries to differ from debt maturity (thereby treating options as true compound options on the firm asset value), and derive full analytical solutions to option prices.[9]

In contrast to the aforementioned papers on the level of credit spreads, a number of

[8]For instance, a strategy of selling an equally weighted portfolio of option straddles (appropriately sized) yields a Sharpe ratio of 1.744 in the CDX market compared to a Sharpe ratio of 0.659 in the SPX market.

[9]Allowing option expiries to differ from debt maturity is important in our setting where option expiries are typically less than four months while the underlying credit index has a maturity of approximately five years. Bai et al. (2019b) derive option prices up to an expectation that is computed via numerical integration.

papers provide evidence that points towards imperfectly integrated equity and corporate credit markets. Collin-Dufresne, Goldstein, and Martin (2001) find that a large fraction of changes in credit spreads cannot be explained by variables suggested by the Merton model; further, the unexplained residuals seem to be driven by few common factors which subsequent papers have linked to illiquidity factors (Friewald and Nagler (2019)) or intermediary balance-sheet factors (He, Khorrami, and Song (2020)). A number of recent papers (Chordia, Goyal, Nozawa, Subrahmanyam, and Tong (2017), Choi and Kim (2018), and Bai, Bali, and Wen (2019a)) document differences in the set of factors and characteristics that explain the cross-sections of corporate bond and stock returns. Schaefer and Strebulaev (2008) find that the Merton model produces reasonable sensitivities of bond returns to stock returns, although a sizable excess bond return volatility remains, which Bao and Pan (2013) link to time-varying bond illiquidity. Kapadia and Pu (2012) find short-lived divergences between CDS and stock prices, especially for firms with high arbitrage costs. A common feature of all these papers is that they study bond returns or credit spread changes of individual firms, for which illiquidity effects are likely to be important. In contrast, we focus on a highly liquid credit index and its options.

Finally, the paper is related to a recent literature on the relative pricing of CDX tranche swaps and SPX options (Coval, Jurek, and Stafford (2009), Collin-Dufresne et al. (2012), and Seo and Wachter (2018)). In principle, this literature also provides insights into the integration of equity and credit derivatives markets. However, in practice the relative pricing of these instruments is complicated by several factors: CDX tranche swaps are long-dated contracts, while the most liquid SPX options have short expiries;[10] the range of (negative) economic states that are spanned by CDX tranche swaps is much wider than that spanned by SPX options (Collin-Dufresne et al. (2012)); and trading in CDX tranche swaps has languished after the financial crisis. In contrast, CDX and SPX options are much more

[10]The literature, therefore, uses less liquid long-term SPX options that are traded over the counter.

closely aligned in terms of which option maturities are liquid and the range of (negative) economic states that are spanned. Moreover, CDX options have flourished after the financial crisis.[11]

The paper is structured as follows: Section 2 describes the CDX options market and the transaction and quote data. Section 3 characterizes the relation between CDX and SPX options. Section 4 presents a structural model for pricing index options, Section 5 describes the calibration results, and Section 6 discusses possible explanations for our findings. Section 7 concludes. Closed-form valuation formulas and proofs are given in the Appendix, and an Internet Appendix contains supplementary results.

2 CDX and CDX options

2.1 CDX

A CDX is a credit default swap that provides default protection on a set of companies belonging to an index, with the notional of the swap divided evenly among the index constituents. We focus on the investment-grade CDX that provides default protection on 125 investment-grade companies. CDX contracts are issued with initial maturities between one and ten years. A new set of CDX contracts referencing a "refreshed" index is issued every March and September.[12] The most recently launched contracts are called on-the-run; all previously launched contracts are referred to as off-the-run. Most trading activity is in the five-year on-the-run contract. Virtually all such trades are centrally cleared and executed on dedicated trading platforms (so-called swap execution facilities or SEFs) at very low transaction costs;

[11] Based on all (capped) trade reports since 2013 and aggregating across all North American credit indexes, we find that trading volume in tranche swaps is only 9% of the trading volume in options.

[12] These *roll dates* are March 20 and September 20 (in the second half of 2014, the roll date was postponed to October 6, due to delays in signing up market participants to the 2014 ISDA Credit Derivatives Definitions). The index constituents are selected among the investment-grade companies that have the most liquid single-name CDSs traded on them. Each index is identified by its series number.

see Collin-Dufresne et al. (2020) for details about the market structure and transaction costs of CDX.

Each swap has a fixed coupon of $C = 100$ bps and, when entering into the swap, the counterparties exchange an upfront amount equal to the present value of the swap.[13] When an index constituent defaults, the loss is settled in the same way as a single-name CDS, and the outstanding notional of the swap is reduced. From then on, the swap references a new version of the index without the defaulted name. For quotation purposes, the upfront amount of the swap is converted to a spread, which is the value of the fixed coupon such that the upfront amount is zero. This conversion is explained in Section IA.1 of the Internet Appendix.

2.2 CDX options

A CDX option is an option to enter into a CDX contract at a given strike price. A payer option gives the right to buy credit protection (paying the strike and the subsequent coupons) while a receiver option gives the right to sell credit protection (receiving the strike and the subsequent coupons). Options are European style and are quoted for a wide set of strikes and monthly expirations. Options expire on the third Wednesday of each month. Contractually, the option payoff is given in upfront terms. However, for quotation purposes it is standard practice to write the payoff in spread terms and express the option price as a log-normal spread implied volatility. Details—including how defaults during the life of the option are handled—are provided in Section IA.1 of the Internet Appendix. Note that a payer (receiver) option is a call (put) option on the upfront amount/spread.

[13] Throughout the paper, we assume that coupons are paid continuously at a rate C, which greatly simplifies notation. In reality, coupons are paid quarterly on standardized coupon dates.

2.3 Trading of CDX options

To understand the trading activity in CDX options, we analyze all transactions from December 31, 2012 (when reporting of trades in CDX options became mandatory) to the end of our sample period on April 30, 2020.[14] Table 1 displays descriptive statistics of the transaction data. For completeness, the table also reports statistics on CDX transactions.[15] In contrast to CDX, trading in CDX options predominantly takes place over the counter, and the SEF trades that we do observe are almost exclusively interdealer trades. Central clearing is also less prevalent in CDX options than in CDX.[16]

CDX option trades are relatively infrequent (18 trades per day, on average) but large in size. The median of the reported trade sizes is USD 100 million. However, about two-thirds of the trades are reported with a capped notional which implies that trade sizes are typically much larger.[17] For the subset of trades that take place on the main interdealer trading platform (GFI SEF), we have additional data from which we can infer that the capped trades in that subset have an average trade size of USD 353 million.[18] The average daily trading volume based on the capped trade reports is USD 1.44 billion. Assuming that capped trades in general have the same average trade size as those on the GFI SEF, we obtain an estimate of the true average daily trading volume of USD 4.35 billion.[19]

[14] Trades are reported to swap data repositories, either the Bloomberg Swap Data Repository, the Depository Trust & Clearing Corporation Data Repository, or the Intercontinental Exchange Trade Vault. Note that the reporting requirement only concerns trades for which at least one counterparty is a US institution. Therefore, the true trading activity is larger than what we report here.

[15] Collin-Dufresne et al. (2020) provide a detailed analysis of CDX transactions during a two-year period starting on October 2, 2013.

[16] For CDX, five-year on-the-run (and immediate off-the-run) trades are, with a few exceptions, required to be executed on SEFs and be centrally cleared. For CDX options, there are no such requirements.

[17] The level of the cap is determined by the Commodity Futures Trading Commission and varies over time and with option strike. In most trade reports, the notional is capped at either USD 100 million or USD 110 million.

[18] Daily market activity reports from the GFI SEF show that the aggregate uncapped notional amount traded is USD 108,410 million for CDX options during the period from October 2, 2013 to April 30, 2020. Identifying GFI SEF trades in the transaction data shows that the aggregate capped notional amount is USD 34,829 million, with 300 capped trades that have an average capped trade size of USD 108 million. This implies that the true average trade size of the capped trades is USD 353.27 (=108 + (108,410 - 34,829)/300) million.

[19] Compared with CDX option trades, CDX trades are more frequent (202 trades per day, on average) but

Figure 1 shows the evolution in trading activity on a monthly basis. Panels A and B show the average daily trading volume for CDX and CDX options, respectively, while Panels C and D show the average number of trades per day. Underscoring the growing popularity of CDX options, the trading volume exhibits an upward trend during the sample period. The average daily trading volume based on the capped trade reports (estimated true volume) has increased from USD 0.88 billion (USD 2.72 billion) in January 2013 to USD 2.08 billion (USD 6.23 billion) in April 2020. Trading volume peaks at the height of the Covid-19 crisis in March 2020 at USD 3.59 billion (USD 11.08 billion) per day. The highest trade count for CDX options is in February 2020 at 88 trades per day, on average.

Table 1 also shows that in the vast majority of option trades, the underlying CDX is the five-year on-the-run contract. Therefore, we focus on those options in the remainder of the paper.

Table 2 shows the distribution of trading volume across moneyness and option maturity. We define moneyness as

$$m = \frac{\log\left(\frac{K}{F(\tau)}\right)}{\sigma^{ATM}\sqrt{\tau}}, \tag{1}$$

where K is the strike, $F(\tau)$ is the forward spread, σ^{ATM} is the ATM log-normal spread implied volatility, and τ is the maturity. Intuitively, m measures the number of standard deviations that an option is in or out of the money.[20] The table shows that there is more trading in high-strike than low-strike options. It also shows that trading is concentrated in relatively short-term options with maturities out to three to four months.

smaller in size with a median trade size of USD 50 million and less than a quarter of the trade sizes being above the cap. The average daily trading volume based on the capped trade reports is USD 11.13 billion but we estimate that the true volume is USD 17.80 billion using the same method as for CDX options.

[20] More precisely, m measures the number of standard deviations that the log strike is away from the log forward in the Black model (see Black (1976)). Alternatively, we could express moneyness in terms of the Black-model delta, Δ, of the option. Since for a call option $\Delta = N(-m + \frac{1}{2}\sigma^2\tau)$, we have that for a two-month call option with a typical volatility of $\sigma = 0.5$, m-values of -2, -1, 0, 1, and 2 correspond to Δ-values of 0.978, 0.846, 0.508, 0.164, and 0.024, respectively.

2.4 CDX option quotes

To have synchronized data across the option surface, we use quotes rather than trades. Quotes are obtained from Markit and are composites of "dealer runs" sent from dealers to clients. We use end-of-day quotes. The sample period is from February 24, 2012 until April 30, 2020.

Details on the quote data is given in Sections IA.2 and IA.3 of the Internet Appendix. There, we find that when option maturities become very short (typically less than one week), dealers stop quoting prices. Beyond that, there are almost always quotes for at least three monthly expirations. At longer maturities, quotes are more sporadic. In light of these findings as well as the evidence on option transactions (Table 2), on each observation date we select the first three monthly expirations among the options that have more than two weeks to expiration. These options are denoted M1, M2, and M3. The average option maturities are 29.9, 60.2, and 90.6 calendar days, respectively.

For each maturity, we consider 13 moneyness "buckets": $-3.25 < m \leq -2.75$, $-2.75 < m \leq -2.25$, ... , $2.75 < m \leq 3.25$, where m is defined in (1). Within each bucket, we search for the option that is closest to the mid of the interval. We only search among OTM options due to their higher liquidity. In the ATM category, we give priority to payer options.

The result of this data-sorting is a uniform maturity-moneyness grid that preserves the information in the data without overweighing those dates on which more maturities and/or strikes are quoted. In the Internet Appendix we show that quotations are tilted towards higher-strike options. This probably reflects both the higher interest in trading those options (Table 2) and the fact that the risk-neutral spread distribution is heavily skewed towards higher spreads (see below) so that deep OTM payer options (by our moneyness measure) have meaningful prices even when deep OTM receiver options have little value.

2.5 SPX option quotes

SPX options trade on the Chicago Board Options Exchange (CBOE) and from there we get end-of-day quotes.[21] Regular SPX options expire on the third Friday of each month.[22] On each observation date, we search for the three SPX option maturities that are closest to the three CDX option maturities. These SPX options either expire two days after or five days before; hence, there is a close match in maturity between SPX and CDX options. The average SPX option maturities are 30.6, 61.2, and 91.5 calendar days, respectively. For each maturity, we then follow the same procedure as for CDX options to select 13 SPX options according to moneyness (where moneyness is again defined in (1), but with $F(\tau)$ denoting the forward SPX value).

3 Stylized facts

To provide an initial sense of the data, Figure 2 shows weekly CDX and SPX implied volatility smiles for the M2 maturity. It is immediately apparent that implied volatility smiles for CDX options are positively skewed, in stark contrast to the negatively skewed SPX implied volatility smiles. This is economically intuitive in that bad economic states are characterized by low equity prices and high credit spreads; therefore, if such states carry a high risk and/or price of risk, prices of OTM SPX put options and OTM CDX call options will be elevated.

To summarize the information in implied volatilities across moneyness, option maturity, and time, we follow the approach in Foresi and Wu (2005). On each date and for each option maturity, we run the following cross-sectional regression

$$\sigma^{IV}(m) = \beta_0 + \beta_1 m + \beta_2 m^2 + \epsilon, \tag{2}$$

[21] Specifically, we use prices at 3:45 p.m. Eastern Time.

[22] There are also weekly and end-of-month expirations that we do not consider.

where m is the measure of moneyness given in (1), and ϵ is an error term. In this regression, β_0 captures the ATM implied volatility, β_1 captures the skewness of the implied volatility smile, and β_2 captures the curvature of the implied volatility smile. The β-coefficients are very highly correlated across option maturity; therefore, for ease of exposition, we average the β-coefficients across option maturity to produce single time series of β_0, β_1, and β_2.[23] Note that β_2 is sensitive to the moneyness range which varies over time, especially for CDX options (see Figure IA3 in the Internet Appendix). This variation introduces noise in the estimate of curvature. For this reason, we mainly focus on the dynamics of volatility and skewness.

Figure 3 provides an overview of the data with the left (right) panels showing data for the CDX (SPX) market. The top-left panel shows time series of the 1Y and 5Y CDX spreads. Normally, the CDX term structure is strongly upward sloping; however, during the Covid-19 crisis the slope flattens as the 1Y spread increases more than the 5Y. At the peak of the crisis, the 5Y spread reaches 151 bps.

The middle-left panel (blue line) shows the time series of CDX volatility. Clearly, CDX volatility exhibits significant variation; in particular, it spikes during the Covid-19 crisis in March 2020 when it reaches a maximum of 1.36 relative to the sample average of 0.47. Moreover, variation in CDX and SPX volatility (middle-right panel) appear to be highly correlated.

The lower-left panel (blue line) shows the time series of CDX skewness. This confirms the observation in Figure 2 that the CDX implied volatility smiles are always positively skewed. CDX skewness varies over time and reaches a maximum of 0.187 during the Covid-19 crisis relative to a sample average of 0.074. It appears that variation in CDX and SPX skewness (lower-right panel) is moderately negatively correlated so that, when the SPX volatility smile

[23] For β_0, the correlations between the individual coefficients and the averaged coefficient in case of SPX (CDX) are between 0.995 (0.991) and 0.999 (0.998). For β_1, the correlations are between 0.959 (0.898) and 0.984 (0.948). And for β_2, the correlations are between 0.771 (0.789) and 0.899 (0.824).

becomes more skewed towards OTM put options, the CDX volatility smile tends to become more skewed towards OTM call options. One exception is during the Covid-19 crisis; initially, both CDX and SPX skewness becomes more pronounced, but CDX skewness reverses already on March 9 while SPX skewness reverses on March 18.[24]

Next, we investigate more formally the joint dynamics of the underlying index (SPX or CDX spread), volatility, and skewness—both within each market (in Table 3) and across markets (in Table 4). To make sure that our findings are not driven by the Covid-19 crisis, we report results both for the full sample and for an ex-Covid-19 sample that ends on December 31, 2019. Table 3 reports correlations (in weekly changes) between the log CDX spread, CDX volatility, and CDX skewness and between the log SPX, SPX volatility, and SPX skewness. For CDX, there is a highly positive correlation between changes in spread and volatility (0.675), a somewhat weaker positive correlation between changes in spread and skewness (0.255), and a moderately positive correlation between changes in volatility and skewness (0.397). For SPX, the table confirms the well-known negative return-volatility relation, positive return-skewness relation, and negative volatility-skewness relation. In general, the correlations (in absolute value) tend to be stronger within the SPX market than the CDX market. The correlation patterns are robust to excluding the Covid-19 crisis; indeed, the correlation between CDX volatility and skewness is stronger in the ex-Covid-19 sample (0.525).

Table 4 shows cross-market correlations (in weekly changes) between index levels, between index volatilities, and between index skewness. There is a strongly negative correlation between CDX spread changes and SPX returns (-0.802), a highly positive correlation between volatility changes (0.749), and a somewhat more moderate negative correlation between skewness changes (-0.368).[25] This correlation structure also holds true in the ex-Covid-19

[24]Figure IA5 in the Internet Appendix shows the smile dynamics during the Covid-19 crisis.

[25]In the interest of brevity, we focus on these three key cross-market correlations. In Section IA.4 of the Internet Appendix, we report additional cross-market correlations. Market practitioners often focus on the

sample.

Figure 4 illustrates the within- and cross-market interactions for the full sample. The scatterplots along the diagonal show the cross-market interactions, while the scatterplots below (above) the diagonal show the CDX-market (SPX-market) interactions. The red lines show the fits of linear regressions and provide a visual representation of the correlations reported in Tables 3 and 4 (the yellow lines are discussed in Section 5 below).

4 A structural model for pricing index options

We now propose a structural model to price credit and equity index options consistently with the debt and equity claims on each firm in the index. We model each individual firm's CDS and equity following Merton's (1974) seminal paper as, respectively, a put and call option on the underlying asset value of the firm. To address the term structure of credit spreads, we allow the outstanding debt to have different maturities (as in Geske (1977)), and to better match short-term credit spreads as well as index options, we model the dynamics of firm asset value as a jump-diffusion process (as in Merton (1976)).[26] We follow Vasicek (1987) in modeling the index portfolio as a large homogeneous portfolio and use the law of large numbers to obtain an explicit solution for credit and equity index dynamics and, consequently, for index options. Our model setup shares many features with Bai et al. (2019b). Among the key differences is that while they assume an identical maturity for the firm's outstanding debt and for the equity options, we allow for different maturities. This is important because the maturities of the credit and equity index options are much shorter

relation between the CDX spread and SPX volatility (VIX). Our structural model, laid out in Section 4, shows that this is not the most natural relation to consider given that CDX is an option on firm value, while SPX options are compound options. A more apples-to-apples comparison is between index changes or between index volatility changes. Indeed, we find that the correlation between CDX spread changes and SPX volatility changes is 0.710 which is lower (in absolute value) than the correlations between CDX spread changes and SPX returns as well as between index volatility changes.

[26] Allowing for jumps is crucial to fit the term structure of credit risk; see, e.g., Collin-Dufresne et al. (2012).

than the maturity of the underlying credit index. Further, while they rely on numerical integration to price equity index options, we derive closed-form expressions for all derivative prices, which considerably speeds up the calibration of the model.

4.1 The firms' assets

We assume that each individual firm in the index has an asset value A_t^i that is driven by a component A_t, which is common to all firms and exposed to systematic Brownian (dW_t) and pure-jump (dN_t) shocks, and a firm-specific residual component, which is exposed to idiosyncratic Brownian (dW_t^i) and pure-jump (dN_t^i) shocks. Specifically, we assume that the risk-neutral asset dynamics of (ex-ante identical) individual firms are given by

$$\frac{dA_t^i}{A_t^i} = \frac{dA_t}{A_t} + \sqrt{1-\rho}\sigma dW_t^i + (e^{\gamma_i} - 1)dN_t^i - \lambda_i \nu_i dt$$
$$\frac{dA_t}{A_t} = (r - \delta)dt + \sqrt{\rho}\sigma dW_t + (e^{\gamma} - 1)dN_t - \lambda \nu dt,$$

where W_t and W_t^i are independent Brownian motions, N_t and N_t^i are independent Poisson counting processes with intensities λ and λ_i, respectively, $\gamma \sim \mathcal{N}(m, v)$ and $\gamma_i \sim \mathcal{N}(m_i, v_i)$ are independent normal random variables, and we define $\nu = \mathbb{E}[e^{\gamma} - 1] = e^{m+\frac{v}{2}} - 1$ and $\nu_i = \mathbb{E}[e^{\gamma_i} - 1] = e^{m_i+\frac{v_i}{2}} - 1$. We assume that all the asset payouts, δA_t^i, go to equity holders.[27]

We can rewrite the individual firm asset value as[28]

$$A_T^i = A_T e^{-\frac{1}{2}(1-\rho)\sigma^2 T + \sqrt{1-\rho}\sigma W_T^i} e^{-\lambda_i \nu_i T + \gamma_i N_T^i}, \tag{3}$$

[27] For expositional ease, we assume a constant risk-free interest rate, r. It is straightforward to incorporate a deterministic term structure into the model, and we do so when implementing the model.

[28] Note the abuse of notation here (and throughout the paper): γN means the sum of N i.i.d. random variables with the same distribution as γ.

where the common factor A_T is given by

$$A_T = A_0 e^{(r-\delta)T} e^{-\frac{1}{2}\rho\sigma^2 T + \sqrt{\rho}\sigma W_T} e^{-\lambda\nu T + \gamma N_T}. \tag{4}$$

Note that conditional on the number of idiosyncratic and systematic jumps, A_T^i has a log-normal distribution.

4.2 The firms' debt

We consider a simplified debt structure with two outstanding bonds: a short-term bond with principal D_1 and maturity date T_1, and a long-term bond with principal D_2 and maturity date $T_2 > T_1$.[29] We assume that repayments of principals are made by equity holders, via 'out-of-pocket' side payments, so that the asset value process is not affected.[30] Thus, equity holders will choose to default at T_1 if the continuation value from holding on to the equity is worth less than the principal payment D_1 they owe to debt holders at that time. This determines an endogenous default threshold, Φ, at T_1, where Φ is the asset value such that, right after D_1 has been paid by equity holders, the equity value equals D_1. At T_2, the default threshold is D_2, as in the standard Merton (1974) model. In case of default, we assume that a fraction α of assets is paid out to debt holders, while a fraction $1-\alpha$ is lost because of bankruptcy costs. Finally, if the firm defaults at T_1, we assume that payments to debt holders are proportional to principal, so that holders of the short-term bond are paid a fraction $R_1 = \alpha\frac{D_1}{D_1+D_2}$ of assets, while holders of the long-term bond are paid a fraction $R_2 = \alpha\frac{D_2}{D_1+D_2}$. Therefore, the loss-given-default per dollar of principal is $1 - \frac{\alpha A_{T_1}^i}{D_1+D_2}$ on both bonds if the firm defaults at T_1 and $1 - \frac{\alpha A_{T_2}^i}{D_2}$ on the long-term bond if the firm defaults at T_2.

[29] This is the most parsimonious debt structure that allows us to address the term structure of credit spreads and to generate variation in the risky annuity factor for long-term CDX contracts. In principle, the model can be solved with an arbitrary number of bonds.

[30] This is a standard assumption in dynamic capital structure models; see, for example, Black and Cox (1976) and Leland (1994).

4.3 Bond, equity, and CDS valuation

We value bonds, equity, and CDS contracts at time T_0, the expiration of options contracts. The value of the short-term bond is given by

$$B_1^i(T_0) = e^{-r(T_1-T_0)}\Big(D_1\mathbb{E}_{T_0}[\mathbf{1}_{\{A_{T_1}^i\geq\Phi\}}] + \mathbb{E}_{T_0}[R_1 A_{T_1}^i \mathbf{1}_{\{A_{T_1}^i<\Phi\}}]\Big),$$

and the value of the long-term bond is given by

$$\begin{aligned} B_2^i(T_0) = {} & e^{-r(T_2-T_0)}\Big(D_2\mathbb{E}_{T_0}[\mathbf{1}_{\{A_{T_1}^i\geq\Phi, A_{T_2}^i\geq D_2\}}] + \mathbb{E}_{T_0}[\alpha A_{T_2}^i \mathbf{1}_{\{A_{T_1}^i\geq\Phi, A_{T_2}^i<D_2\}}]\Big) \\ & + e^{-r(T_1-T_0)}\mathbb{E}_{T_0}[R_2 A_{T_1}^i \mathbf{1}_{\{A_{T_1}^i<\Phi\}}]. \end{aligned}$$

The equity value is given by the asset value less the value of the two bonds and the present value of the expected bankruptcy costs; that is,

$$\begin{aligned} S_{T_0}^i(A_{T_0}^i) = A_{T_0}^i & - e^{-r(T_1-T_0)}\Big(D_1\mathbb{E}_{T_0}[\mathbf{1}_{\{A_{T_1}^i\geq\Phi\}}] + \mathbb{E}_{T_0}[A_{T_1}^i \mathbf{1}_{\{A_{T_1}^i<\Phi\}}]\Big) \\ & - e^{-r(T_2-T_0)}\Big(D_2\mathbb{E}_{T_0}[\mathbf{1}_{\{A_{T_1}^i\geq\Phi, A_{T_2}^i\geq D_2\}}] + \mathbb{E}_{T_0}[A_{T_2}^i \mathbf{1}_{\{A_{T_1}^i\geq\Phi, A_{T_2}^i<D_2\}}]\Big). \end{aligned}$$

Finally, consider a CDS contract from T_0 to T_2 with unit notional. The value of the protection leg is

$$\mathrm{Prot}_2^i(T_0) = e^{-r(T_1-T_0)}\mathbb{E}_{T_0}[(1-\frac{\alpha A_{T_1}^i}{D_1+D_2})\mathbf{1}_{\{A_{T_1}^i<\Phi\}}]+e^{-r(T_2-T_0)}\mathbb{E}_{T_0}[(1-\frac{\alpha A_{T_2}^i}{D_2})\mathbf{1}_{\{A_{T_1}^i\geq\Phi, A_{T_2}^i<D_2\}}],$$

and the value of the risky annuity (assuming that coupons are paid continuously) is

$$\mathcal{A}_2^i(T_0) = \int_{T_0}^{T_1} e^{-r(t-T_0)}dt + \int_{T_1}^{T_2} e^{-r(t-T_0)}dt\mathbb{E}_{T_0}[\mathbf{1}_{\{A_{T_1}^i\geq\Phi\}}].$$

With a coupon rate of C, the upfront amount of the CDS contract is

$$\begin{aligned}
U_2^i(T_0) &= \mathrm{Prot}_2^i(T_0) - C \times \mathcal{A}_2^i(T_0) \\
&= e^{-r(T_1-T_0)}\mathbb{E}_{T_0}[(1 - \frac{\alpha A_{T_1}^i}{D_1 + D_2} + C_1)\mathbf{1}_{\{A_{T_1}^i < \Phi\}}] \\
&\quad + e^{-r(T_2-T_0)}\mathbb{E}_{T_0}[(1 - \frac{\alpha A_{T_2}^i}{D_2})\mathbf{1}_{\{A_{T_1}^i \geq \Phi, A_{T_2}^i < D_2\}}] - C_0 - C_1 e^{-r(T_1-T_0)},
\end{aligned}$$

where we have defined

$$C_0 = C\int_{T_0}^{T_1} e^{-r(t-T_0)}dt \quad \text{and} \quad C_1 = C\int_{T_1}^{T_2} e^{-r(t-T_1)}dt.$$

4.4 CDX and SPX

We value the CDX and SPX indexes at time T_0. The upfront amount of the CDX is a simple average of the upfront amounts of the $N = 125$ single-name CDSs for the index constituents. Because N is large, we approximate the index upfront amount by letting $N \to \infty$. In this case, we obtain a simple analytical expression for the index upfront amount via the law of large numbers, which in turn allows us to price CDX options analytically. The index upfront amount, conditional on the common factor A_{T_0}, is given by[31]

$$\begin{aligned}
U_{T_0}(A_{T_0}) &= \lim_{N\to\infty} \frac{1}{N}\sum_{i=1}^{N} U_2^i(T_0) \\
&= \mathbb{E}[U_2^i(T_0)|A_{T_0}] \\
&= e^{-r(T_1-T_0)}\Big((1 + C_1)\mathbb{E}[\mathbf{1}_{\{A_{T_1}^i < \Phi\}} \mid A_{T_0}] - \frac{\alpha}{D_1 + D_2}\mathbb{E}[A_{T_1}^i \mathbf{1}_{\{A_{T_1}^i < \Phi\}} \mid A_{T_0}]\Big) \\
&\quad + e^{-r(T_2-T_0)}\Big(\mathbb{E}[\mathbf{1}_{\{A_{T_1}^i \geq \Phi, A_{T_2}^i < D_2\}} \mid A_{T_0}] - \frac{\alpha}{D_2}\mathbb{E}[A_{T_2}^i \mathbf{1}_{\{A_{T_1}^i \geq \Phi, A_{T_2}^i < D_2\}} \mid A_{T_0}]\Big) \\
&\quad - C_0 - C_1 e^{-r(T_1-T_0)}.
\end{aligned}$$

[31] In case of an infinite number of firms, A_t is identifiable as the limit of the firms' average asset value at time t.

Similarly, the value of the SPX is given by

$$
\begin{aligned}
S_{T_0}(A_{T_0}) = & \lim_{N\to\infty} \frac{1}{N} \sum_{i=1}^{N} S^i_{T_0}(A_{T_0}) \\
&= \mathbb{E}[S^i_{T_0}|A_{T_0}] \\
&= A_{T_0} - e^{-r(T_1-T_0)}\Big(D_1\mathbb{E}[\mathbf{1}_{\left\{A^i_{T_1}\geq\Phi\right\}} \mid A_{T_0}] + \mathbb{E}[A^i_{T_1}\mathbf{1}_{\left\{A^i_{T_1}<\Phi\right\}} \mid A_{T_0}]\Big) \\
&\quad - e^{-r(T_2-T_0)}\Big(D_2\mathbb{E}[\mathbf{1}_{\left\{A^i_{T_1}\geq\Phi, A^i_{T_2}\geq D_2\right\}} \mid A_{T_0}] + \mathbb{E}[A^i_{T_2}\mathbf{1}_{\left\{A^i_{T_1}\geq\Phi, A^i_{T_2}<D_2\right\}}\} \mid A_{T_0}]\Big).
\end{aligned}
$$

Closed-from solutions for all the expectations in the index formulas in terms of univariate and bivariate normal distributions are given in Appendix A.1.

4.5 CDX and SPX options

The time-0 value of a CDX call option with strike K and expiration at T_0 is

$$
\begin{aligned}
C_0^{CDX} &= e^{-rT_0}\mathbb{E}_0[\max(U_{T_0}(A_{T_0}) - K, 0)] \\
&= e^{-rT_0}\mathbb{E}_0\Bigg[\Bigg(e^{-r(T_1-T_0)}\Big((1+C_1)\mathbb{E}[\mathbf{1}_{\left\{A^i_{T_1}<\Phi\right\}} \mid A_{T_0}] - \frac{\alpha}{D_1+D_2}\mathbb{E}[A^i_{T_1}\mathbf{1}_{\left\{A^i_{T_1}<\Phi\right\}} \mid A_{T_0}]\Big) \\
&\quad + e^{-r(T_2-T_0)}\Big(\mathbb{E}[\mathbf{1}_{\left\{A^i_{T_1}\geq\Phi, A^i_{T_2}<D_2\right\}} \mid A_{T_0}] - \frac{\alpha}{D_2}\mathbb{E}[A^i_{T_2}\mathbf{1}_{\left\{A^i_{T_1}\geq\Phi, A^i_{T_2}<D_2\right\}} \mid A_{T_0}]\Big)\Bigg)\mathbf{1}_{\left\{A_{T_0}<\overline{A}\right\}}\Bigg] \\
&\quad - e^{-rT_0}\tilde{K}\mathbb{E}_0[\mathbf{1}_{\left\{A_{T_0}<\overline{A}\right\}}] \\
&= e^{-rT_1}\Big((1+C_1)\mathbb{E}_0[\mathbf{1}_{\left\{A_{T_0}<\overline{A}, A^i_{T_1}<\Phi\right\}}] - \frac{\alpha}{D_1+D_2}\mathbb{E}_0[A^i_{T_1}\mathbf{1}_{\left\{A_{T_0}<\overline{A}, A^i_{T_1}<\Phi\right\}}]\Big) \\
&\quad + e^{-rT_2}\Big(\mathbb{E}_0[\mathbf{1}_{\left\{A_{T_0}<\overline{A}, A^i_{T_1}\geq\Phi, A^i_{T_2}<D_2\right\}}] - \frac{\alpha}{D_2}\mathbb{E}_0[A^i_{T_2}\mathbf{1}_{\left\{A_{T_0}<\overline{A}, A^i_{T_1}\geq\Phi, A^i_{T_2}<D_2\right\}}]\Big) \\
&\quad - e^{-rT_0}\tilde{K}\mathbb{E}_0[\mathbf{1}_{\left\{A_{T_0}<\overline{A}\right\}}],
\end{aligned}
$$

where

$$\tilde{K} = K + C_0 + C_1 e^{-r(T_1-T_0)}$$

and $\overline{A}$ is the unique value such that $U_{T_0}(\overline{A}) = K$, and we use the fact that $U_T(A)$ is decreasing in A.

The time-0 value of an SPX call option with strike K and expiration at T_0 is

$$
\begin{aligned}
C_0^{SPX} &= e^{-rT_0}\mathbb{E}_0[\max(S_{T_0}(A_{T_0}) - K, 0)] \\
&= e^{-rT_0}\mathbb{E}_0\Bigg[\Bigg(A_{T_0} - e^{-r(T_1-T_0)}\Big(D_1\mathbb{E}[\mathbf{1}_{\{A^i_{T_1}\geq\Phi\}} \mid A_{T_0}] + \mathbb{E}[A^i_{T_1}\mathbf{1}_{\{A^i_{T_1}<\Phi\}} \mid A_{T_0}]\Big) \\
&\quad - e^{-r(T_2-T_0)}\Big(D_2\mathbb{E}[\mathbf{1}_{\{A^i_{T_1}\geq\Phi, A^i_{T_2}\geq D_2\}} \mid A_{T_0}] + \mathbb{E}[A^i_{T_2}\mathbf{1}_{\{A^i_{T_1}\geq\Phi, A^i_{T_2}<D_2\}} \mid A_{T_0}]\Big)\Bigg)\mathbf{1}_{\{A_{T_0}\geq\overline{A}\}}\Bigg] \\
&\quad - e^{-rT_0}K\mathbb{E}_0[\mathbf{1}_{\{A_{T_0}\geq\overline{A}\}}] \\
&= e^{-rT_0}\mathbb{E}_0[A_{T_0}\mathbf{1}_{\{A_{T_0}\geq\overline{A}\}}] - e^{-rT_1}\Big(D_1\mathbb{E}_0[\mathbf{1}_{\{A_{T_0}\geq\overline{A}, A^i_{T_1}\geq\Phi\}}] + \mathbb{E}_0[A^i_{T_1}\mathbf{1}_{\{A_{T_0}\geq\overline{A}, A^i_{T_1}<\Phi\}}]\Big) \\
&\quad - e^{-rT_2}\Big(D_2\mathbb{E}_0[\mathbf{1}_{\{A_{T_0}\geq\overline{A}, A^i_{T_1}\geq\Phi, A^i_{T_2}\geq D_2\}}] + \mathbb{E}_0[A^i_{T_2}\mathbf{1}_{\{A_{T_0}\geq\overline{A}, A^i_{T_1}\geq\Phi, A^i_{T_2}<D_2\}}]\Big) \\
&\quad - e^{-rT_0}K\mathbb{E}_0[\mathbf{1}_{\{A_{T_0}\geq\overline{A}\}}],
\end{aligned}
$$

where $\overline{A}$ is the unique value such that $S_{T_0}(\overline{A}) = K$, and we use the fact that $S_T(A)$ is increasing in A.

Closed-from solutions for all the expectations in the index option formulas in terms of univariate, bivariate, and trivariate normal distributions are given in Appendix A.1.

4.6 In-sample fit to index option smiles

Before using the model to study the joint valuation of CDX and SPX options, we verify that it is sufficiently flexible to match the CDX and SPX implied volatility smiles, individually. To show the importance of the various components of the asset return process, we start with the pure-diffusion version of the model, then add the systematic jumps, and finally add the idiosyncratic jumps. For illustration, we consider the pricing of two-month (M2) options on the last trading day in 2019, December 31. On this day, the 1Y and 5Y CDX spreads are

8.3 and 45.3 bps, respectively, and the level of the SPX is 3226.7. We calibrate the model to match the 5Y CDX spread and the SPX level perfectly, and minimize the sum of squared pricing errors for index options—either CDX or SPX options.[32]

The diffusion version is basically the Merton (1974) model applied to multiple firms and allowing for two debt maturities. The red line in the left panel in Figure 5 displays the in-sample fit to the CDX implied volatility curve. In striking contrast to the data, the fitted implied volatility curve is not only much too flat, but also exhibits a negative slope. That is, the diffusion version does not even qualitatively match the pattern in the data. This is a robust result that obtains on each trading day in the sample. We elaborate on this finding in Section IA.5 of the Internet Appendix, where we prove analytically that in the classic diffusion-based Merton (1974) setting the leverage effect generates a negative implied volatility skew for both credit and equity options. The pure diffusion model also vastly underestimates the 1Y CDX spread, with a model-implied value of less than one basis point.

The blue line in the figure shows a very good fit for the version with systematic jumps. Intuitively, a negative (risk-neutral) mean systematic jump size in firms' asset values makes the (risk-neutral) CDX spread distribution more positively skewed and increases the value of high-strike options relative to low-strike options. The root mean squared error (RMSE) in terms of implied volatilities drops from 0.1862 to 0.0128. Having systematic jumps in the asset value process is, therefore, critical for matching the observed CDX implied volatility curves.[33] Despite the jump component, this version still significantly underestimates the 1Y CDX spread.

To match both the CDX implied volatility curves and the CDX term structure, we also

[32] We also calibrate to the SPX dividend yield, and the index leverage ratios. The general calibration procedure is described in more detail in Section 5. The calibrated parameters for each version of the model are given in Table IA.2 in the Internet Appendix.

[33] An alternative device for improving the basic model is adding stochastic volatility to the asset value process with a negative correlation between asset returns and innovations to volatility. This would also make the (risk-neutral) CDX spread distribution more positively skewed. We focus on jumps because the options in our data set have short maturities and jumps are better at generating skewed distributions over short horizons. Furthermore, jumps have the advantage of preserving closed-form solutions to index options.

need idiosyncratic jumps in the asset value process. For this version, we add the 1Y CDX spread to the set of instruments that are matched perfectly; yet, the fit to CDX options is virtually unchanged with a CDX implied volatility curve that is visually indistinguishable (and, therefore, not displayed in the figure) and an RMSE of 0.0121.

For completeness, we also illustrate the model's in-sample performance when we fit to SPX options instead of CDX options (all the other aspects of the calibration are the same). The right panel in Figure 5 displays the fitted SPX implied volatility curves. The diffusion version (red line) correctly generates a downward-sloping curve, although it is much too flat. In contrast, the version with systematic jumps (blue line) has a very good fit consistent with results in Bai et al. (2019b).

These results show that our structural model can successfully match CDX and SPX option prices, separately. In the next section, we investigate if the model can also jointly match these option prices.

5 The relative pricing of index options

5.1 Calibration procedure

The overall empirical strategy is to calibrate the model to the CDX term structure, the SPX level, and SPX options, and then study the out-of-sample fit to CDX options. Specifically, the calibration procedure forces a perfect fit to the 1Y and 5Y CDX and the SPX level (as well as the SPX dividend yield and the short- and long-term index leverage ratios), and minimizes the sum of squared pricing errors for SPX options.[34] It is especially important to price the 5Y CDX and the SPX level accurately; otherwise, it is difficult to interpret

[34] See Section IA.6 in the Internet Appendix for details on the computation of the index leverage ratios using Compustat data. The SPX dividend yield is obtained from the put-call parity relation for SPX options.

option pricing errors. The model is re-calibrated each Wednesday in the sample.[35] Note that idiosyncratic jump risk is largely pinned down by the 1Y CDX, which is essentially a deep out-of-the-money put option on firm assets. This makes it difficult to identify all idiosyncratic jump parameters; therefore, we follow Collin-Dufresne et al. (2012) in fixing $m_i = -2$ and $v_i = 0$ which implies that an idiosyncratic jump leads to almost certain default for a company. We set bankruptcy costs to 20%, corresponding to $\alpha = 0.80$. This is roughly in line with empirical estimates (see, for example, Andrade and Kaplan (1998) and Davydenko, Strebulaev, and Zhao (2012)), but we show below that our results are not very sensitive to the level of bankruptcy costs. Interest rates are obtained by first bootstrapping the LIBOR/swap curve and then interpolating. In total, there are 10 parameters to be calibrated: A_0, D_1, D_2, δ, σ, ρ, λ, m, v, and λ_i.[36] More details on the calibration procedure are given in Section IA.7 of the Internet Appendix.

5.2 Results

Table 5 reports the sample mean and sample standard deviation of the parameters. The systematic jump intensity is 0.953, on average, with a mean jump size of -0.088 and a jump size standard deviation of 0.077—all of which appear plausible. The idiosyncratic jump intensity is 0.0032, on average, suggesting a small jump-to-default risk. The instantaneous (risk-neutral) quadratic variation of log asset returns is

$$\frac{1}{dt}Var(d\log A_t^i) = \rho\sigma^2 + (1-\rho)\sigma^2 + \lambda(m^2+v) + \lambda_i(m_i^2+v_i),$$

[35] If Wednesday is not a trading day, we calibrate on the preceding Tuesday instead. The sample comprises 426 weekly observations from February 29, 2012 to April 29, 2020. Date-by-date model re-calibration is typical of papers that study the relative pricing of derivatives securities; see, e.g., Coval et al. (2009) on the relative pricing of CDX tranche swaps and SPX options and Kelly, Lustig, and Nieuwerburgh (2016) on the relative pricing of stock option baskets and equity index options.

[36] Because we re-calibrate the model on each date, we do not distinguish between state variables and parameters.

the sample average of which is 0.142, corresponding to a volatility of 0.376. The sample average of the systematic part, $\rho\sigma^2 + \lambda(m^2 + v)$, is 0.0159, corresponding to a volatility of 0.126. The sample average of the instantaneous (risk-neutral) asset correlation between any two index constituents is 0.113.

From the calibrated model, we price CDX options and compare the model-implied prices to the data. Specifically, on each date, we compute the mean pricing error (ME) and RMSE across all CDX options in terms of implied volatilities. For comparison, we do the same for SPX options. Table 6 reports the sample means of the resulting ME and RMSE time series. The model fits SPX options very well with an average ME of essentially zero and an average RMSE of roughly one percentage point implied volatility. On the other hand, there is a large difference between the model-implied CDX option prices and the data with an average ME of minus 21 percentage points implied volatility and an average RMSE of roughly 22 percentage points. That the out-of-sample CDX RMSE is larger than the in-sample SPX RMSE is not surprising. More striking is the fact that the model-implied CDX option prices are systematically much lower than the prices in the data.

To determine which dimensions of CDX option prices the model has difficulty matching, we run the regression (2) on the fitted implied volatilities and measure the model fit in terms of how close the β-estimates obtained from the fitted data are to the original β-estimates. In Figure 3, the red lines show the β-estimates from the fitted data. The figure confirms the model's accurate (in-sample) fit to SPX options in terms of both volatility (middle-right panel) and skewness (lower-right panel). The figure also shows that the model has a relatively accurate (out-of-sample) fit to CDX skewness (lower-left panel). However, the figure shows that the model has a poor (out-of-sample) fit to CDX volatility. While the model appears to capture the variation in volatility relatively well, the level of model-implied volatility is consistently too low; indeed, the sample means of β_0^{CDX} in the data and the fitted data are 0.471 and 0.285, respectively.

As an example, Figure 6 plots the fit to the SPX and CDX implied volatility smiles on the last Wednesday in the sample, April 29, 2020. The model has a very good fit to SPX options and correctly generates a positively skewed CDX volatility smile. However, the model clearly underestimates the level of the CDX volatility smile.

Figure 7 shows the time series of CDX option pricing errors in terms of β_0^{CDX}. The left panel displays the difference between β_0^{CDX} in the data and the fitted data (i.e., the difference between the blue and red line in the middle-left panel of Figure 3), while the right panel displays the relative difference. In absolute terms, pricing errors trend downwards in the second half of the sample until the onset of the Covid-19 crisis, when they increase sharply. In relative terms, we observe the same downward trend, and the effect of the Covid-19 crisis is much less noticeable.

Next, we investigate the extent to which the within- and cross-market correlations computed from the fitted data match the patterns discussed in Section 3. For SPX, Table 3 shows a close (in-sample) match to the correlations in the data. More importantly, for CDX the table shows a relatively good (out-of-sample) match to the correlations between spread and volatility (0.517 vs. 0.675 in the data) and between volatility and skewness (0.286 vs. 0.397 in the data); however, contrary to the data, the correlation between spread and skewness is not significantly different from zero.

Table 4 shows that the model (again, out-of-sample) correctly generates a highly positive (if slightly too high) correlation between SPX and CDX volatility (0.873 vs. 0.749 in the data) and accurately matches the moderately negative correlation between SPX and CDX skewness (-0.368 vs. -0.380 in the data).[37] All these results also hold true in the ex-Covid-19 sample.

Finally, the yellow lines in Figure 4 show the fits of linear regressions applied to the fitted data. Focusing on the out-of-sample results, Panels E and I show the cross-market

[37] Note that, by design of the calibration procedure, the correlation between SPX returns and CDX spread changes is matched exactly.

interactions while panels D, G, and H show the CDX-market interactions. These are largely in line with the observations from Tables 3 and 4.

5.3 Robustness

Robustness checks are reported in Tables 5 and 6.

5.3.1 Increasing bankruptcy costs, $\alpha = 0.5$

We increase bankruptcy costs to 50%, corresponding to $\alpha = 0.50$. With higher expected loss-given-default, the default likelihood needs to decrease to preserve the fit to the CDX term structure. This is achieved via increasing A_0 slightly and decreasing idiosyncratic diffusive risk (lower σ and higher ρ) and jump risk (lower λ_i) in such a way that the SPX level is preserved. Table 6 shows that the fit to CDX options improves slightly from the main specification.

5.3.2 No idiosyncratic jumps, $\lambda_i = 0$

Without idiosyncratic jumps it is not possible to fit the 1Y CDX (see Section 4.6). Therefore, when calibrating the model, we remove the 1Y CDX from the objective function. Table 6 shows that the fit to CDX options is slightly better than in the main specification.

5.3.3 No jumps, $\lambda = \lambda_i = 0$

In a pure diffusion model, it is not possible to fit the entire implied volatility smile (see, again, Section 4.6). Therefore, when calibrating the model, we remove OTM SPX options (as well as the 1Y CDX) from the objective function. In this case, Table 6 shows the fit to ATM options only. Clearly, the discrepancy between model-implied and actual CDX option prices is as large for ATM options in this very parsimonious model as it is for all options in the general model.

To summarize, the model captures many aspects of the joint dynamics of the credit and equity index options data; however, it is not able to capture the relative levels of CDX and SPX option prices.

6 Interpretation of results

In interpreting the results, we face the joint-hypothesis problem (e.g., Fama (1970)) that we can never definitively tell whether the results reflect lack of integration between the two markets or a misspecified pricing model, or some combination. Instead, in this section, we discuss different potential explanations for our results.

6.1 Model misspecification

Although Section 5.3 shows that our results are robust within the boundaries of the model, the model itself relies on a number of simplifying assumptions, some of which we discuss here. First, the model assumes that firms are ex-ante identical, when in fact they exhibit significant heterogeneity (see below). In the Internet Appendix, Section IA.8 we solve an extended version of the model that allows for heterogeneity in leverage across firms. We show that, relative to the benchmark model, matching the mean, dispersion, and skewness of the leverage distribution for index constituents leads to lower CDX option prices relative to SPX option prices, hence exacerbating the valuation puzzle.

Second, the model prices index options assuming an infinite number of index constituents. In the Internet Appendix, Section IA.9, we use simulations to price index options for a finite number of index constituents and quantify the bias in the analytical option pricing formulas. We show that the (downward) bias is small, but greater for CDX options than for SPX options because the CDX index has fewer constituents; hence, accounting for the actual number of index constituents would raise CDX option prices relative to SPX option prices.

However, the effect is small relative to the magnitude of the valuation puzzle.

Third, the model does not incorporate stochastic volatility in the asset process. Instead, we compensate for this by re-calibrating model parameters on each trading day. From a time-series perspective, it would clearly be relevant to introduce stochastic asset volatility. However, from a cross-sectional perspective using short-term options, which is the focus of our paper, the effect is likely to be more muted because jumps are more important than stochastic volatility for valuing short-term options; see, e.g., Das and Sundaram (1999).[38]

6.2 Differences in index compositions

Our analysis does not require the two indexes to be identical in terms of names, but rather in terms of risk characteristics. To assess the similarity of the indexes, we focus on four characteristics that are central to the structural model: rating (as a proxy for the physical-measure default probability), leverage, and total and systematic asset return volatility.[39]

Figure 8 compares the indexes in terms of leverage and ratings. Panels A and B show the distribution of firm-quarter leverage observations for the CDX and SPX constituents, respectively.[40] Clearly, the distribution for SPX constituents has a higher dispersion with relatively more low-leverage (even unlevered) and high-leverage firms. However, on average, leverage is similar across the two indexes with a mean (median) of 0.277 (0.244) for CDX vs. 0.238 (0.200) for SPX.

Panels C and D show the distribution of firm-quarter rating observations for the two sets

[38] Du et al. (2019) investigate the effect of stochastic asset volatility on credit spreads and find that it mainly affects medium- to long-term spreads. Introducing stochastic asset volatility into our framework would significantly increase complexity because of the need to value compound options with multiple state variables.

[39] Section IA.10 in the Internet Appendix details the computation of asset return volatility. In a nutshell, asset returns are leverage-weighted averages of stock and synthetic bond returns, where stock returns are from CRSP and synthetic bond returns are computed using single-name CDS data from Markit. The systematic component of asset return volatility is obtained from a one-factor model.

[40] In the figure, we focus on total leverage. In the Internet Appendix, we split total leverage into short- and long-term leverage and find similar results, see Figure IA8. The fraction of CDX (SPX) constituents for which we are able to compute leverage varies between 0.832 and 0.888 (0.892 and 0.984).

of index constituents.[41] Again, the distribution for SPX constituents has a higher dispersion, but for both indexes the mean and median rating is BBB+.[42]

Figure 8 compares the indexes in terms of asset return volatility. Panels A and B show the distribution of firm-quarter observations of total asset return volatility for the CDX and SPX index constituents, respectively. While the distribution for SPX constituents displays slightly higher dispersion (standard deviation of 0.068 for CDX vs. 0.080 for SPX), the average asset volatility is very similar with a mean (median) of 0.167 (0.154) for CDX vs. 0.173 (0.158) for SPX.

Since the non-diversifiable component of volatility is the crucial driver of index option value, we plot the distribution of firm-quarter observations of systematic asset return volatility in Panels C and D. These distributions are strikingly similar with a mean (median) [standard deviation] of 0.092 (0.085) [0.045] for CDX vs. 0.098 (0.089) [0.052] for SPX.

Given these results, it seems unlikely that differences in the risk characteristics that drive valuation in our structural model (such as leverage, total and systematic volatility) can explain our findings. In particular, a potential explanation for the overpricing of CDX options could be a relatively higher systematic asset return volatility among CDX constituents, but this is clearly not what we observe in the data.

6.3 Differences in economic states spanned by options

For the comparison between model-implied and actual CDX option prices to be meaningful, we need that SPX options span roughly the same set of economic states as CDX options. To check this, we translate the strike ranges of CDX and SPX options into strike ranges in

[41] Note that ratings data in Compustat is only available up until third quarter of 2017. During this time period, the fraction of CDX (SPX) constituents with ratings information varies between 0.888 and 0.912 (0.864 and 0.892).

[42] When the CDX index is refreshed every six months, it consists only of investment-grade firms (i.e., those rated BBB- and above). The few BB-observations in the figure come from firms that were downgraded after index launch.

terms of the common factor, A.

For CDX options, A^{min} is the value of the common factor below which the highest-strike call option expires in the money, and A^{max} is the value above which the lowest-strike put option expires in the money.[43] Similarly, for SPX options, A^{min} is the value of the common factor below which the lowest-strike put option expires in the money, and A^{max} is the value above which the highest-strike call option expires in the money.[44]

Figure 10 plots the time series of the strike range of CDX and SPX options in terms of the common factor. Specifically, on each observation date and for each option maturity, we express A^{min} and A^{max} relative to the forward value of the common factor, A^{fwd}; that is, as $\frac{A^{min}-A^{fwd}}{A^{fwd}}$ and $\frac{A^{max}-A^{fwd}}{A^{fwd}}$. Clearly, CDX and SPX options span roughly the same economic states.

6.4 Stochastic bankruptcy costs

The spanning result in the previous section only holds true in the context of the model. A richer model with a credit-specific factor would break the tight link between CDX and SPX options and would also provide an economic rationale for why both types of options are traded. What might such a credit-specific factor be? A natural candidate would be systematic variation in bankruptcy costs which would impact bond recovery upon default and thus affect credit derivatives, but not equity derivatives since equity always recovers zero in bankruptcy.[45] In the Internet Appendix, Section IA.11 we add stochastic bankruptcy costs to the model and derive analytical solutions for all derivatives. Specifically, we assume that systematic bankruptcy costs follow a continuous-time Markov chain independent of A_t and A_t^i. We show that the CDX depends on the conditional expectation of bankruptcy costs,

[43] Recall that $U_{T_0}(A)$ is decreasing in A; therefore, A^{min} solves $U_{T_0}(A^{min}) = K^{max}$ and A^{max} solves $U_{T_0}(A^{max}) = K^{min}$.
[44] Here, A^{min} solves $S_{T_0}(A^{min}) = K^{min}$ and A^{max} solves $S_{T_0}(A^{max}) = K^{max}$.
[45] An alternative could be a credit-specific liquidity factor along the lines of He and Xiong (2012) or He et al. (2020), for example.

while CDX options also depend on bankruptcy cost volatility.

To illustrate the potential for this model to account for the discrepancy in CDX option prices, we consider a simple three-state Markov chain. We assume that bankruptcy costs in the three states are 40%, 20%, and zero, corresponding to α-values of 0.6, 0.8, and 1. We start out in the middle state, and assume that the transition matrix has the form

$$Q = \begin{bmatrix} -q_{in} & q_{in} & 0 \\ q_{out} & -2q_{out} & q_{out} \\ 0 & q_{in} & -q_{in} \end{bmatrix},$$

where q_{out} (q_{in}) determines the probability of moving away from (towards) the middle state. Because states one and three are equally likely and persistent, conditional on being in the middle state, the expected future bankruptcy costs are 20% ($\alpha = 0.80$) as in our benchmark model. Therefore, the CDX term structure is unchanged, and q_{out} and q_{in} only affect CDX options. On each day in the sample, we take the calibrated parameters of the benchmark model as given (and, hence, preserve the fit to all dimensions of the data except CDX options) and then calibrate q_{out} and q_{in} to minimize the sum of squared pricing errors for ATM CDX options.[46]

The left panel in Figure 11 shows time series of the mean error (in terms of implied volatilities) for ATM CDX options. Except during the Covid-19 crisis, the mean error is virtually zero. The right panel shows the three-month conditional (risk-neutral) standard deviation of bankruptcy costs. This fluctuates around 0.15 indicating that very high uncertainty about systematic bankruptcy costs is needed to reconcile the pricing of CDX and SPX options. It is not clear whether this implied volatility of bankruptcy costs is consistent with the actual variability and risk premium associated with bankruptcy costs, which are

[46] In our very parsimonious setting, we only have two degrees of freedom; therefore, we focus on matching ATM CDX options. We leave for future research the question of whether with more states and/or more parameters in the transition matrix it is possible to match the entire CDX option surface.

notoriously difficult to measure (e.g., Almeida and Philippon (2007)).

6.5 Structural demand for CDX options

Another possibility, along the lines of Gârleanu, Pedersen, and Poteshman (2009), is that demand pressure in CDX options pushes their prices above fair values implied by SPX options. Indeed, anecdotal evidence suggests that there is a structural demand for CDX call options to hedge against widening of credit spreads. Specifically, there appears to be a significant regulatory-driven demand by banks who seek to hedge their credit valuation adjustment (CVA) exposures in order to reduce their regulatory capital.[47] Unfortunately, we cannot directly quantify this demand because we do not have access to trader identities in our transaction data set. However, via regulatory filings we can quantify the amount of risk-weighted assets (RWAs) attributed to CVA risk across large banks to get an idea about the magnitudes of CVA exposures and, hence, the potential demand for CDX call options. Figure IA16 in the Internet Appendix shows the evolution of RWAs for CVA risk across the eight US global systemically important banks. Between Q4 2015 and Q1 2020 it averages 228 bln USD (it jumps markedly to 271 bln USD in Q1 2020); hence, the regulatory-driven demand can potentially account for a significant fraction of the trading volume documented in Section 2.3.[48]

6.6 Trading CDX vs. SPX options

Finally, we compare the profitability of selling volatility in the two markets. We consider a strategy of selling ATM straddles within each maturity category on a daily basis and with

[47] In the aftermath of the financial crisis, the Basel III regulation introduced a new capital charge—the CVA risk charge—to cover the risk of deterioration in the credit worthiness of counterparties. Both CDX and CDX options are eligible hedge instruments, but due to a discrepancy between the regulatory and accounting treatment of counterparty risk, many banks prefer to use CDX options; see, e.g., Becker (2014).

[48] Because traded CDX options have short maturities, a bank that hedges CVA risk exposures via options would need to frequently roll over its positions.

a holding period of one day (a short holding period ensures that the delta remains close to zero). In addition to holding the option premium in a margin account, we assume that an initial amount of capital is required when selling options. We further assume that the required capital is proportional to the option premium and adjust the proportionality factor to achieve a 10% unconditional annualized volatility of realized excess returns within each option maturity category.[49]

Table 7 shows summary statistics of returns for each option maturity as well as for an equally weighted (EW) portfolio of the three option maturities.[50] Across all maturities and both including and excluding the Covid-19 crisis, selling CDX volatility generates higher and more statistically significant average excess returns and higher Sharpe ratios than selling SPX volatility. For instance, for the full sample (Panel A), the EW portfolio generates an annualized Sharpe ratio of 1.744 in the CDX market vs. 0.659 in the SPX market. Because of the large increase in volatility during the Covid-19 crisis, the strategy in both markets performs better during the ex-Covid-19 sample (Panel B).[51]

We also consider a short-long strategy of selling CDX straddles vs. buying SPX straddles.[52] This strategy generates high Sharpe ratios, that are typically higher than that of selling SPX volatility outright, but lower than selling CDX volatility outright. For instance, for the full sample, trading the EW portfolios against each other generates an annualized Sharpe ratio of 0.877. Further, the higher-order moments of the long-short strategy are more attractive, with the return distributions being roughly symmetric (instead of highly

[49] A similar approach is taken in Duarte, Longstaff, and Yu (2007) in their analysis of fixed income arbitrage strategies. The choice of 10% is inconsequential for our conclusions. Section IA.12 in the Internet Appendix provides more details on the trading strategy. It also shows that the results are robust to assuming that the required capital is constant over time (rather than varying with the option premium).

[50] When computing performance, we only consider returns on those days where returns are available for all option maturities and for both markets.

[51] A contemporaneous paper by Ammann and Moerke (2019) constructs synthetic variance swap contracts from CDX options and finds that selling CDX variance swaps generates higher Sharpe ratios than selling SPX variance swaps in a pre-Covid-19 sample. See also Chen, Doshi, and Seo (2020).

[52] We assume that the same amount of capital is required when buying SPX straddles as when selling them so that we maintain a 10% unconditional annualized volatility of realized excess returns. The short-long strategy then allocates 50% of funds to selling CDX straddles and 50% to buying SPX straddles.

negatively skewed) and much less leptokurtic. Figure 12 shows the evolution of one dollar invested in each of the EW strategies at the beginning of the sample. Clearly, the short-long strategy avoids the occasional large drawdowns from selling volatility outright.

Together, these results are consistent with the demand-pressure hypothesis (Section 6.5). However, the results could also be consistent with the bankruptcy-cost hypothesis (Section 6.4) provided sellers of CDX options require a large compensation for bearing systematic bankruptcy cost uncertainty.

7 Conclusion

In recent years, a liquid market for credit index (CDX) options has developed. We study the extent to which these options are priced consistently with S&P 500 (SPX) equity index options. We consider a rich structural credit risk model in which firm assets follow a jump-diffusion process with idiosyncratic and systematic risk, and we derive analytical expressions for CDX and SPX options. Calibrating the model, we find that it captures many aspects of the joint dynamics of CDX and SPX options. However, it cannot reconcile the relative levels of option prices, suggesting that credit and equity markets are not fully integrated. We discuss several potential explanations for this finding, and we show that a strategy of selling CDX volatility yields significantly higher average excess returns and Sharpe ratios than selling SPX volatility.

A.1 Pricing formulas

This Appendix contains the pricing formulas for the model in Section (4).

A.1.1 Valuation of CDX and SPX

From (3) and (4) we have

$$
\begin{aligned}
A_{T_0} &= A_0 e^{(r-\delta-\lambda\nu)T_0+\gamma N_{T_0}+y} \\
A^i_{T_1} &= A_0 e^{(r-\delta-\lambda_i\nu_i-\lambda\nu)T_1+\gamma N_{T_1}+\gamma_i N^i_{T_1}+y+z} = A_{T_0} e^{(r-\delta-\lambda\nu)(T_1-T_0)-\lambda_i\nu_i T_1+\gamma(N_{T_1}-N_{T_0})+\gamma_i N^i_{T_1}+z} \qquad (5) \\
A^i_{T_2} &= A_0 e^{(r-\delta-\lambda_i\nu_i-\lambda\nu)T_2+\gamma N_{T_2}+\gamma_i N^i_{T_2}+y+z+x} = A_{T_0} e^{(r-\delta-\lambda\nu)(T_2-T_0)-\lambda_i\nu_i T_2+\gamma(N_{T_2}-N_{T_0})+\gamma_i N^i_{T_2}+z+x},
\end{aligned}
$$

where y, z, and x are independent normal random variables with

$$
\begin{aligned}
v_y &= \rho\sigma^2 T_0 & m_y &= -\frac{1}{2}v_y \\
v_z &= (1-\rho)\sigma^2 T_0 + \sigma^2(T_1-T_0) = \sigma^2(T_1-\rho T_0) & m_z &= -\frac{1}{2}v_z \\
v_x &= \sigma^2(T_2-T_1) & m_x &= -\frac{1}{2}v_x.
\end{aligned}
$$

Because, conditional on the number of jumps, future asset values are log-normally distributed, we obtain the following closed-form solutions for all the expectations (basically variants of the standard Merton (1976) jump-diffusion model formula):

$$
\begin{aligned}
&\mathbb{E}[\mathbf{1}_{\{A^i_{T_1}<\Phi\}} \mid A_{T_0}] = \sum_{n_1,j_1=0}^{\infty} \mathcal{P}_{\lambda}^{T_1-T_0}(n_1)\mathcal{P}_{\lambda_i}^{T_1}(j_1)\mathcal{N}\left(-d_1^-\right) \\
&\mathbb{E}[A^i_{T_1}\mathbf{1}_{\{A^i_{T_1}<\Phi\}} \mid A_{T_0}] = \sum_{n_1,j_1=0}^{\infty} \mathcal{P}_{\lambda}^{T_1-T_0}(n_1)\mathcal{P}_{\lambda_i}^{T_1}(j_1)A_{T_0}e^{(r-\delta-\lambda\nu)(T_1-T_0)-\lambda_i\nu_i T_1+n_1 m+j_1 m_i+\frac{1}{2}(n_1 v+j_1 v_i)}\mathcal{N}\left(-d_1^+\right) \\
&\mathbb{E}[\mathbf{1}_{\{A^i_{T_1}\geq\Phi, A^i_{T_2}<D_2\}} \mid A_{T_0}] = \sum_{n_1,n_2,j_1,j_2=0}^{\infty} \mathcal{P}_{\lambda}^{T_1-T_0}(n_1)\mathcal{P}_{\lambda}^{T_2-T_1}(n_2)\mathcal{P}_{\lambda_i}^{T_1}(j_1)\mathcal{P}_{\lambda_i}^{T_2-T_1}(j_2)\mathcal{N}_2(d_1^-,-d_2^-;-\rho) \\
&\mathbb{E}[A^i_{T_2}\mathbf{1}_{\{A^i_{T_1}\geq\Phi, A^i_{T_2}<D_2\}} \mid A_{T_0}] = \sum_{n_1,n_2,j_1,j_2=0}^{\infty} \mathcal{P}_{\lambda}^{T_1-T_0}(n_1)\mathcal{P}_{\lambda}^{T_2-T_1}(n_2)\mathcal{P}_{\lambda_i}^{T_1}(j_1)\mathcal{P}_{\lambda_i}^{T_2-T_1}(j_2) \\
&\quad A_{T_0}e^{(r-\delta-\lambda\nu)(T_2-T_0)-\lambda_i\nu_i T_2+(n_1+n_2)m+(j_1+j_2)m_i+(n_1+n_2)\frac{v}{2}+(j_1+j_2)\frac{v_i}{2}}\mathcal{N}_2\left(d_1^+,-d_2^+;-\rho\right),
\end{aligned}
$$

where $\mathcal{N}_2$ denotes the bivariate normal cumulative distribution function,

$$\mathcal{P}_\lambda^T(n) = e^{-\lambda T}\frac{(\lambda T)^n}{n!} \tag{6}$$

is the probability of n jumps over a time interval of length T for a Poisson jump counter with intensity λ, and we define

$$\begin{aligned}
d_1^- &= \frac{\log\frac{A_{T_0}}{\Phi} + (r-\delta-\lambda\nu)(T_1-T_0) - \lambda_i\nu_i T_1 + n_1 m + j_1 m_i - \frac{1}{2}v_z}{\sqrt{v_z + n_1 v + j_1 v_i}}\\
d_1^+ &= \frac{\log\frac{A_{T_0}}{\Phi} + (r-\delta-\lambda\nu)(T_1-T_0) - \lambda_i\nu_i T_1 + n_1 m + j_1 m_i + \frac{1}{2}v_z + n_1 v + j_1 v_i}{\sqrt{v_z + n_1 v + j_1 v_i}}\\
d_2^- &= \frac{\log\frac{A_{T_0}}{D_2} + (r-\delta-\lambda\nu)(T_2-T_0) - \lambda\nu_i T_2 + (n_1+n_2)m + (j_1+j_2)m_i - \frac{1}{2}(v_z+v_x)}{\sqrt{v_z + v_x + (n_1+n_2)v + (j_1+j_2)v_i}}\\
d_2^+ &= \frac{\log\frac{A_{T_0}}{D_2} + (r-\delta-\lambda\nu)(T_2-T_0) - \lambda\nu_i T_2 + (n_1+n_2)m + (j_1+j_2)m_i + \frac{1}{2}(v_z+v_x) + (n_1+n_2)v + (j_1+j_2)v_i}{\sqrt{v_z + v_x + (n_1+n_2)v + (j_1+j_2)v_i}}\\
\rho &= \sqrt{\frac{v_z + n_1 v + j_1 v_i}{v_z + v_x + (n_1+n_2)v + (j_1+j_2)v_i}}.
\end{aligned} \tag{7}$$

We only show the derivation of the explicit solution for the second expectation, since all the other expectations can be derived similarly. Substituting from Equation (5) above and conditioning on the number of jumps we obtain:

$$\begin{aligned}
\mathbb{E}[A_{T_1}^i \mathbf{1}_{\left\{A_{T_1}^i < \Phi\right\}} \,|\, A_{T_0}] \quad &= \sum_{n_1, j_1 = 0}^{\infty} \mathcal{P}_\lambda^{T_1 - T_0}(n_1)\mathcal{P}_{\lambda_i}^{T_1}(j_1) A_{T_0} e^{(r-\delta-\lambda\nu)(T_1-T_0) - \lambda_i\nu_i T_1} \times \\
&\qquad \mathbb{E}[e^{z+\gamma n_1 + \gamma_i j_1}\mathbf{1}_{\left\{A_{T_1}^i < \Phi\right\}} \,|\, A_{T_0}, N_{T_1}^i = j_1, N_{T_1} - N_{T_0} = n_1].
\end{aligned}$$

Now, since[53] $z + \gamma n_1 + \gamma_i j_1 \sim \mathcal{N}(m_z + m n_1 + m_i j_1, v_z + v n_1 + v_i j_1)$ we obtain:

$$\mathbb{E}[e^{z+\gamma n_1+\gamma_i j_1}\mathbf{1}_{\left\{A_{T_1}^i<\Phi\right\}} \,|\, A_{T_0}, N_{T_1}^i = j_1, N_{T_1} - N_{T_0} = n_1] = e^{m_z + m n_1 + m_i j_1 + \frac{1}{2}(v_z + v n_1 + v_i j_1)}\tilde{\mathbb{E}}[\mathbf{1}_{\left\{\frac{z+\gamma n_1+\gamma_i j_1 - \tilde{M}}{\sqrt{\tilde{V}}} < -d_1^+\right\}}],$$

where d_1^+ is as defined in Equation (7) above and the expectation $\tilde{\mathbb{E}}[\cdot]$ is taken with respect to a probability measure $\tilde{P}$ equivalent to Q under which $z+\gamma n_1+\gamma_i j_1 \sim \mathcal{N}(\tilde{M}, \tilde{V})$ with the mean

[53] Recall that γn_1 $(\gamma_i j_1)$ is our short-hand notation for a sum of n_1 (j_1) i.i.d. normal random variables each distributed like γ (γ_i).

and variance under $\tilde{P}$ given by $\tilde{M} = m_z+v_z+(m+v)n_1+(m_i+v_i)j_1$ and $\tilde{V} = v_z+vn_1+v_ij_1$.[54] Using the definition of m_z and the fact that $\tilde{\mathbb{E}}[\mathbf{1}_{\left\{\frac{z+\gamma n_1+\gamma_i j_1-\tilde{M}}{\sqrt{\tilde{V}}}<-d_1^+\right\}}] = \mathcal{N}(-d_1^+)$ completes the derivation. Similar derivations apply to all other expectations.

A.1.2 Valuation of CDX and SPX options

Again, we obtain closed-form solution for all the expectations in the CDX option formula

$$
\begin{aligned}
&\mathbb{E}_0[\mathbf{1}_{\left\{A_{T_0}<\overline{A}\right\}}] = \sum_{n_0=0}^{\infty} \mathcal{P}_\lambda^{T_0}(n_0)\mathcal{N}(-d_0^-)\\
&\mathbb{E}_0[\mathbf{1}_{\left\{A_{T_0}<\overline{A},A^i_{T_1}<\Phi\right\}}] = \sum_{n_0,n_1,j_1=0}^{\infty} \mathcal{P}_\lambda^{T_0}(n_0)\mathcal{P}_\lambda^{T_1-T_0}(n_1)\mathcal{P}_{\lambda_i}^{T_1}(j_1)\mathcal{N}_2(-d_0^-;-d_1^-;\rho_{01})\\
&\mathbb{E}_0[A^i_{T_1}\mathbf{1}_{\left\{A_{T_0}<\overline{A},A^i_{T_1}<\Phi\right\}}] = \sum_{n_0,n_1,j_1=0}^{\infty} \mathcal{P}_\lambda^{T_0}(n_0)\mathcal{P}_\lambda^{T_1-T_0}(n_1)\mathcal{P}_{\lambda_i}^{T_1}(n_2)\\
&\quad A_0e^{(r-\delta-\lambda\nu-\lambda_i\nu_i)T_1+(n_0+n_1)m+j_1m_i+\frac{1}{2}(n_0+n_1)v+\frac{1}{2}j_1v_i}\mathcal{N}_2(-d_0^+,-d_1^+;\rho_{01})\\
&\mathbb{E}_0[\mathbf{1}_{\left\{A_{T_0}<\overline{A},A^i_{T_1}\geq\Phi,A^i_{T_2}<D_2\right\}}] = \sum_{n_0,n_1,n_2,j_1,j_2=0}^{\infty} \mathcal{P}_\lambda^{T_0}(n_0)\mathcal{P}_\lambda^{T_1-T_0}(n_1)\mathcal{P}_\lambda^{T_2-T_1}(n_2)\mathcal{P}_{\lambda_i}^{T_1}(j_1)\mathcal{P}_{\lambda_i}^{T_2-T_1}(j_2)\\
&\quad \mathcal{N}_3(-d_0^-,d_1^-,-d_2^-;-\rho_{01},\rho_{02},-\rho_{12})\\
&\mathbb{E}_0[A^i_{T_2}\mathbf{1}_{\left\{A_{T_0}<\overline{A},A^i_{T_1}\geq\Phi,A^i_{T_2}<D_2\right\}}] = \sum_{n_0,n_1,n_2,j_1,j_2=0}^{\infty} \mathcal{P}_\lambda^{T_0}(n_0)\mathcal{P}_\lambda^{T_1-T_0}(n_1)\mathcal{P}_\lambda^{T_2-T_1}(n_2)\mathcal{P}_{\lambda_i}^{T_1}(j_1)\mathcal{P}_{\lambda_i}^{T_2-T_1}(j_2)\\
&\quad A_0e^{(r-\delta-\lambda\nu-\lambda_i\nu_i)T_2+(n_0+n_1+n_2)m+(j_1+j_2)m_i+\frac{1}{2}(n_0+n_1+n_2)v+\frac{1}{2}(j_1+j_2)v_i}\mathcal{N}_3(-d_0^+,d_1^+,-d_2^+;-\rho_{01},\rho_{02},-\rho_{12}),
\end{aligned}
$$

and the SPX option formula

$$
\begin{aligned}
&\mathbb{E}_0[\mathbf{1}_{\left\{A_{T_0}\geq\overline{A}\right\}}] = \sum_{n_0=0}^{\infty} \mathcal{P}_\lambda^{T_0}(n_0)\mathcal{N}(d_0^-)\\
&\mathbb{E}_0[A_{T_0}\mathbf{1}_{\left\{A_{T_0}\geq\overline{A}\right\}}] = \sum_{n_0=0}^{\infty} \mathcal{P}_\lambda^{T_0}(n_0)A_0e^{(r-\delta-\lambda\nu)T_0+n_0m+\frac{1}{2}n_0v}\mathcal{N}(d_0^+)\\
&\mathbb{E}_0[\mathbf{1}_{\left\{A_{T_0}\geq\overline{A},A^i_{T_1}\geq\Phi\right\}}] = \sum_{n_0,n_1,j_1=0}^{\infty} \mathcal{P}_\lambda^{T_0}(n_0)\mathcal{P}_\lambda^{T_1-T_0}(n_1)\mathcal{P}_{\lambda_i}^{T_1}(j_1)\mathcal{N}_2(d_0^-,d_1^-;\rho_{01})
\end{aligned}
$$

[54]Recall that if $z \sim \mathcal{N}(m_z, v_z)$ then $\mathbb{E}[e^zH(z)] = e^{m_z+\frac{1}{2}v_z}\tilde{\mathbb{E}}[H(z)]$ where under $\tilde{P} \sim Q$ we have $z \sim \mathcal{N}(m_z + v_z, v_z)$. To see that note that $d\tilde{P} = e^{z-m_z-\frac{1}{2}v_z}dQ$ and that the Laplace transform of z under $\tilde{P}$ is $\tilde{\mathbb{E}}[e^{kz}] = \mathbb{E}[e^{z-m_z-\frac{1}{2}v_z+kz}] = e^{k(m_z+v_z)+\frac{1}{2}k^2v_z}$.

$$\mathbb{E}_0[A^i_{T_1}\mathbf{1}_{\left\{A_{T_0}\geq\overline{A},A^i_{T_1}<\Phi\right\}}] = \sum_{n_0,n_1,j_1=0}^{\infty}\mathcal{P}^{T_0}_{\lambda}(n_0)\mathcal{P}^{T_1-T_0}_{\lambda}(n_1)\mathcal{P}^{T_1}_{\lambda_i}(n_2)$$

$$A_0 e^{(r-\delta-\lambda\nu-\lambda_i\nu_i)T_1+(n_0+n_1)m+j_1m_i+\frac{1}{2}(n_0+n_1)v+\frac{1}{2}j_1v_i}\mathcal{N}_2(d^+_0,-d^+_1;-\rho_{01})$$

$$\mathbb{E}_0[\mathbf{1}_{\left\{A_{T_0}\geq\overline{A},A^i_{T_1}\geq\Phi,A^i_{T_2}\geq D_2\right\}}] = \sum_{n_0,n_1,n_2,j_1,j_2=0}^{\infty}\mathcal{P}^{T_0}_{\lambda}(n_0)\mathcal{P}^{T_1-T_0}_{\lambda}(n_1)\mathcal{P}^{T_2-T_1}_{\lambda}(n_2)\mathcal{P}^{T_1}_{\lambda_i}(j_1)\mathcal{P}^{T_2-T_1}_{\lambda_i}(j_2)$$

$$\mathcal{N}_3(d^-_0,d^-_1,d^-_2;\rho_{01},\rho_{02},\rho_{12})$$

$$\mathbb{E}_0[A^i_{T_2}\mathbf{1}_{\left\{A_{T_0}\geq\overline{A},A^i_{T_1}\geq\Phi,A^i_{T_2}<D_2\right\}}] = \sum_{n_0,n_1,n_2,j_1,j_2=0}^{\infty}\mathcal{P}^{T_0}_{\lambda}(n_0)\mathcal{P}^{T_1-T_0}_{\lambda}(n_1)\mathcal{P}^{T_2-T_1}_{\lambda}(n_2)\mathcal{P}^{T_1}_{\lambda_i}(j_1)\mathcal{P}^{T_2-T_1}_{\lambda_i}(j_2)$$

$$A_0 e^{(r-\delta-\lambda\nu-\lambda_i\nu_i)T_2+(n_0+n_1+n_2)m+(j_1+j_2)m_i+\frac{1}{2}(n_0+n_1+n_2)v+\frac{1}{2}(j_1+j_2)v_i}\mathcal{N}_3(d^+_0,d^+_1,-d^+_2;\rho_{01},-\rho_{02},-\rho_{12}),$$

where $\mathcal{N}_2$ and $\mathcal{N}_3$ denote the bivariate and trivariate normal cumulative distribution functions, $\mathcal{P}^T_\lambda(n)$ is given in (6), and we define

$$d^-_0 = \frac{\log(\frac{A_0}{\overline{A}})+(r-\delta-\lambda\nu)T_0+n_0m-\frac{1}{2}v_y}{\sqrt{v_y+n_0v}}$$

$$d^+_0 = \frac{\log(\frac{A_0}{\overline{A}})+(r-\delta-\lambda\nu)T_0+n_0m+\frac{1}{2}v_y+n_0v}{\sqrt{v_y+n_0v}}$$

$$d^-_1 = \frac{\log\frac{A_0}{\Phi}+(r-\delta-\lambda\nu-\lambda\nu_i)T_1+(n_0+n_1)m+j_1m_i-\frac{1}{2}(v_y+v_z)}{\sqrt{v_y+v_z+(n_0+n_1)v+j_1v_i}}$$

$$d^+_1 = \frac{\log\frac{A_0}{\Phi}+(r-\delta-\lambda\nu-\lambda\nu_i)T_1+(n_0+n_1)m+j_1m_i+\frac{1}{2}(v_y+v_z)+(n_0+n_1)v+j_1v_i}{\sqrt{v_y+v_z+(n_0+n_1)v+j_1v_i}}$$

$$d^-_2 = \frac{\log\frac{A_0}{D_2}+(r-\delta-\lambda\nu-\lambda\nu_i)T_2+(n_0+n_1+n_2)m+(j_1+j_2)m_i-\frac{1}{2}(v_y+v_z+v_x)}{\sqrt{v_y+v_z+v_x+(n_0+n_1+n_2)v+(j_1+j_2)v_i}}$$

$$d^+_2 = \frac{\log\frac{A_0}{D_2}+(r-\delta-\lambda\nu-\lambda\nu_i)T_2+(n_0+n_1+n_2)m+(j_1+j_2)m_i+\frac{1}{2}(v_y+v_z+v_x)+(n_0+n_1+n_2)v+(j_1+j_2)v_i}{\sqrt{v_y+v_z+v_x+(n_0+n_1+n_2)v+(j_1+j_2)v_i}}$$

$$\rho_{01} = \sqrt{\frac{v_y+n_0v}{v_y+v_z+(n_0+n_1)v+j_1v_i}}$$

$$\rho_{02} = \sqrt{\frac{v_y+n_0v}{v_y+v_z+v_x+(n_0+n_1+n_2)v+(j_1+j_2)v_i}}$$

$$\rho_{12} = \sqrt{\frac{v_y+v_z+(n_0+n_1)v+j_1v_i}{v_y+v_z+v_x+(n_0+n_1+n_2)v+(j_1+j_2)v_i}}.$$

References

Almeida, Heitor, and Thomas Philippon, 2007, The risk-adjusted cost of financial distress, *The Journal of Finance* 62, 2557–2586.

Ammann, Manuel, and Mathis Moerke, 2019, Credit variance risk premiums, Working paper, University of St.Gallen.

Andrade, Gregor, and Steven N. Kaplan, 1998, How costly is financial (not economic) distress? Evidence from highly leveraged transactions that became distressed, *Journal of Finance* 53, 1443–1494.

Bai, Jennie, Turan G. Bali, and Quan Wen, 2019a, Common risk factors in the cross-section of corporate bond returns, *Journal of Financial Economics* 131, 619–642.

Bai, Jennie, Robert S. Goldstein, and Fan Yang, 2019b, The leverage effect and the basket-index put spread, *Journal of Financial Economics* 131, 186–205.

Bao, Jack, and Jun Pan, 2013, Bond illiquidity and excess volatility, *Review of Financial Studies* 26, 3068–3103.

Becker, Lucas, 2014, CVA hedge losses prompt focus on swaptions and guarantees, *Risk Magazine* .

Black, Fischer, 1976, The pricing of commodity contracts, *Journal of Financial Economics* 3, 167–179.

Black, Fischer, and John C. Cox, 1976, Valuing corporate securities: Some effects of bond indentures provisions, *Journal of Finance* 31, 351–367.

Chen, Long, Pierre Collin-Dufresne, and Robert S. Goldstein, 2009, On the relation between the credit spread puzzle and the equity premium puzzle, *Review of Financial Studies* 22, 3367–3409.

Chen, Steven Shu-Hsi, Hitesh Doshi, and Sang Byung Seo, 2020, Ex ante risk in the corporate bond market: Evidence from synthetic options, Working paper, University of Houston.

Chen, Zhiwu, and Peter J. Knez, 1995, Measurement of market integration and arbitrage, *The Review of Financial Studies* 8, 287–325.

Choi, Jaewon, and Yongjun Kim, 2018, Anomalies and market (dis)integration, *Journal of Monetary Economics* 100, 16–34.

Chordia, Tarun, Amit Goyal, Yoshio Nozawa, Avanidhar Subrahmanyam, and Qing Tong, 2017, Are capital market anomalies common to equity and corporate bond markets? an empirical investigation, *Journal of Financial and Quantitative Analysis* 52, 1301–1342.

Collin-Dufresne, Pierre, Robert S. Goldstein, and J. Spencer Martin, 2001, The determinants of credit spread changes, *Journal of Finance* 56, 2177–2207.

Collin-Dufresne, Pierre, Robert S. Goldstein, and Fan Yang, 2012, On the relative pricing of long-maturity index options and collateralized debt obligations, *Journal of Finance* 67, 1983–2014.

Collin-Dufresne, Pierre, Benjamin Junge, and Anders B. Trolle, 2020, Market structure and transaction costs of index CDSs, *Journal of Finance* 75, 2719–2763.

Coval, Joshua, Jakub Jurek, and Erik Stafford, 2009, Economic catastrophe bonds, *American Economic Review* 99, 628–666.

Cremers, Martijn, Joost Driessen, and Pascal Maenhout, 2008, Explaining the level of credit spreads: Option-implied jump risk premia in a firm value model, *Review of Financial Studies* 21, 2209–2242.

Culp, Christopher L., Yoshio Nozawa, and Pietro Veronesi, 2018, Option-based credit spreads, *American Economic Review* 108, 454–488.

Das, Sanjiv R., and Rangarajan K. Sundaram, 1999, Of smiles and smirks: A term structure perspective, *Journal of Financial and Quantitative Analysis* 34, 211–239.

Davydenko, Sergei A., Ilya A. Strebulaev, and Xiaofei Zhao, 2012, A market-based study of the cost of default, *Review of Financial Studies* 25, 2959–2999.

Du, Du, Redouane Elkamhi, and Jan Ericsson, 2019, Time-varying asset volatility and the credit spread puzzle, *Journal of Finance* 74, 1841–1885.

Duarte, Jefferson, Francis A. Longstaff, and Fan Yu, 2007, Risk and return in fixed-income arbitrage: Nickels in front of a steamroller?, *Review of Financial Studies* 20, 769–811.

Fama, Eugene F., 1970, Efficient capital markets: A review of theory and empirical work, *Journal of Finance* 25, 383–417.

Foresi, Silverio, and Liuren Wu, 2005, Crash-o-phobia: A domestic fear or a worldwide concern, *Journal of Derivatives* 13, 8–21.

Friewald, Nils, and Florian Nagler, 2019, Over-the-counter market frictions and yield spread changes, *Journal of Finance* 74, 3217–3257.

Gârleanu, Nicolae, Lasse H. Pedersen, and Allen M. Poteshman, 2009, Demand-based option pricing, *Review of Financial Studies* 22, 4259–4299.

Geske, Robert, 1977, The valuation of corporate liabilities as compound options, *Journal of Financial and Quantitative Analysis* 12, 541–552.

He, Zhiguo, Paymon Khorrami, and Zhaogang Song, 2020, Commonality in credit spread changes: Dealer inventory and intermediary distress, Working paper, University of Chicago.

He, Zhiguo, and Wei Xiong, 2012, Rollover risk and credit risk, *The Journal of Finance* 67, 391–430.

Huang, Jing-Zhi, and Ming Huang, 2012, How much of the corporate-treasury yield spread is due to credit risk?, *Review of Asset Pricing Studies* 2, 153–202.

Jones, Philip E., Scott P. Mason, and Eric Rosenfeld, 1984, Contingent claims analysis of corporate capital structures: An empirical investigation, *Journal of Finance* 39, 611–25.

Kapadia, Nikunj, and Xiaoling Pu, 2012, Limited arbitrage between equity and credit markets, *Journal of Financial Economics* 105, 542–564.

Kelly, Bryan, Hanno Lustig, and Stijn Van Nieuwerburgh, 2016, Too-systemic-to-fail: What option markets imply about sector-wide government guarantees, *American Economic Review* 106, 1278–1319.

Leland, Hayne E., 1994, Optimal capital structure, endogenous bankruptcy, and the term structure of credit spreads, *Journal of Finance* 49, 1213–1252.

Merton, Robert C., 1974, On the pricing of corporate debt: The risk structure of interest rates, *Journal of Finance* 29, 449–470.

———, 1976, Option pricing when underlying stock returns are discontinuous, *Journal of Financial Economics* 3, 125–144.

Newey, Whitney K., and Kenneth D. West, 1987, A simple, positive semi-definite, heteroskedasticity and autocorrelation consistent covariance matrix, *Econometrica* 55, 703–708.

Sandulescu, Mirela, 2020, How integrated are corporate bond and stock markets? Working paper, University of Michigan.

Schaefer, Stephen M., and Ilya A. Strebulaev, 2008, Structural models of credit risk are useful: Evidence from hedge ratios on corporate bonds, *Journal of Financial Economics* 90, 1–19.

Seo, Sang Byung, and Jessica Wachter, 2018, Do rare events explain CDX tranche spreads?, *Journal of Finance* 73, 2343–2383.

Vasicek, Oldrich, 1987, Probability of loss on a loan portfolio, KMV Corporation.

	CDX	CDX options
Trades per day	202	18
Median trade size (in million USD)	50	100
Average daily volume (in million USD)	11,133	1,442
Five-year tenor (% of trades)	96.1	98.1
On-the-run series (% of trades)	88.9	94.0
Bespoke contract terms (% of trades)	1.2	8.0
Cleared (% of trades)	90.4	17.6
Block size (% of trades)	24.9	64.3
Capped trade size (% of trades)	22.3	66.5
On-SEF execution (% of trades)	83.9	3.8
Payer (% of trades)	—	63.1

Table 1: Descriptive statistics for CDX and CDX option trades

The table shows descriptive statistics for CDX and CDX option trades. Tenor is the initial time to expiration of the CDX contract (the underlying CDX contract in case of CDX options). The on-the-run series is the most recently launched CDX contract. A trade is block-sized if the notional amount traded exceeds a certain minimum block size. Typically, reported trade sizes are capped when the notional amount traded exceeds USD 100 million or USD 110 million. The sample period is from December 31, 2012 to April 30, 2020. The sample comprises 371,693 CDX trades and 32,669 CDX option trades.

	Days to expiration						
Moneyness	< 15	15–44	45–74	75–104	105–134	≥ 135	Total
$m < -1.5$	0.20	0.24	0.06	0.01	0.00	0.00	0.52
$-1.5 \leq m < -0.5$	0.94	3.99	2.94	1.62	0.54	0.39	10.42
$\lvert m \rvert \leq 0.5$	2.12	15.28	9.61	6.48	2.27	1.28	37.03
$0.5 < m \leq 1.5$	1.53	9.01	10.34	8.75	4.17	2.30	36.10
$m > 1.5$	1.42	5.96	4.45	2.65	0.97	0.47	15.92
Total	6.21	34.47	27.40	19.51	7.95	4.45	

Table 2: Distribution of trading volume across the volatility surface

The table shows the percentage of CDX option volume across the volatility surface. Moneyness is defined as $m = \log(K/F(\tau))/(\sigma\sqrt{\tau})$, where K is the strike, $F(\tau)$ is the front-end-protected τ-forward spread, σ is at-the-money implied volatility, and $\tau = d/365$ is time to expiration, and d is days to expiration. The underlying of all options is the five-year on-the-run index. The sample period is from December 31, 2012 to April 30, 2020. The sample comprises 28,409 CDX option trades.

	Data		Model	
Panel A: Full sample				
	$\Delta log(CDX)$	$\Delta\beta_0^{CDX}$	$\Delta log(CDX)$	$\Delta\beta_0^{CDX}$
$\Delta\beta_0^{CDX}$	0.675		0.517	
	[0.620,0.724]		[0.444,0.584]	
$\Delta\beta_1^{CDX}$	0.255	0.397	0.037	0.286
	[0.164,0.342]	[0.313,0.474]	[-0.058,0.132]	[0.196,0.371]
	$\Delta log(SPX)$	$\Delta\beta_0^{SPX}$	$\Delta log(SPX)$	$\Delta\beta_0^{SPX}$
$\Delta\beta_0^{SPX}$	-0.881		-0.851	
	[-0.901,-0.858]		[-0.875,-0.822]	
$\Delta\beta_1^{SPX}$	0.765	-0.897	0.676	-0.870
	[0.722,0.801]	[-0.914,-0.876]	[0.620,0.724]	[-0.891,-0.845]
Panel B: Ex-Covid-19 sample				
	Data		Model	
	$\Delta log(CDX)$	$\Delta\beta_0^{CDX}$	$\Delta log(CDX)$	$\Delta\beta_0^{CDX}$
$\Delta\beta_0^{CDX}$	0.615		0.525	
	[0.550,0.672]		[0.451,0.592]	
$\Delta\beta_1^{CDX}$	0.243	0.525	-0.031	0.309
	[0.150,0.333]	[0.451,0.592]	[-0.128,0.066]	[0.219,0.395]
	$\Delta log(SPX)$	$\Delta\beta_0^{SPX}$	$\Delta log(SPX)$	$\Delta\beta_0^{SPX}$
$\Delta\beta_0^{SPX}$	-0.858		-0.838	
	[-0.881,-0.830]		[-0.864,-0.806]	
$\Delta\beta_1^{SPX}$	0.681	-0.836	0.689	-0.873
	[0.625,0.730]	[-0.863,-0.804]	[0.634,0.737]	[-0.894,-0.848]

Table 3: Within-market correlations

The top part of each panel shows correlations between weekly changes in the log CDX spread ($\Delta log(CDX)$), CDX volatility ($\Delta\beta_0^{CDX}$), and CDX skewness ($\Delta\beta_1^{CDX}$). The bottom part of each panel shows correlations between weekly SPX returns ($\Delta log(SPX)$) and changes in the SPX volatility ($\Delta\beta_0^{SPX}$) and SPX skewness ($\Delta\beta_1^{SPX}$). Correlations to the left ("Data") are computed from the data. Correlations to the right ("Model") are computed from the fitted data using the benchmark specification of the model in Section 4. 95% confidence intervals are given in brackets. The full sample period is February 29, 2012 to April 29, 2020 (426 weekly observations). The ex-Covid-19 sample period is February 29, 2012 to December 31, 2019 (409 weekly observations).

	Data	Model
Panel A: Full sample		
$\Delta log(CDX), \Delta log(SPX)$	-0.802	-0.802
	[-0.834,-0.766]	[-0.834,-0.766]
$\Delta\beta_0^{CDX}, \Delta\beta_0^{SPX}$	0.749	0.873
	[0.704,0.788]	[0.848,0.894]
$\Delta\beta_1^{CDX}, \Delta\beta_1^{SPX}$	-0.368	-0.380
	[-0.448,-0.283]	[-0.459,-0.296]
Panel B: Ex-Covid-19 sample		
$\Delta log(CDX), \Delta log(SPX)$	-0.786	-0.786
	[-0.821,-0.746]	[-0.821,-0.746]
$\Delta\beta_0^{CDX}, \Delta\beta_0^{SPX}$	0.679	0.930
	[0.623,0.728]	[0.916,0.942]
$\Delta\beta_1^{CDX}, \Delta\beta_1^{SPX}$	-0.372	-0.462
	[-0.453,-0.286]	[-0.535,-0.382]

Table 4: Cross-market correlations

Each panel shows correlations between weekly SPX returns ($\Delta log(SPX)$) and log CDX spread changes ($\Delta log(CDX)$), between weekly changes in SPX and CDX volatility ($\Delta\beta_0^{SPX}$ and $\Delta\beta_0^{CDX}$), and between weekly changes in SPX and CDX skewness ($\Delta\beta_1^{SPX}$ and $\Delta\beta_1^{CDX}$). Correlations to the left ("Data") are computed from the data. Correlations to the right ("Model") are computed from the fitted data using the benchmark specification of the model in Section 4. 95% confidence intervals are given in brackets. The full sample period is February 29, 2012 to April 29, 2020 (426 weekly observations). The ex-Covid-19 sample period is February 29, 2012 to December 31, 2019 (409 weekly observations).

	A_0	D_1/A_0	D_2/A_0	δ	σ	ρ	λ	m	$\sqrt{v}$	λ_i
Main	2893.8	0.0339	0.2279	0.0149	0.3405	0.0526	0.9531	-0.0875	0.0770	0.0032
	(408.8)	(0.0026)	(0.0132)	(0.0023)	(0.0150)	(0.0158)	(0.8756)	(0.0231)	(0.0164)	(0.0017)
$\alpha = 0.5$	2899.2	0.0339	0.2274	0.0149	0.3096	0.0608	0.9676	-0.0864	0.0764	0.0026
	(409.1)	(0.0025)	(0.0132)	(0.0023)	(0.0154)	(0.0192)	(0.8807)	(0.0228)	(0.0162)	(0.0014)
$\lambda_i = 0$	2894.5	0.0339	0.2278	0.0149	0.3580	0.0436	0.9832	-0.0877	0.0767	0
	(408.8)	(0.0026)	(0.0132)	(0.0023)	(0.0122)	(0.0128)	(0.8648)	(0.0223)	(0.0160)	
$\lambda = \lambda_i = 0$	2894.6	0.0339	0.2278	0.0149	0.3756	0.0894	0	0	0	0
	(408.8)	(0.0026)	(0.0132)	(0.0023)	(0.0112)	(0.0324)				

Table 5: Parameter estimates

For each model specification, the table reports the sample mean and sample standard deviation of the calibrated parameters. All specifications have $m_i = -2$ and $v_i = 0$. The first, third, and fourth specification have $\alpha = 0.8$. The sample period is February 29, 2012 to April 29, 2020 (426 weekly observations).

	SPX options		CDX options		1Y CDX	
	ME	RMSE	ME	RMSE	err	|err|
Main	-0.003	0.012	-0.215	0.220	0	0
$\alpha = 0.5$	-0.003	0.012	-0.186	0.193	0	0
$\lambda_i = 0$	-0.002	0.011	-0.185	0.191	-15.10	15.10
$\lambda = \lambda_i = 0$	-0.000	0.007	-0.218	0.220	-15.15	15.15

Table 6: Pricing errors

For each model specification and on each Wednesday in the sample, we compute the mean pricing error (ME) and root mean squared pricing error (RMSE) for CDX options and SPX options. Pricing errors are the differences between fitted and actual implied volatilities. The table reports sample means of the resulting ME and RMSE time series. For the specifications $\lambda_i = 0$ and $\lambda = \lambda_i = 0$, the 1Y CDX is not fitted perfectly, and the table reports sample means of the pricing error (difference between fitted and actual quoted spread) and absolute pricing error. For the specification $\lambda = \lambda_i = 0$, the MEs and RMSEs are computed for ATM options only. The sample period is February 29, 2012 to April 29, 2020 (426 weekly observations).

	CDX options				SPX options				CDX vs. SPX options			
	M1	M2	M3	EW	M1	M2	M3	EW	M1	M2	M3	EW
Panel A: Full sample												
Mean	0.122	0.154	0.189	0.155	0.052	0.073	0.069	0.064	0.035	0.041	0.060	0.045
t-stat	3.125	3.842	4.742	4.208	1.514	2.052	1.919	1.880	1.865	2.153	3.167	2.623
Std.dev.	0.100	0.100	0.100	0.089	0.100	0.100	0.100	0.098	0.057	0.057	0.057	0.052
SR	1.217	1.539	1.888	1.744	0.515	0.726	0.692	0.659	0.613	0.710	1.051	0.877
Skewness	-2.051	-2.378	-1.493	-2.219	-2.497	-2.277	-2.101	-2.285	-0.236	0.069	0.205	0.142
Kurtosis	14.167	19.322	19.149	17.586	17.593	16.775	15.177	16.125	9.008	10.395	12.045	9.772
Panel B: Ex-Covid-19 sample												
Mean	0.157	0.206	0.238	0.200	0.081	0.119	0.125	0.108	0.038	0.043	0.057	0.046
t-stat	4.105	5.344	6.276	5.757	2.418	3.481	3.635	3.269	1.932	2.163	2.815	2.539
Std.dev.	0.100	0.100	0.100	0.087	0.100	0.100	0.100	0.098	0.059	0.059	0.059	0.053
SR	1.568	2.055	2.383	2.291	0.811	1.187	1.248	1.106	0.647	0.731	0.963	0.868
Skewness	-1.802	-1.781	-1.122	-1.717	-2.598	-2.285	-1.980	-2.314	-0.327	0.020	0.175	0.072
Kurtosis	12.718	14.466	19.333	14.476	19.176	18.696	15.770	17.950	9.399	10.810	12.372	10.226

Table 7: Summary statistics of trading strategies

In each market and for each option maturity category, the strategy sells closest-to-ATM straddles each trading day with a holding period of one day. We assume that the strategy requires an initial amount of capital proportional to the option premium, and we adjust the proportionality factor to achieve a 10% unconditional annualized volatility of realized excess returns for each option maturity. "EW" denotes an equally weighted portfolio of the three option maturities. "CDX vs. SPX options" denotes a short-long strategy that allocates 50% of funds to selling CDX straddles and 50% to buying SPX straddles. Means, standard deviations, and Sharpe ratios ("SR") are annualized. t-statistics are corrected for heteroscedasticity and serial correlation up to four lags using the approach of Newey and West (1987). The full sample consists of 1881 daily returns between February 28, 2012 and April 30, 2020. The ex-Covid-19 sample consists of 1801 daily returns between February 28, 2012 and December 31, 2019.

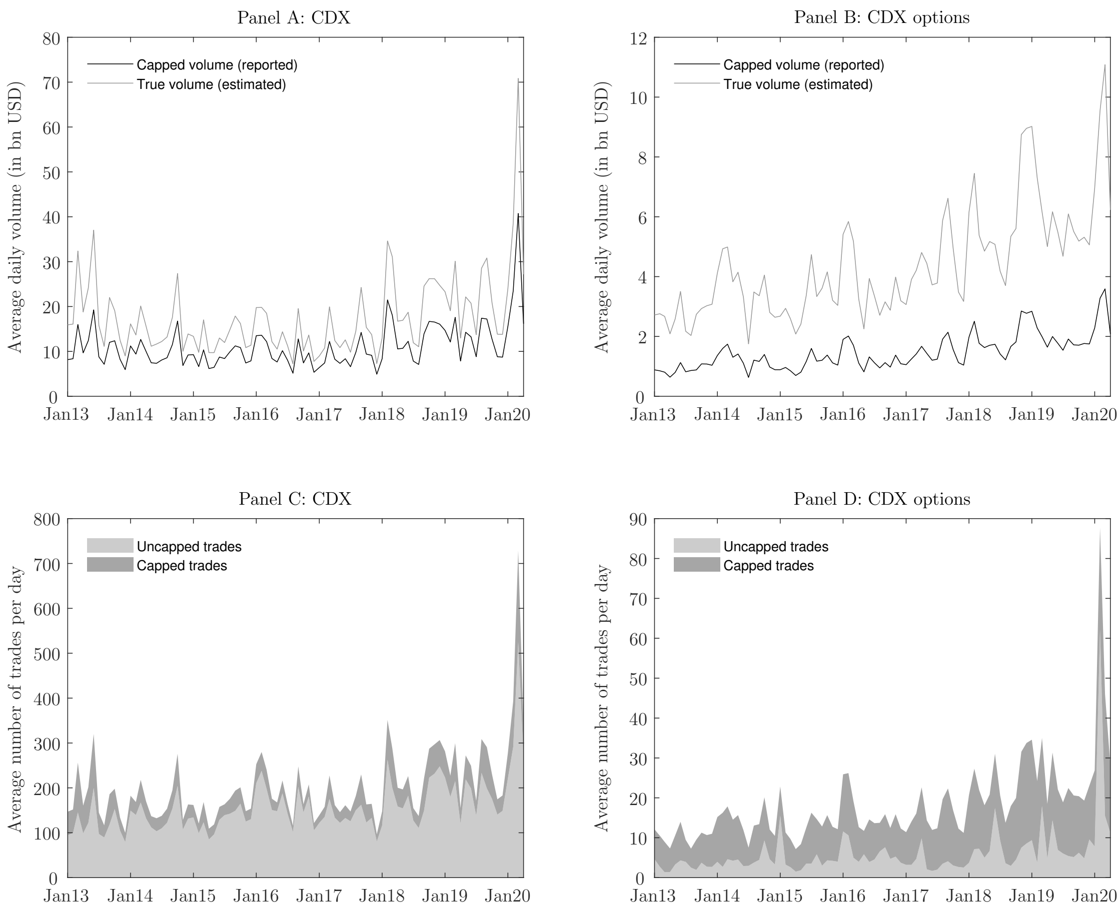

Figure 1: Trading activity for CDX and CDX options

Panels A and B show the average daily trading volume for CDX and CDX options. Panels C and D show the average number of trades per day for CDX and CDX options. Daily market activity reports from the GFI SEF are used to compute the average amount by which the actual notionals of capped trades on the GFI SEF exceed the reported notionals. This is done separately for CDX and CDX options (see Footnote 18 for details). The estimated true volume in Panels A and B is obtained by adding the average amount to the reported notionals for all capped trades. The frequency of observations is monthly. The sample period is December 31, 2012 to April 30, 2020 (88 observations).

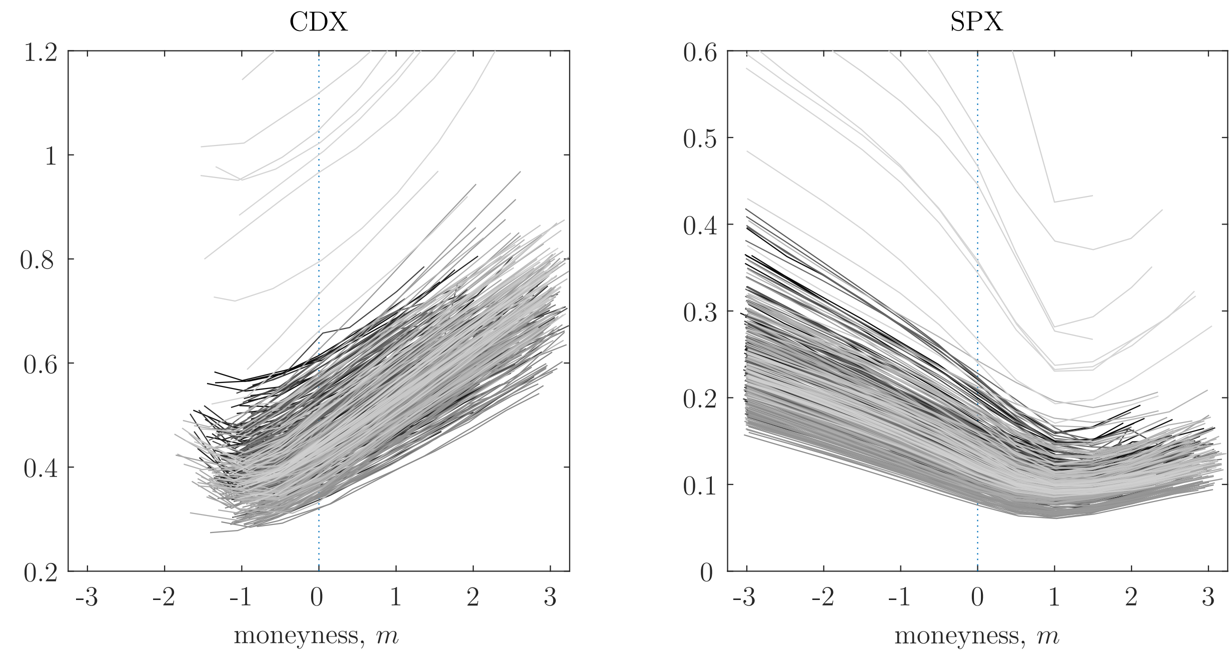

Figure 2: CDX and SPX implied volatility smiles

The figure shows weekly (Wednesday) two-month implied volatility smiles for CDX and SPX. CDX data is displayed in the left panel and SPX data is displayed in the right panel. Moneyness is defined as $m = \log(K/F(\tau))/(\sigma\sqrt{\tau})$, where K is the strike, $F(\tau)$ is the forward (front-end-protected) spread in case of CDX options and the forward price in case of SPX options), σ is the at-the-money implied volatility, and τ is the maturity. Sample period is from February 29, 2012 until April 29, 2020 (426 observations).

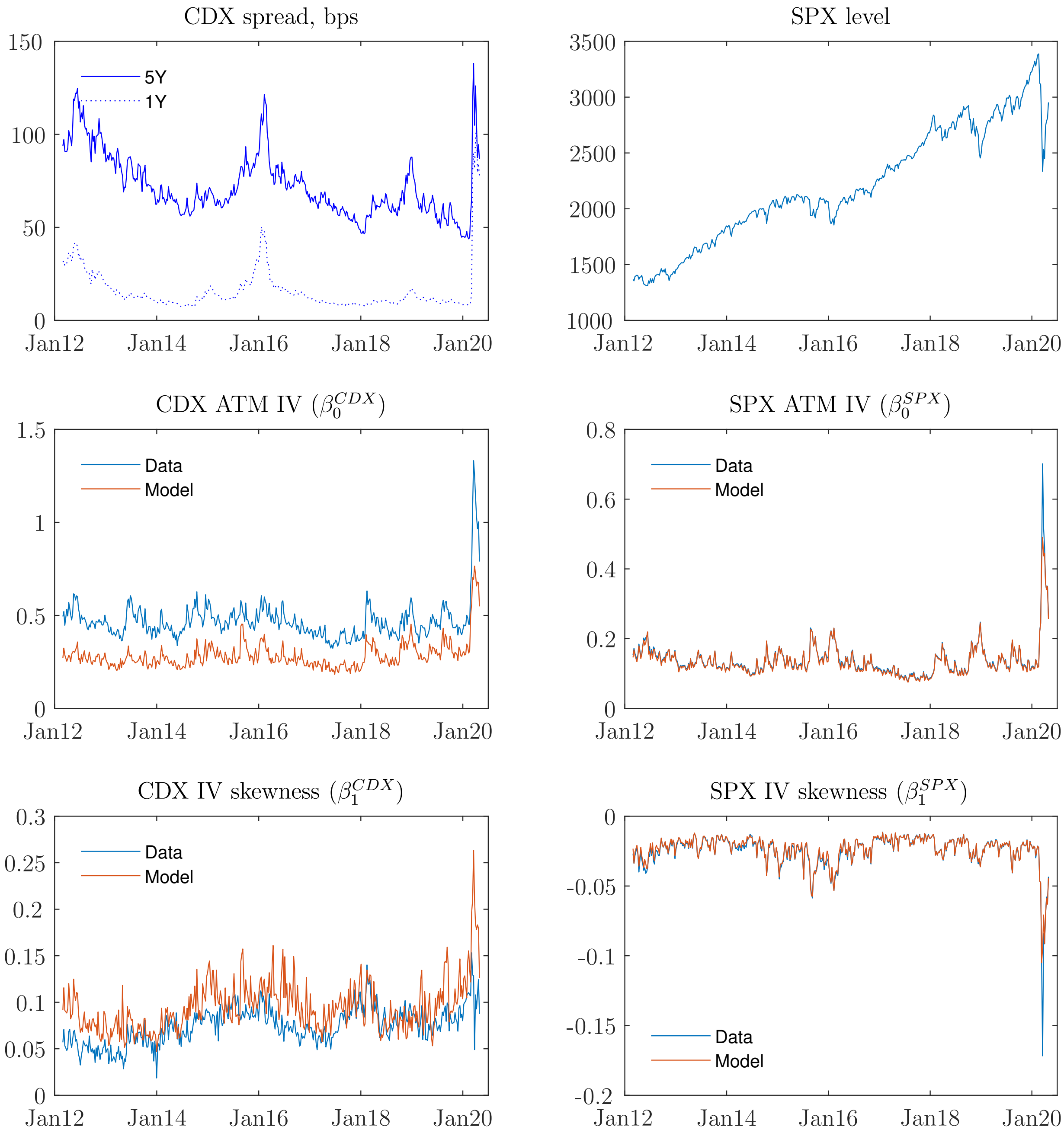

Figure 3: Summary of CDX and SPX options markets

The top left (right) panel shows time series of the CDX spread (SPX level). The middle left (right) panel shows time series of the at-the-money CDX (SPX) implied volatility proxied by β_0. The bottom left (right) panel shows time series of the skewness of the CDX (SPX) implied volatility smile proxied by β_1. Weekly data from February 29, 2012 until April 29, 2020 (426 observations).

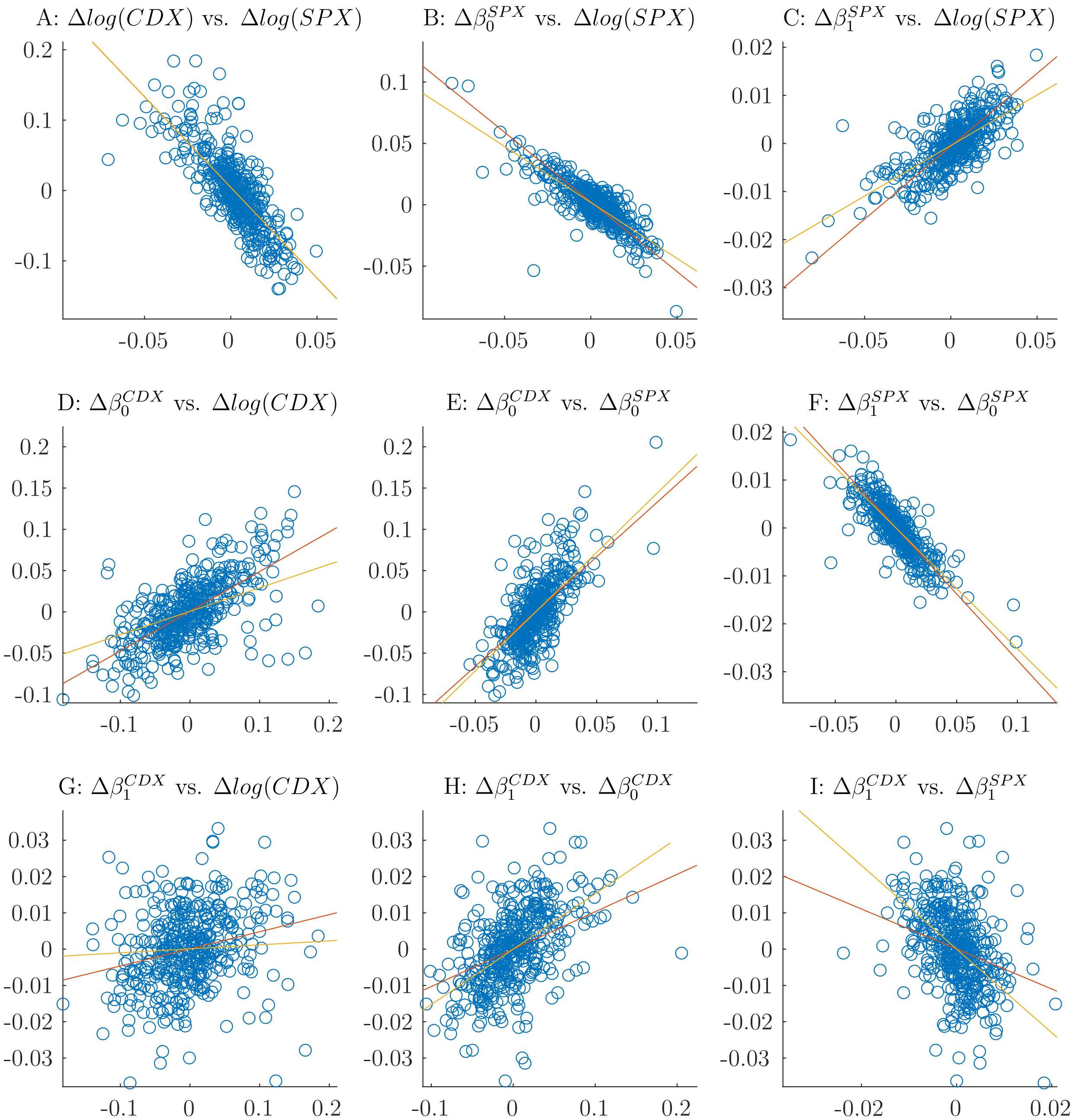

Figure 4: Within- and cross-market interactions

The scatterplots along the diagonal show the cross-market interactions: Weekly log CDX spread changes ($\Delta log(CDX)$) vs. SPX returns ($\Delta log(SPX)$) in Panel A; weekly CDX volatility changes ($\Delta\beta_0^{CDX}$) vs. SPX volatility changes ($\Delta\beta_0^{SPX}$) in Panel E; and weekly CDX skewness changes ($\Delta\beta_1^{CDX}$) vs. SPX skewness changes ($\Delta\beta_1^{SPX}$) in Panel I. Scatterplots below the diagonal show the CDX-market interactions: Weekly CDX volatility changes vs. log CDX spread changes in Panel D; weekly CDX skewness changes vs. log CDX spread changes in Panel G; and weekly CDX skewness changes vs. CDX volatility changes in Panel H. Scatterplots above the diagonal show the SPX-market interactions: Weekly SPX volatility changes vs. SPX returns in Panel B; weekly SPX skewness changes vs. SPX returns in Panel C; and weekly SPX skewness changes vs. SPX volatility changes in Panel F. We only display observations that fall within the 0.5th and 99.5th percentile of the univariate distributions. The red (yellow) lines show the fits of linear regressions applied to the data (fitted data using the benchmark specification of the model in Section 4). The sample period is February 29, 2012 to April 29, 2020 (426 weekly observations).

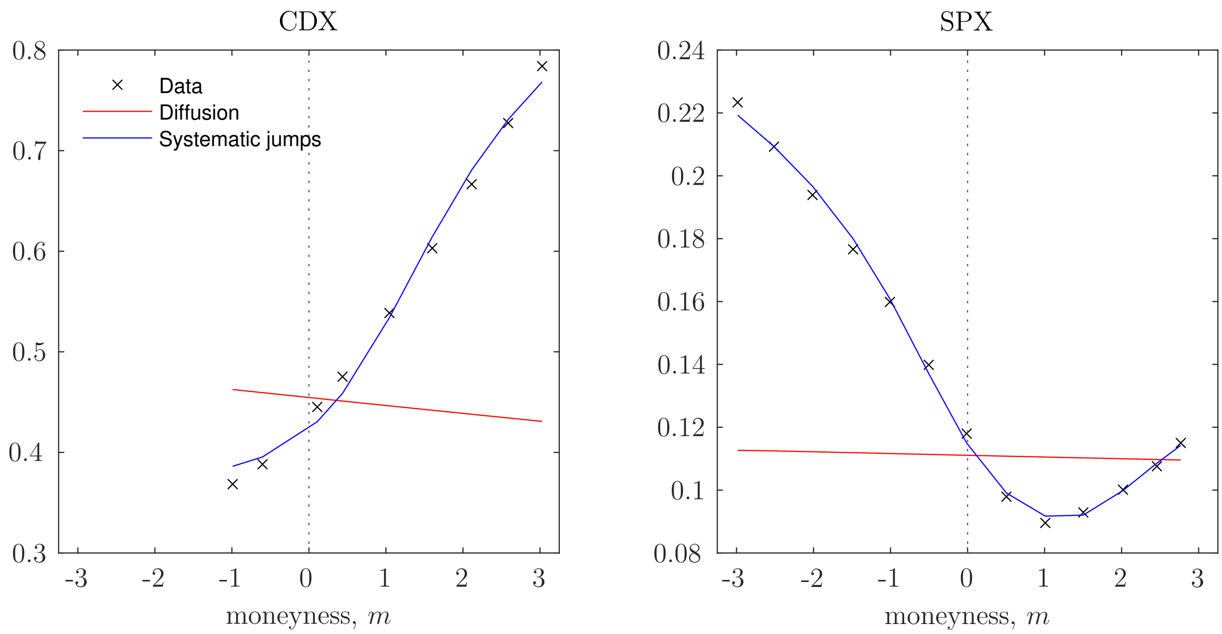

Figure 5: In-sample fit to CDX and SPX implied volatility smiles

The figure shows actual and fitted two-month implied volatility smiles for CDX and SPX on December 31, 2019. CDX data is displayed in the left panel and SPX data is displayed in the right panel. Moneyness is defined as $m = \log(K/F(\tau))/(\sigma\sqrt{\tau})$, where K is the strike, $F(\tau)$ is the forward (front-end-protected) spread in case of CDX options and the forward price in case of SPX options), σ is the at-the-money implied volatility, and τ is the option maturity. Crosses show data. The red lines show the implied volatility curves in the pure-diffusion version of the model. The blue lines show the curves when adding systematic jumps.

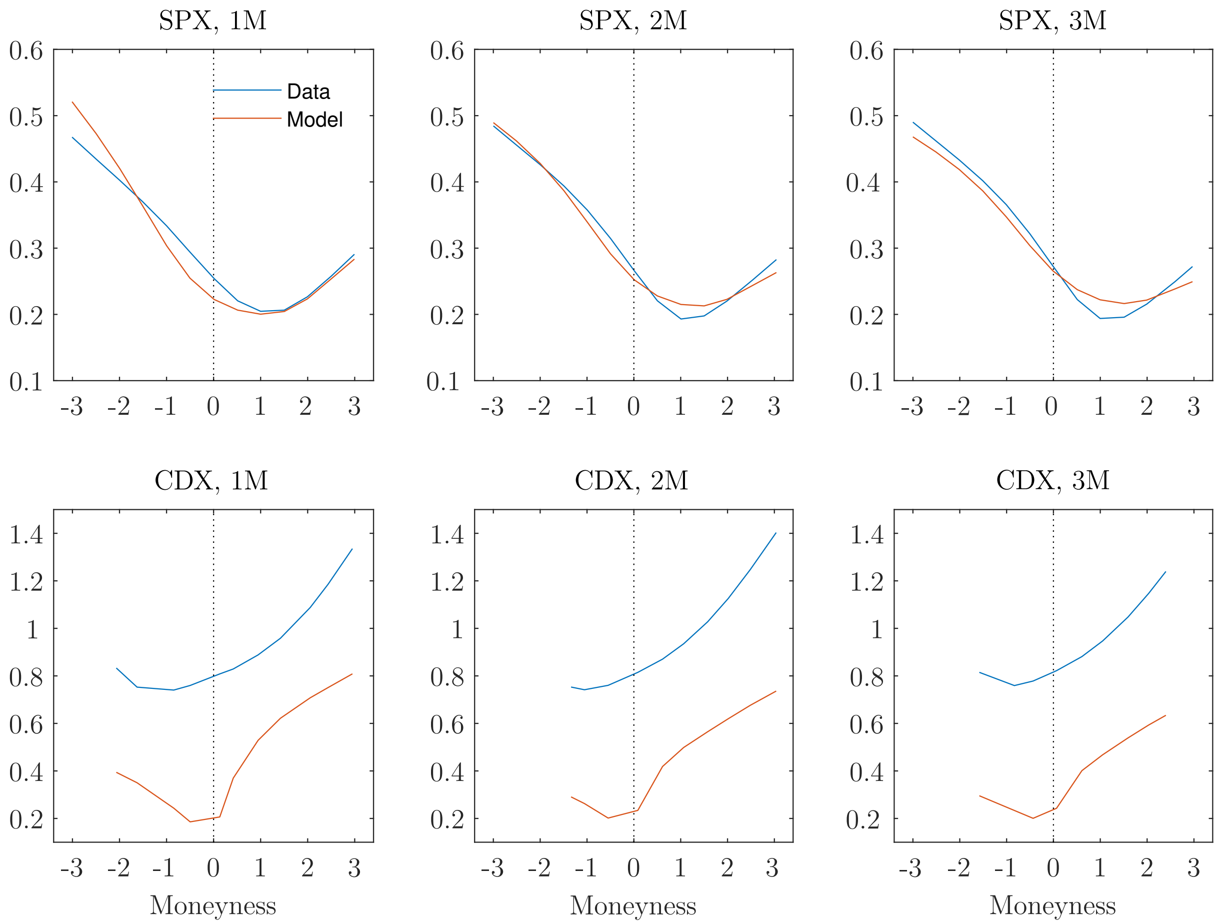

Figure 6: Fit to SPX and CDX implied volatility smiles on last Wednesday in sample

First row shows the fit to 1M, 2M, and 3M SPX implied volatility smiles on April 29, 2020. Second row shows the fit to 1M, 2M, and 3M CDX implied volatility smiles.

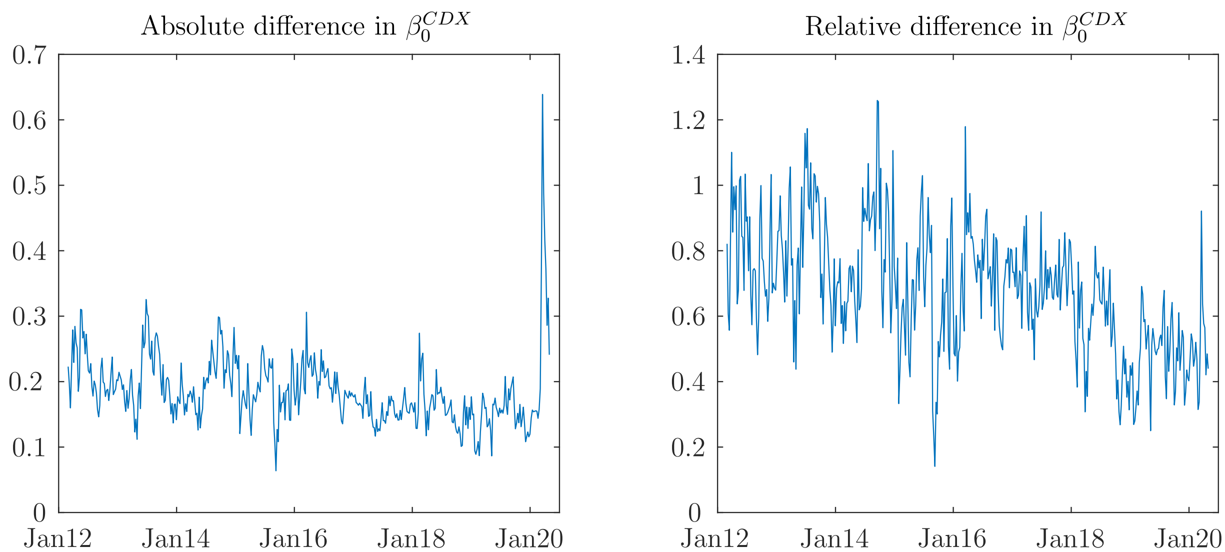

Figure 7: Time series of CDX option pricing errors

The left (right) panel shows the time series of the difference (relative difference) between β_0^{CDX} inferred from the data and the fitted data. Weekly data from February 29, 2012 until April 29, 2020 (426 observations).

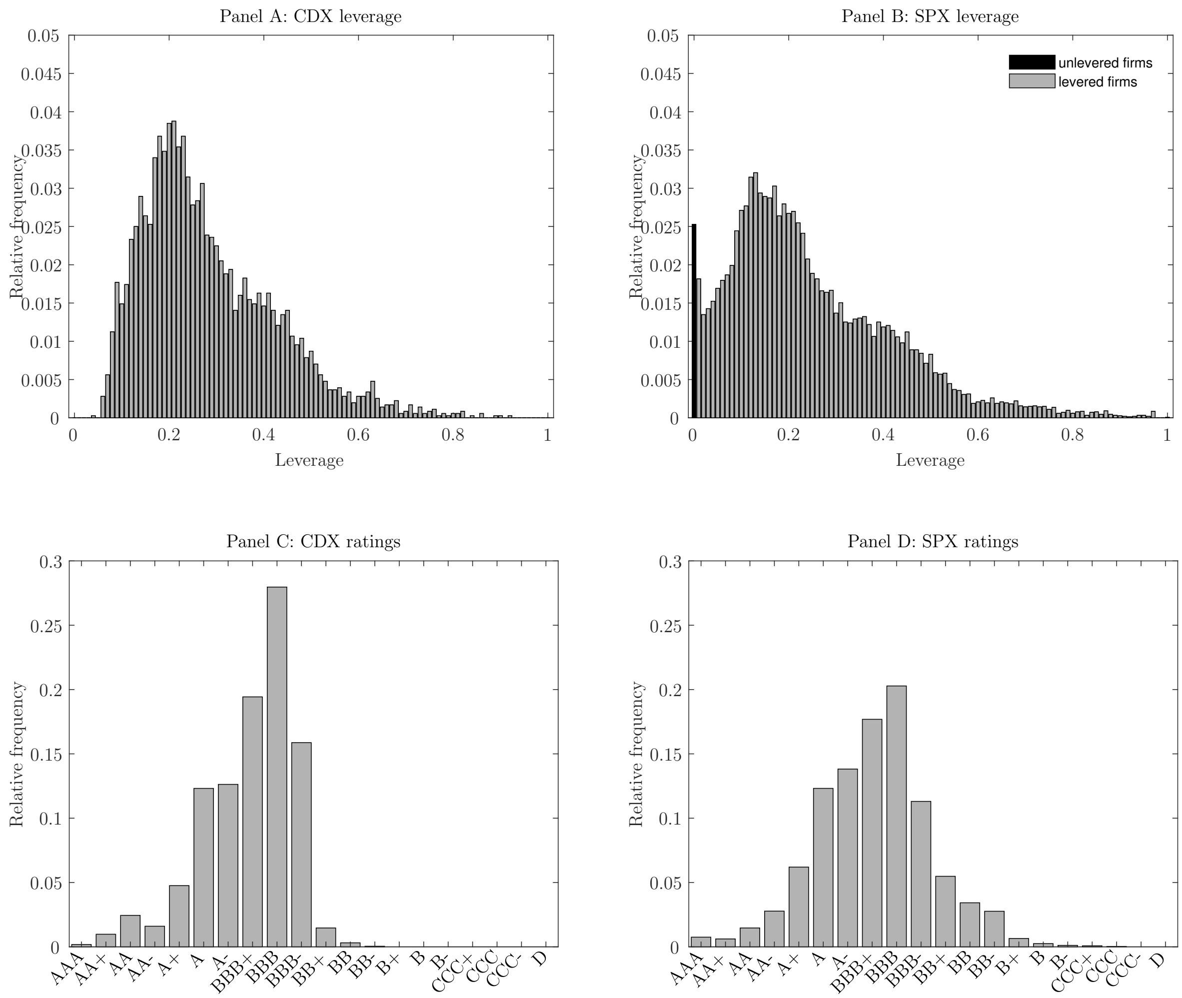

Figure 8: Distributions of leverage and ratings across index constituents
Panels A and B show the distribution of firm-quarter leverage observations for the constituents of the CDX and SPX, respectively, between the first quarter of 2012 and the first quarter of 2020. Leverage is defined as book value of debt over the sum of book value of debt and market value of equity. Panels C and D show the distribution of firm-quarter rating observations for the constituents of the CDX and SPX, respectively, between the first quarter of 2012 and the third quarter of 2017.

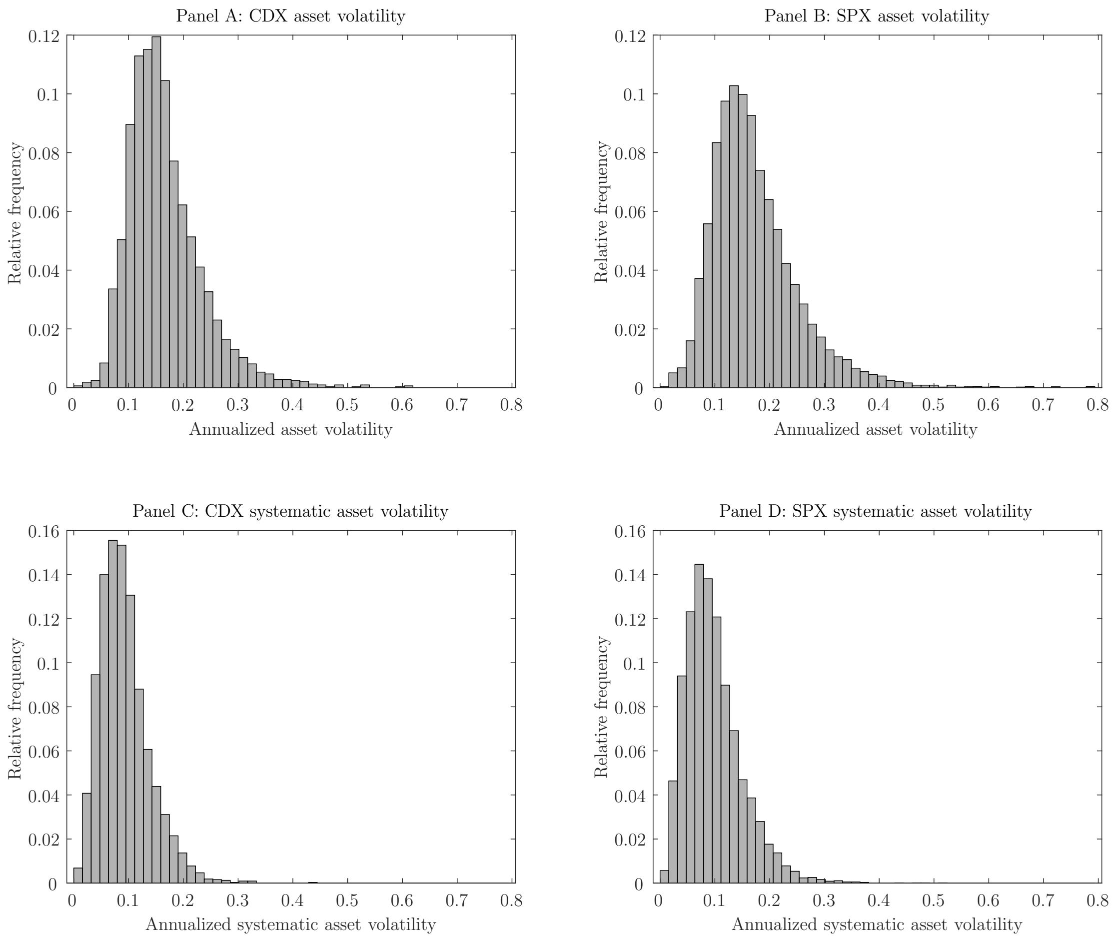

Figure 9: Distributions of asset volatility across index constituents

Panels A and B (C and D) show the distribution of firm-quarter total (systematic) asset return volatility for the constituents of the CDX and SPX, respectively. Asset returns are computed using daily data from January 3, 2012 until December 31, 2019.

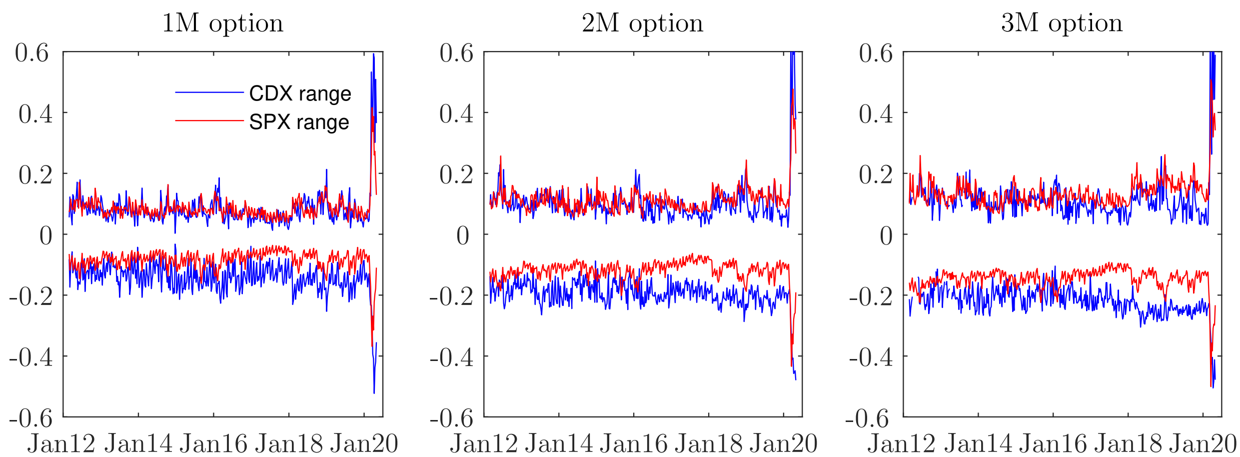

Figure 10: Range of economic states spanned by options

The figure shows $\frac{A^{min}-A^{fwd}}{A^{fwd}}$ and $\frac{A^{max}-A^{fwd}}{A^{fwd}}$ for CDX and SPX options. A^{fwd} is the forward value of the common factor. For CDX options, A^{min} solves $U_{T_0}(A^{min}) = K^{max}$ and A^{max} solves $U_{T_0}(A^{max}) = K^{min}$. For SPX options, A^{min} solves $S_{T_0}(A^{min}) = K^{min}$ and A^{max} solves $S_{T_0}(A^{max}) = K^{max}$. The sample period is February 29, 2012 to April 29, 2020 (426 weekly observations).

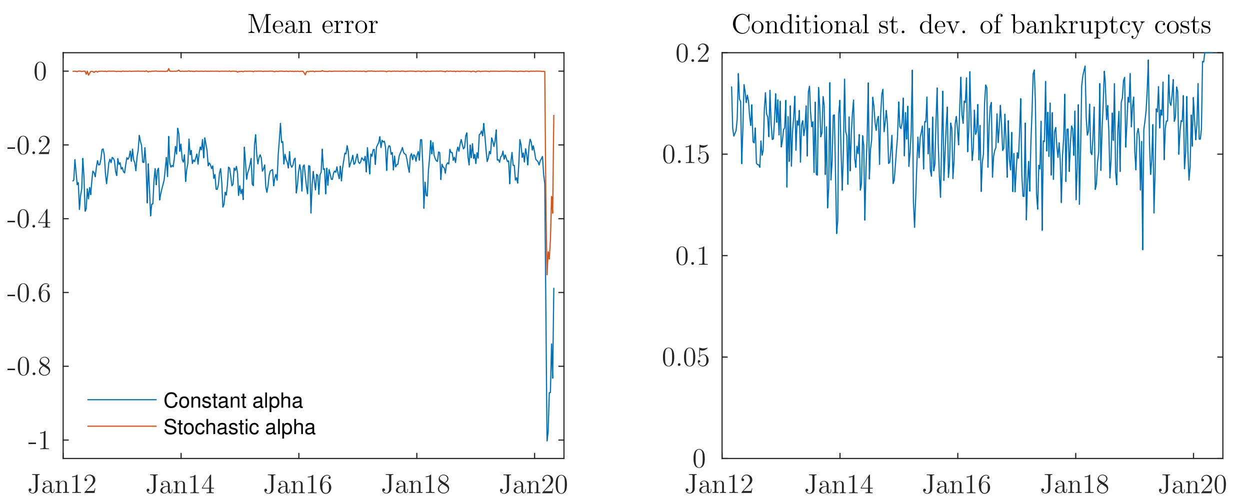

Figure 11: Fit to CDX options for stochastic alpha model

For each model specification (constant bankruptcy costs with $\alpha = 0.8$ and stochastic bankruptcy costs with expected $\alpha = 0.8$) and on each Wednesday in the sample, we compute the mean error for ATM CDX options, where the error is the difference between fitted and actual implied volatilities. The left panel shows the resulting time series. The right panel shows the three-month conditional standard deviation of bankruptcy costs in the model where costs are stochastic. The sample period is February 29, 2012 to April 29, 2020 (426 weekly observations).

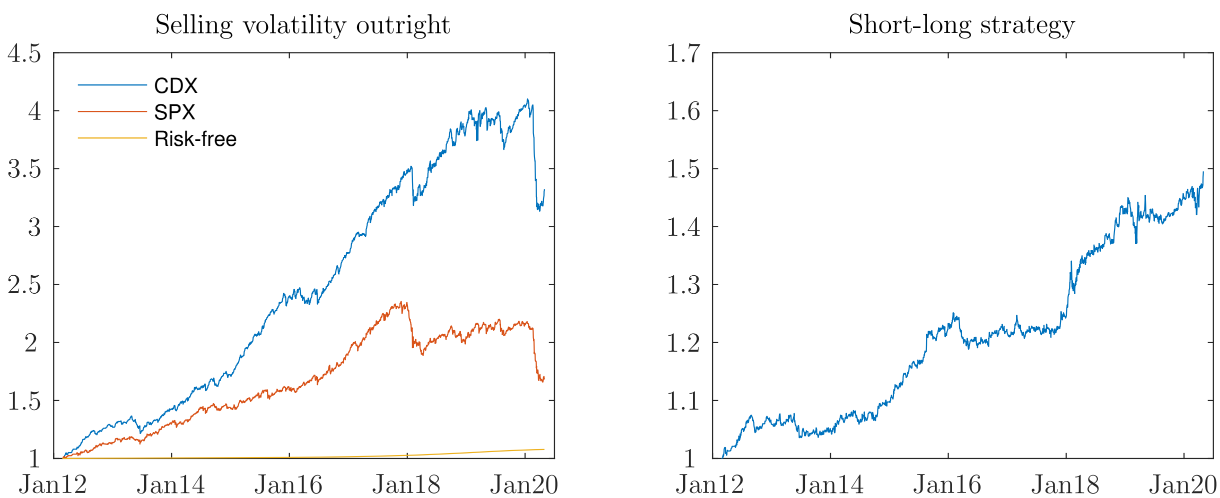

Figure 12: Cumulative performance of trading strategies

The figure shows the evolution of one dollar invested in each of the EW strategies at the beginning of the sample (see Table 7 for details on the trading strategies). The left panel shows the performance of selling CDX and SPX straddles outright. The right panel shows the performance of the short-long strategy that allocates 50% of funds to selling CDX straddles and 50% to buying SPX straddles. On those trading days where options returns on unavailable, we invest at the risk-free rate. The sample period is from February 24, 2012 to April 30, 2020 (2042 daily observations).

Internet Appendix to: How integrated are credit and equity markets? Evidence from index options

IA.1 CDX spreads and implied volatilities

This section explains how to convert upfront amounts to spreads and option prices to spread implied volatilities.

IA.1.1 CDX spread

Consider a CDX contract with $N = 125$ equally-weighted constituents, maturity T, and premium paid continuously at a rate of C. To lighten notation, we assume that the initial notional is one. The fraction of index constituents that have not defaulted at time t (which corresponds to the outstanding notional) is then given by

$$f(t) = \frac{1}{N} \sum_{i=1}^{N} \mathbf{1}_{\{\tau_i > t\}},$$

where τ_i is the default time of firm i. Similarly, the cumulative default losses between index inception and time t is given by

$$L(t) = \frac{1}{N} \sum_{i=1}^{N} \ell_i \mathbf{1}_{\{\tau_i \leq t\}},$$

where ℓ_i is the default loss of firm i.

The time-t value of the contract from the perspective of the buyer of protection is

$$V(t,T) = V^{Prot}(t,T) - C \times \mathcal{A}(t,T),$$

where $V^{Prot}(t,T)$ is the value of the protection leg given by

$$V^{Prot}(t,T) = \mathbb{E}_t \left[\int_t^T e^{-\int_t^u r(s)ds} dL(u) \right],$$

and $\mathcal{A}(t,T)$ is the risky annuity value given by

$$\mathcal{A}(t,T) = \mathbb{E}_t \left[\int_t^T e^{-\int_t^u r(s)ds} f(u) du \right].$$

Although CDX contracts are *traded* in terms of an upfront amount and a fixed coupon, they are typically *quoted* in terms of a spread, which is the size of the coupon such that the upfront amount is zero. When converting between upfront amount and spread, the market standard is to assume i) that index constituents are homogenous (i.e., identical in terms of default intensity and default loss), ii) a constant default intensity λ, iii) a loss-given-default of $(1-R)$ with a recovery rate of $R = 40\%$, and iv) that interest rates and defaults are independent.[1] With these assumptions, we have

$$\overline{V}^{Prot}(t,T) = \lambda(1-R)f(t) \int_t^T P(t,u)e^{-\lambda(u-t)} du$$

and

$$\overline{\mathcal{A}}(t,T) = f(t) \int_t^T P(t,u)e^{-\lambda(u-t)} du.$$

For a given $V(t,T)$, λ is first calibrated so that

$$V(t,T) = \overline{V}^{Prot}(t,T) - C \times \overline{\mathcal{A}}(t,T) = (\lambda(1-R) - C)\,\overline{\mathcal{A}}(t,T),$$

and the spread is then given by

$$\overline{Spr}(t,T) = \lambda(1-R).$$

Alternatively, CDX contracts can be quoted in terms of *points upfront* (PUF) which is the

[1] These are the assumptions behind the so-called the ISDA Standard Model. In the following, overlined quantities are calculated under these assumptions.

upfront amount per unit of outstanding notional. In our case, this is given by

$$U(t,T) = \frac{1}{f(t)} V(t,T).$$

IA.1.2 Forward CDX spread

Consider a CDX call option bought at time 0, with option expiry at time T_0, CDX maturity at time T, and strike in PUF terms of K^U. The option payoff is

$$\left(V(T_0,T) + (L(T_0) - L(0)) - f(0)K^U\right)^+.$$

Exercise will cost $f(0)K^U$. In return, the option-holder enters into the version of the CDX contract that prevails at time T_0 (which has a value of $V(T_0,T)$) and receives the realized default losses during the life of the option (which has a value of $L(T_0) - L(0)$). The latter feature is called *front-end protection* (FEP).

Equivalently, we can write the option payoff as

$$\left(V^{FEP}(T_0,T) - f(0)K^U\right)^+, \tag{IA1}$$

where $V^{FEP}(T_0,T)$ is the value of a front-end protected CDX contract for which the protection leg incorporates the default losses between times 0 and T_0.

At time $0 \le t < T_0$, the value of this *forward-starting* CDX contract is

$$V^{FEP}(t;T_0,T) = V^{Prot,FEP}(t;T_0,T) - C \times \mathcal{A}(t;T_0,T),$$

where

$$V^{Prot,FEP}(t;T_0,T) = \mathbb{E}_t\left[\int_{T_0}^{T} e^{-\int_t^u r(s)ds} dL(u)\right] + \mathbb{E}_t\left[e^{-\int_t^{T_0} r(s)ds}(L(T_0) - L(0))\right]$$

and

$$\mathcal{A}(t;T_0,T) = \mathbb{E}_t\left[\int_{T_0}^{T} e^{-\int_t^u r(s)ds} f(u)du\right].$$

To express this value as a spread, we use the same assumptions as above so that

$$\overline{V}^{Prot,FEP}(t;T_0,T) = \lambda(1-R)f(t)\int_{T_0}^{T} P(t,u)e^{-\lambda(u-t)}du + (1-R)P(t,T_0)\left(f(0) - f(t)e^{-\lambda(T_0-t)}\right)$$

and

$$\overline{\mathcal{A}}(t;T_0,T) = f(t)\int_{T_0}^{T} P(t,u)e^{-\lambda(u-t)}du.$$

For a given $V^{FEP}(t;T_0,T)$ (obtained via put-call parity, see Section IA.2 in the Internet Appendix for details), λ is first calibrated so that

$$V^{FEP}(t;T_0,T) = \overline{V}^{Prot,FEP}(t;T_0,T) - C \times \overline{\mathcal{A}}(t;T_0,T),$$

and the front-end protected forward spread is then given by

$$\overline{Spr}^{FEP}(t;T_0,T) = \frac{\overline{V}^{Prot,FEP}(t;T_0,T)}{\overline{\mathcal{A}}(t;T_0,T)}. \tag{IA2}$$

IA.1.3 Spread implied volatilities

For the purpose of expressing option prices as implied volatilities, we write the option payoff (IA1) in spread terms as

$$\left(\left(\overline{Spr}^{FEP}(T_0,T) - C\right)\overline{\mathcal{A}}(T_0,T) - f(0)K^U\right)^+ = \left(\overline{Spr}^{FEP}(T_0,T) - K^{Spr}\right)^+\overline{\mathcal{A}}(T_0,T),$$

where

$$K^{Spr} = \frac{f(0)K^U}{\overline{\mathcal{A}}(T_0,T)} + C.$$

is the strike in spread terms. K^{Spr} is itself stochastic and to get a strike known at $0 \leq t < T_0$ we replace $\overline{\mathcal{A}}(T_0, T)$ with its time-t forward value, $\frac{1}{P(t,T_0)}\overline{\mathcal{A}}(t; T_0, T)$, to get

$$K^{Spr} \approx \frac{f(0)K^U P(t, T_0)}{\overline{\mathcal{A}}(t; T_0, T)} + C. \tag{IA3}$$

This is the equation we will use to convert between strikes in upfront terms and spread terms.[2]

The CDX call option price is given by

$$\begin{aligned} C(t; T_0, T, K) &= \mathbb{E}_t \left[e^{-\int_t^{T_0} r(s)ds} \left(\overline{Spr}^{FEP}(T_0, T) - K^{Spr} \right)^+ \overline{\mathcal{A}}(T_0, T) \right] \\ &= \overline{\mathcal{A}}(t; T_0, T) \tilde{\mathbb{E}}_t \left[\left(\overline{Spr}^{FEP}(T_0, T) - K^{Spr} \right)^+ \right], \end{aligned}$$

where $\tilde{\mathbb{E}}_t[\cdot]$ denotes expectation taken with respect to the annuity measure that has $\overline{\mathcal{A}}(t; T_0, T)$ as numeraire.[3] The forward spread (IA2) is a martingale under the annuity measure and—assuming that it follows a driftless geometric Brownian motion—we get a Black (1976)-type option price formula. This allows us to express option prices as log-normal spread implied volatilities.[4]

IA.2 Markit credit option data

This section describes Markit's credit option data and the cleaning and data processing procedures we employ.

[2]Clearly, the conversion is exact for $K^U = 0$.

[3]A technical issue arises if all the index constituents were to default prior to option expiry; see, e.g., Morini and Brigo (2011). However, the risk of this is negligible given realistic spreads and short option maturities.

[4]Pedersen (2003) presents an alternative model that can be used to back out log-normal spread implied volatilities. That model must be solved numerically, but avoids the strike approximation (IA3). As shown by White (2014), the two models generate very similar implied volatilities.

IA.2.1 Data description

As part of its credit option data, Markit records pricing information for European options on the CDX North American Investment Grade (hereafter, CDX) index. Each record uniquely identifies the CDX option contracts it refers to by specifying the underlying CDX contract as well as the strike price and maturity of the options.[5] The underlying CDX contract is identified by the index's series and version numbers and the contract tenor, i.e., the time to maturity with which the contract was initially launched. The option maturity is identified by the month and the year in which the option expires. The option strike is not given directly in terms of the points upfront (PUF) used for settlement, see (IA1). Instead, the strike is given in terms of a spread. At option maturity, this spread is converted to PUF using the ISDA Standard Model along with the prevailing discount curve.[6] Because of interest rate uncertainty, the strike in terms of PUF is, strictly speaking, not known before option expiry. However, interest rate uncertainty is second-order in our context; therefore, at any point in time prior to option expiry, we convert the strike from spread to PUF by assuming that the discount curve at expiry coincides with the prevailing forward curve.

The pricing information consists of bid and offer composite quotes and the corresponding quote mid-points. Quotes are relative to a so-called reference level because CDX options are conventionally traded with "with delta", i.e., together with a delta hedge in the underlying CDX contract. The quoted spread at which the delta hedge will be executed is called the reference level. The amount that will be executed is a percentage of the option's notional amount and specified via a quoted delta.[7] Both the reference level and the delta are con-

[5] Records contain pricing information for payer and receiver options with the same strike price and maturity.

[6] The zero curve used by the ISDA Standard Model is constructed from LIBOR money market rates (for maturities up to one year) and swap rates (for longer maturities). Specifically, it uses 1M, 2M, 3M, 6M, and 1Y USD LIBOR rates (before June 3, 2013 the 9M rate was used as well) and annual USD LIBOR swap rates from the 2Y maturity onwards (with quarterly floating leg payments and semi-annual fixed leg payments). For details, see the interest rate curve specifications on the homepage of the ISDA CDS Standard Model.

[7] The quoted delta actually is the percentage of the option's notional that will be executed for hedging purposes and therefore it is not necessarily equal to the option's delta. In particular, it is positive for both payer and receiver options.

ventionally quoted along with the option's bid and offer prices. The composite quotes are averages over the most recent quotes that market-making credit derivatives dealers contribute for a given reference level prior to 5:30 p.m. New York time. Both the reference level and averages of the quoted payer and receiver deltas are recorded in addition to the composite quotes.

The pricing information also contains the number of dealers who contribute quotes to the calculation of the composite and the number of unique quotes that dealers contributed throughout the trading day. In this context unique means that the quote count does not increase if a dealer repeatedly contributes the same quote for a given reference level.

Markit made some changes to the reporting format of the credit option data since they initially offered the data. Specifically, data coverage expanded to options for which Markit does not observe dealer quotes on a given date and instead uses a proprietary pricing model to determine option prices. These records are flagged as "estimated" in the data and we disregard them entirely. We only use "observed" records that are based on actual dealer quotes and collected in the same way as described above.[8]

IA.2.2 Data cleaning

The raw data comprise 301,673 records for CDX options. We remove 150 duplicate records. Where necessary, we determine the option expiry date as the third Wednesday of the month that corresponds to the expiry-month-expiry-year tuple specified in the raw data, and we remove one record with quote date after the determined expiry date. We also remove three records with negative bid-ask spreads and 73 records with quote dates that do not fall on a

[8]There are minor changes to the reporting format such as expiry dates being recorded instead of the month and year in which the option expires. The records also provide additional information that was not available in the original reporting format such as front-end protected forward prices and spreads. We prefer to determine front-end protected forward spreads ourselves (see next section) to have a consistent set of data throughout. Our data comprises of records in the original reporting format for the period up to and including September 11, 2017. Thereafter, all records are in the new reporting format.

weekday. Finally, we remove 176 records that do not specify the strike price of the options.

IA.2.3 Data processing

The remaining 301,270 records are grouped into 22,296 option strips. Each strip of options is characterized by the underlying CDX contract, the options' expiry date, and the reference level at which the options are quoted on a given day.[9] Formally, on a given day and for a given underlying CDX contract, expiry date, and reference level, a strip comprises of a set of strikes, $\Sigma_C = \{K_{C,1}, K_{C,2}, \ldots, K_{C,m}\}$, at which payer options are quoted and a set of strikes, $\Sigma_P = \{K_{P,1}, K_{P,2}, \ldots, K_{P,n}\}$, at which receiver options are quoted.

To compute the spread implied volatilities of the options in a strip, we need the value of the underlying forward-starting front-end protected CDX contract. This value is not directly observable. However, it can be inferred via put-call parity. Specifically, it is backed out from that part of the strip's strike grid on which both payer and receiver options are quoted, which is denoted by $\Sigma = \Sigma_C \cap \Sigma_P$. If $\Sigma = \emptyset$, there is no strike at which both payer and receiver options are quoted and we discard the option strip, which is the case for three strips. On the other hand, if $\Sigma \neq \emptyset$, there is at least one strike at which payer and receiver options are quoted and we proceed as follows.

Let $C(t; T_0, T, K^U)$ and $P(t; T_0, T, K^U)$ denote the time-t mid-quotes of payer and receiver options, respectively, with expiry at T_0 and PUF strike K^U on the current CDX version. Then, put-call parity asserts that

$$C(t; T_0, T, K^U) - P(t; T_0, T, K^U) = V^{FEP}(t; T_0, T) - D(t, T_0) f(t) K^U,$$

[9] Often, there are several reference levels for the same option expiry. In this case, we take that reference level whose strip length is longest (i.e., the one with the largest number of strikes). Should that not result in a unique match then we consider the number of quotes (we select the reference level with the largest number of quotes), the number of quoting dealers (again selecting the reference level that is quoted by the largest number of dealers), and the average spread across the options (selecting the reference level that is quoted with the tightest spread).

where $D(t, T_0)$ is the discount factor for date T_0, and $V^{FEP}(t; T_0, T)$ is the time-t value of the T_0-starting front-end protected CDX contract. Therefore, V^{FEP} can be inferred as the constant term in the following linear regression across all strikes in Σ:

$$C(t; T_0, T, K_n^U) - P(t; T_0, T, K_n^U) = \alpha + \beta D(t, T_0) f(t) K_n^U + \epsilon_n, \qquad K_n^U \in \Sigma. \tag{IA4}$$

If $N = |\Sigma| > 1$, we estimate the regression in Equation (IA4) by least-squares and remove 13 strips for which $R^2 < 98.5\%$. For the remaining strips, we re-estimate the regression in Equation (IA4) imposing the restriction $\beta = -1$, in which case the least-square estimate of V^{FEP} is given by

$$\widehat{V}^{FEP} = \frac{1}{N} \sum_{n=1}^{N} \left\{ C(t; T_0, T, K_n^U) - P(t; T_0, T, K_n^U) + D(t, T_0) f(t) K_n^U \right\}.$$

Then, we proceed to compute the corresponding front-end protected forward spread (as described in Section IA.1.2) and the spread implied volatilities for all the options in the strip (as described in Section IA.1.3).

Finally, we drop all records for options on off-the-run index series, leaving us with 282,861 records for 20,794 option strips.

IA.3 Details on option quotes

Figure IA1 shows time series of the CDX option maturities (in calendar days) that are quoted. The time series are color-coded according to the option expiry grid (recall that options expire on the third Wednesday of each month), so that the blue line at the bottom of the figure shows the first maturity on the expiry grid (i.e., the options that expire on the first third Wednesday following the observation date), the red line above the blue line shows the second maturity on the expiry grid, etc. The time series are broken whenever there are no option quotes for a given maturity.

Clearly, the range of quoted maturities increases over the sample period. This is consistent with the growing trading volume in CDX options (Figure 1).

The left panels in Figure IA2 show time series of the M1, M2, and M3 CDX option maturities (in calendar days). The right panels in Figure IA2 show time series of the maturity difference (in calendar days) between the M1, M2, and M3 CDX options and the maturity-matched SPX options.

The left (right) panels in Figure IA3 show time series of the range of moneyness spanned by CDX (SPX) options.

The left (right) panels in Figure IA4 show time series of the relative bid-ask spreads of at-the-money CDX (SPX) options. Unfortunately, there is a period in 2017 and 2018, when bid and ask prices are missing from the Markit data.

IA.4 Additional cross-market correlations

In the paper, we focus on three key cross-market correlations. Table IA.1 complements Table 4 in the paper by showing the remaining six cross-market correlations. Among these, the highest correlation is between CDX spread changes and SPX volatility changes (0.710). Figure IA6 illustrates all nine cross-market interactions for the full sample.[10]

IA.5 Understanding the pure-diffusion model credit skew

In the paper (Figure 5) we show that the implied credit skew has a negative slope in case of the pure-diffusion version of the model. To understand this result, we first look at the model-implied instantaneous forward CDX spread volatility. Next, we prove analytically that the slope of the credit (and equity) skew is negative in the special case where i) the underlying

[10]Note that the scatterplots along the diagonal are identical to those in Figure 4 in the paper.

model is the classic Merton (1974) model, ii) the CDS is paid in full-upfront (i.e., with no periodic coupon payments), and iii) the credit implied volatility is expressed in full-upfront (rather than spread) terms.

IA.5.1 The instantaneous forward CDX spread volatility skew

We first compute the instantaneous volatility of the forward CDX spread, when its value equals the different option strikes.[11] The left panel in Figure IA7 displays both the CDX implied volatility curve (the solid red line) and the instantaneous volatility curve (the dashed red line). The instantaneous volatility curve is downward sloping; in other words, the correlation between the level of CDX spread and its instantaneous volatility is negative. This negative correlation explains the negative slope of the implied volatility curve.[12]

IA.5.2 Credit and equity option skews in the diffusion-based Merton model

We now prove analytically that the classic diffusion-based Merton (1974) model generates a negative implied volatility skew for both credit and equity options.

Recall that in this model the equity value equals the price of a European call option written on the underlying asset value A_t with strike equal to the outstanding debt notional D and maturity T. Let's denote this price by $C(A_t, t)$. It follows from risk-neutral pricing and Itô's lemma that

$$\frac{dC}{C} = rdt + \sigma_C(A_t, t)dZ_t,$$

where $\sigma_C(A, t) = \frac{C_A A \sigma}{C}$ and σ is the volatility of the underlying asset value. Now, as is well-

[11] For instance, the most OTM put (call) option has a moneyness of $m = -0.99$ ($m = 3.03$), which corresponds to a strike of 39 bps (75 bps). For the forward CDX spread to equal this value, the asset value must be $A_0 = 4487.9$ ($A_0 = 3610.8$) at which level the instantaneous volatility of the forward CDX spread is 0.481 (0.407).

[12] The implied volatility curve is less steep than the instantaneous volatility curve because implied variance is approximately equal to the integral of the instantaneous variance along the path of the underlying that joins its initial value to the strike price at expiration, see Gatheral (2006).

known, the sign of the option implied volatility skew will be determined by the sign of the correlation between the underlying and its variance. Specifically, the implied volatility skew will be negatively (positively) sloped if the covariance of $\frac{dC}{C}$ and $d\sigma_C^2$ is negative (positive). In the present model, we have

$$\rho_C = \frac{1}{dt} Cov\left(\frac{dC}{C}, d\sigma_C^2\right) = 2\sigma_C^2 \frac{\partial \sigma_C}{\partial A} \sigma A.$$

Thus, we have

$$\text{sign}(\rho_C) = \text{sign}\left(\frac{\partial \sigma_C}{\partial A}\right) = \text{sign}\left(\frac{\partial \frac{C_A A}{C}}{\partial A}\right) = -\text{sign}\left(\frac{\partial \frac{C}{C_A A}}{\partial A}\right).$$

Now, by homogeneity we have $C = AC_A + DC_D$. It follows that

$$\frac{\sigma}{\sigma_C} = \frac{C}{AC_A} = 1 + \frac{DC_D}{AC_A} = 1 - \frac{De^{-rT}N(d_2)}{AN(d_1)}.$$

We can then compute

$$\frac{\partial \frac{C}{AC_A}}{\partial A} = \frac{De^{-rT}}{A^2 N(d_1)^2 \sigma\sqrt{T}} \left(n(d_1)N(d_2) + N(d_1)N(d_2)\sigma\sqrt{T} - N(d_1)n(d_2)\right).$$

The sign of the expression is that of the function

$$f_s(x) = n(x+s)N(x) + N(x+s)N(x)s - N(x+s)n(x), \tag{IA5}$$

for the positive constant $s = \sigma\sqrt{T}$ and for $x = d_2$. Note in particular that $\lim_{x\to-\infty} f_s(x) = 0$, $\lim_{x\to+\infty} f_s(x) = s > 0$. Thus, if we can show that $f_s'(x) > 0$ this suffices to establish that $f_s(x) > 0 \ \forall x$. We find that $f_s'(x) = N(x+s)n(x)(x+s) - N(x)n(x+s)x = n(x)n(x+s)(\frac{N(x+s)(x+s)}{n(x+s)} - \frac{N(x)x}{n(x)})$. Since $g(x) = \frac{N(x)x}{n(x)}$ is an increasing function, it follows that $f_s'(x) >$

0.[13]

We have established:

Lemma 1. $\frac{\partial \sigma_C}{\partial A} < 0$ *and thus* $\rho_C < 0$.

It follows that when A drops (because of a negative shock $dZ < 0$), the value of the call (i.e., the equity value) decreases, but its variance increases generating the negative equity implied volatility skew.

Turning to the credit side, we assume for analytical purposes that the CDS is paid in full-upfront (so that the underlying of a CDS option is the full-upfront CDS price) and we study the slope of the implied volatility skew expressed in full-upfront terms.[14] In the Merton setting, the CDS value equals the price of a European put option on A_t with strike D and maturity T. Let's denote this price by $P(A_t, t)$. Its risk-neutral dynamics are

$$\frac{dP}{P} = rdt + \sigma_P(A_t, t)dZ_t,$$

where $\sigma_P(A, t) = \frac{P_A A \sigma}{P}$. Similar to before, the credit-option implied volatility skew will be negatively (positively) sloped if the covariance of $\frac{dP}{P}$ and $d\sigma_P^2$ is negative (positive). In the present model, we have

$$\rho_P = \frac{1}{dt} Cov\left(\frac{dP}{P}, d\sigma_P^2\right) = 2\sigma_P^2 \frac{\partial \sigma_P}{\partial A} \sigma A.$$

Thus,

$$\text{sign}(\rho_P) = \text{sign}\left(\frac{\partial \sigma_P}{\partial A}\right) = \text{sign}\left(\frac{\partial \frac{P_A A}{P}}{\partial A}\right) = -\text{sign}\left(\frac{\partial \frac{P}{P_A A}}{\partial A}\right).$$

[13] It can be shown that $g'(x) = \frac{\int_{-\infty}^{x} (x-y)^2 n(y) dy}{n(x)} > 0$.

[14] Instead, and to be consistent with the market convention, in the paper we present implied credit-spread volatilities, where the upfront-to-spread conversion is done using a standard reduced-form model as described in Section IA.1 of the Internet Appendix.

Now, by homogeneity we have $P = AP_A + DP_D$. It follows that

$$\frac{\sigma}{\sigma_P} = \frac{P}{AP_A} = 1 + \frac{DP_D}{AP_A} = 1 - \frac{De^{-rT}N(-d_2)}{AN(-d_1)}$$

We can then compute

$$\frac{\partial \frac{P}{AP_A}}{\partial A} = \frac{De^{-rT}}{A^2 N(-d_1)^2 \sigma\sqrt{T}} \Big(N(-d_1)N(-d_2)\sigma\sqrt{T} + n(-d_2)N(-d_1) - n(-d_1)N(-d_2) \Big) .$$

We see that the sign of the right-hand side is that of the function $f_s(x)$ defined in equation (IA5) above with $x = -d_1$. It follows then immediately from our previous analysis that:

Lemma 2. $\frac{\partial \sigma_P}{\partial A} < 0$ *and thus* $\rho_P < 0$.

Thus, when A drops (because of a negative shock $dZ < 0$), and since $\sigma_P < 0$, the value the put (i.e., the CDS value) increases, but its variance decreases generating a negative credit implied volatility skew.

Combining both lemmas, we see that the classic Merton diffusion framework generates the same (negative) slope for the equity and credit implied volatility skew, contrary to what is observed in the data.

IA.6 Computation of leverage

We distinguish between short-term debt maturing within one year and long-term debt maturing later than one year. For each index constituent, we compute "short-term leverage" as book value of short-term debt relative to the sum of market value of equity and book value of total debt and "long-term leverage" as book value of long-term debt relative to the sum of market value of equity and book value of total debt. We use quarterly Compustat data, where the book values of short-term and long-term debt are items $DLCQ$ and $DLTTQ$, respectively, and market value of equity equals shares outstanding (item $CSHOQ$) times share price (item $PRCCQ$). Leverage ratios for CDX and SPX are obtained by averaging the leverage ratios of the index constituents, and the final leverage ratios used in calibration are obtained by averaging the leverage ratios across the two indexes.

Figure 8 in the paper shows the distributions of leverage across index constituents. Figure IA8 goes one step further and shows the distributions of short- and long-term leverage across index constituents. Panels A and B show the distribution of firm-quarter short-term leverage observations for the CDX and SPX constituents, respectively. Panels C and D do the same for long-term leverage. On average, short- and long-term leverage is similar across the two indexes. The mean (median) short-term leverage is 0.033 and 0.034 (0.021 and 0.015) for the CDX and SPX, respectively, while the mean (median) long-term leverage is 0.244 and 0.204 (0.220 and 0.175) for the CDX and SPX, respectively.

IA.7 Details on calibration

We partition the parameters into two sets,

$$\Theta_1 = \{A_0, D_1, D_2, \delta, \sigma, \lambda_i\}$$

and

$$\Theta_2 = \{\rho, \lambda, m, v\},$$

where Θ_2 determines the amount of systematic risk in the asset process. The optimization procedure has two "layers". In the outer layer, we search for the Θ_2 that minimizes the sum of squared pricing errors for SPX options. In the inner layer, for each Θ_2-guess, we solve for the Θ_1 that achieves an exact match to the 1Y and 5Y CDX, the SPX level, the SPX dividend yield, and the index leverage ratios.

Ideally, we would want to express option pricing errors in terms of implied volatilities. However, this is not practical because computing implied volatilities from prices requires a numerical inversion for each option, which adds an extra layer of complexity to the calibration procedure. Instead, we fit to option prices scaled by their option vegas computed from the Black-type formula described in Section IA.1.3. This converts option pricing errors in terms of prices into option pricing errors in terms of implied volatilities via a linear approximation.

Finally, implementing the pricing formulas in our model involve a couple of numerical choices: The summations in the pricing formulas are truncated at the 0.9999 percentile of the associated Poisson distributions. The bivariate and trivariate normal cumulative distribution functions are computed using the `bvnl.m` and `tvnls.m` Matlab functions developed by Alan Genz.

IA.8 Option pricing with heterogeneity in leverage

In the paper, we assume that firms are ex-ante identical. In this section, we investigate the effect of heterogeneity in leverage on the relative valuation of CDX and SPX options. Figure IA9 shows time series of the mean, standard deviation, and skewness of the distribution of long-term leverage for SPX constituents. Consistent with Panel D in Figure IA8, the leverage distribution is consistently positively skewed. The time-series averages of the mean, standard deviation, and skewness are 0.204, 0.143, and 0.887, respectively. We focus on the impact of this "average" degree of heterogeneity.

IA.8.1 Homogeneous benchmark

As benchmark, we use the homogeneous model. We assume a flat term structure with $r = 0.02$, and set $T_0 = 0.25$, $T_1 = 1$, and $T_2 = 5$. We set parameter values for A_0, δ, σ, ρ,

λ, m, v, and λ_i to those reported in Table 5. We search for D_1 and D_2 so that we match the time-series average of SPX leverage ratios in short-term ($lev_1 = 0.034$) and long-term ($lev_2 = 0.204$). The resulting values are $D_1 = 101.0$ and $D_2 = 605.5$. We compute SPX (2259.0), index dividend yield (0.019), and CDX upfront values for 1Y (-85.7 bps) and 5Y (-195.8 bps),[15] We also compute SPX option prices for a wide range of strikes (m between -3 and 3).

IA.8.2 Heterogenous model

Next, we consider a model that allows for heterogeneity in leverage. Specifically, along the lines of Bai, Goldstein, and Yang (2019b), we assume that there are two types of firms, L and H, that are ex-ante identical except in terms of their long-term leverage, lev_2^L and lev_2^H (type L being the low-leverage firms). A fraction w of index constituents are of type L, while the remaining fraction $1 - w$ are of type H.

As a first step, we search for w, lev_2^L, and lev_2^H so that we match the time-series averages of the first three moments of the distribution of long-term leverage for SPX constituents. The solution is $w = 0.703$, $lev_2^L = 0.111$, and $lev_2^H = 0.424$. The two types of firms are assumed to have the same short-term leverage so that $lev_1^L = lev_1^H = 0.034$.

Next, we calibrate the parameters of the heterogeneous model to the values implied by the homogeneous model, only now we have four debt parameters, D_1^L, D_2^L, D_1^H, and D_2^H,

[15] The corresponding 1Y and 5Y CDX spreads are 13.3 bps and 57.9 bps, respectively.

and four leverage targets

$$
\begin{aligned}
lev_1^L &= \frac{D_1^L}{S_0^{i,L} + D_1^L + D_2^L} \\
lev_2^L &= \frac{D_2^L}{S_0^{i,L} + D_1^L + D_2^L} \\
lev_1^H &= \frac{D_1^H}{S_0^{i,H} + D_1^H + D_2^H} \\
lev_2^H &= \frac{D_2^H}{S_0^{i,H} + D_1^H + D_2^H}.
\end{aligned}
$$

Specifically, we match exactly the 1Y and 5Y CDX, the SPX level, the SPX dividend yield, and the leverage ratios, and minimize the sum of squared pricing errors for SPX options. This way we ensure that the two models (the homogenous and the heterogenous) match the same set of statistics.

Note that equity and CDS values for type L and H firms are obtained with the pricing formulas in the paper, and that the SPX and CDX values are given by

$$
\begin{aligned}
S_0(A_0) &= wS_0^{i,L}(A_0) + (1-w)S_0^{i,H}(A_0) \\
U_0(A_0) &= wU_0^{i,L}(A_0) + (1-w)U_0^{i,H}(A_0).
\end{aligned}
$$

The pricing formula for SPX options is given below.

The resulting parameters for the heterogeneous model are $A_0 = 2895.5$, $\delta = 0.0149$, $\sigma = 0.2771$, $\rho = 0.0807$, $\lambda = 0.9426$, $m = -0.0892$, $\sqrt{v} = 0.0779$, $\lambda_i = 0.0040$, $D_1^L = 99.8$, $D_2^L = 325.5$, $D_1^H = 105.6$, and $D_2^H = 1314.4$. The model has an almost perfect fit to SPX options (RMSE of 0.000037).[16]

Finally, we compare prices for CDX options (the pricing formula for CDX options in the heterogeneous model is given below). The heterogeneous model generates somewhat lower

[16] The equity value and 1Y and 5Y CDS spreads for the low-leverage (high-leverage) firm are 2504.5 (1678.9), 6.2 (30.2) bps, and 10.5 (177.7) bps, respectively.

CDX option prices than the benchmark model across the entire moneyness spectrum. In terms of implied volatilities, the difference between the two models increases with moneyness. This is evident from Figure IA10 which shows the implied volatility smiles for the two models. For the ATM CDX option, the implied volatility drops from 29.7% in the benchmarket model to 28.2% in the heterogenous model. The upshot is that the sort of heterogeneity in leverage that we observe in the data tends to exacerbate the valuation puzzle.

IA.8.3 Pricing formulas for index options

The index upfront amount, conditional on the common factor A_{T_0}, is given by

$$
\begin{aligned}
U_{T_0}(A_{T_0}) &= w\mathbb{E}[U_{T_0}^{i,L}|A_{T_0}] + (1-w)\mathbb{E}[U_{T_0}^{i,H}|A_{T_0}] \\
&= we^{-r(T_1-T_0)}\Big((1+C_1)\mathbb{E}[\mathbf{1}_{\left\{A^i_{T_1}<\Phi^L\right\}} \mid A_{T_0}] - \frac{\alpha}{D_1^L + D_2^L}\mathbb{E}[A^i_{T_1}\mathbf{1}_{\left\{A^i_{T_1}<\Phi^L\right\}} \mid A_{T_0}]\Big) \\
&\quad + we^{-r(T_2-T_0)}\Big(\mathbb{E}[\mathbf{1}_{\left\{A^i_{T_1}\geq\Phi^L, A^i_{T_2}<D_2^L\right\}} \mid A_{T_0}] - \frac{\alpha}{D_2^L}\mathbb{E}[A^i_{T_2}\mathbf{1}_{\left\{A^i_{T_1}\geq\Phi^L, A^i_{T_2}<D_2^L\right\}} \mid A_{T_0}]\Big) \\
&\quad + (1-w)e^{-r(T_1-T_0)}\Big((1+C_1)\mathbb{E}[\mathbf{1}_{\left\{A^i_{T_1}<\Phi^H\right\}} \mid A_{T_0}] - \frac{\alpha}{D_1^H + D_2^H}\mathbb{E}[A^i_{T_1}\mathbf{1}_{\left\{A^i_{T_1}<\Phi^H\right\}} \mid A_{T_0}]\Big) \\
&\quad + (1-w)e^{-r(T_2-T_0)}\Big(\mathbb{E}[\mathbf{1}_{\left\{A^i_{T_1}\geq\Phi^H, A^i_{T_2}<D_2^H\right\}} \mid A_{T_0}] - \frac{\alpha}{D_2^H}\mathbb{E}[A^i_{T_2}\mathbf{1}_{\left\{A^i_{T_1}\geq\Phi^H, A^i_{T_2}<D_2^H\right\}} \mid A_{T_0}]\Big) \\
&\quad - C_0 - C_1 e^{-r(T_1-T_0)}.
\end{aligned}
$$

Therefore, the time-0 value of a CDX call option with strike K and expiration at T_0 is

$$
\begin{aligned}
C_0^{CDX} &= e^{-rT_0}\mathbb{E}_0[\max(U_{T_0}(A_{T_0}) - K, 0)] \\
&= we^{-rT_1}\Big((1+C_1)\mathbb{E}_0[\mathbf{1}_{\{A_{T_0}<\overline{A}, A^i_{T_1}<\Phi^L\}}] - \frac{\alpha}{D_1^L + D_2^L}\mathbb{E}_0[A^i_{T_1}\mathbf{1}_{\{A_{T_0}<\overline{A}, A^i_{T_1}<\Phi^L\}}]\Big) \\
&\quad + we^{-rT_2}\Big(\mathbb{E}_0[\mathbf{1}_{\{A_{T_0}<\overline{A}, A^i_{T_1}\geq\Phi^L, A^i_{T_2}<D_2^L\}}] - \frac{\alpha}{D_2^L}\mathbb{E}_0[A^i_{T_2}\mathbf{1}_{\{A_{T_0}<\overline{A}, A^i_{T_1}\geq\Phi^L, A^i_{T_2}<D_2^L\}}]\Big) \\
&\quad + (1-w)e^{-rT_1}\Big((1+C_1)\mathbb{E}_0[\mathbf{1}_{\{A_{T_0}<\overline{A}, A^i_{T_1}<\Phi^H\}}] - \frac{\alpha}{D_1^H + D_2^H}\mathbb{E}_0[A^i_{T_1}\mathbf{1}_{\{A_{T_0}<\overline{A}, A^i_{T_1}<\Phi^H\}}]\Big) \\
&\quad + (1-w)e^{-rT_2}\Big(\mathbb{E}_0[\mathbf{1}_{\{A_{T_0}<\overline{A}, A^i_{T_1}\geq\Phi^H, A^i_{T_2}<D_2^H\}}] - \frac{\alpha}{D_2^H}\mathbb{E}_0[A^i_{T_2}\mathbf{1}_{\{A_{T_0}<\overline{A}, A^i_{T_1}\geq\Phi^H, A^i_{T_2}<D_2^H\}}]\Big) \\
&\quad - e^{-rT_0}\tilde{K}\mathbb{E}_0[\mathbf{1}_{\{A_{T_0}<\overline{A}\}}],
\end{aligned}
$$

where

$$\tilde{K} = K + C_0 + C_1 e^{-r(T_1-T_0)}$$

and $\overline{A}$ is the unique value such that $U_{T_0}(\overline{A}) = K$ and we use the fact that $U_T(A)$ is decreasing in A.

The value of the SPX, conditional on the common factor A_{T_0}, is given by

$$
\begin{aligned}
S_{T_0}(A_{T_0}) &= w\mathbb{E}[S^{i,L}_{T_0}|A_{T_0}] + (1-w)\mathbb{E}[S^{i,H}_{T_0}|A_{T_0}] \\
&= A_{T_0} - we^{-r(T_1-T_0)}\Big(D_1^L\mathbb{E}[\mathbf{1}_{\{A^i_{T_1}\geq\Phi^L\}} \mid A_{T_0}] + \mathbb{E}[A^i_{T_1}\mathbf{1}_{\{A^i_{T_1}<\Phi^L\}} \mid A_{T_0}]\Big) \\
&\quad - we^{-r(T_2-T_0)}\Big(D_2^L\mathbb{E}[\mathbf{1}_{\{A^i_{T_1}\geq\Phi^L, A^i_{T_2}\geq D_2^L\}} \mid A_{T_0}] + \mathbb{E}[A^i_{T_2}\mathbf{1}_{\{A^i_{T_1}\geq\Phi^L, A^i_{T_2}<D_2^L\}}\} \mid A_{T_0}]\Big) \\
&\quad - (1-w)e^{-r(T_1-T_0)}\Big(D_1^H\mathbb{E}[\mathbf{1}_{\{A^i_{T_1}\geq\Phi^H\}} \mid A_{T_0}] + \mathbb{E}[A^i_{T_1}\mathbf{1}_{\{A^i_{T_1}<\Phi^H\}} \mid A_{T_0}]\Big) \\
&\quad - (1-w)e^{-r(T_2-T_0)}\Big(D_2^H\mathbb{E}[\mathbf{1}_{\{A^i_{T_1}\geq\Phi^H, A^i_{T_2}\geq D_2^H\}} \mid A_{T_0}] + \mathbb{E}[A^i_{T_2}\mathbf{1}_{\{A^i_{T_1}\geq\Phi^H, A^i_{T_2}<D_2^H\}}\} \mid A_{T_0}]\Big).
\end{aligned}
$$

Therefore, the time-0 value of an SPX call option with strike K and expiration at T_0 is

$$
\begin{aligned}
C_0^{SPX} &= e^{-rT_0}\mathbb{E}_0[\max(S_{T_0}(A_{T_0}) - K, 0)] \\
&= e^{-rT_0}\mathbb{E}_0[A_{T_0}\mathbf{1}_{\{A_{T_0}\geq\overline{A}\}}] - we^{-rT_1}\Big(D_1^L\mathbb{E}_0[\mathbf{1}_{\{A_{T_0}\geq\overline{A},A^i_{T_1}\geq\Phi^L\}}] + \mathbb{E}_0[A^i_{T_1}\mathbf{1}_{\{A_{T_0}\geq\overline{A},A^i_{T_1}<\Phi^L\}}]\Big) \\
&\quad - we^{-rT_2}\Big(D_2^L\mathbb{E}_0[\mathbf{1}_{\{A_{T_0}\geq\overline{A},A^i_{T_1}\geq\Phi^L,A^i_{T_2}\geq D_2^L\}}] + \mathbb{E}_0[A^i_{T_2}\mathbf{1}_{\{A_{T_0}\geq\overline{A},A^i_{T_1}\geq\Phi^L,A^i_{T_2}<D_2^L\}}]\Big) \\
&\quad - (1-w)e^{-rT_1}\Big(D_1^H\mathbb{E}_0[\mathbf{1}_{\{A_{T_0}\geq\overline{A},A^i_{T_1}\geq\Phi^H\}}] + \mathbb{E}_0[A^i_{T_1}\mathbf{1}_{\{A_{T_0}\geq\overline{A},A^i_{T_1}<\Phi^H\}}]\Big) \\
&\quad - (1-w)e^{-rT_2}\Big(D_2^H\mathbb{E}_0[\mathbf{1}_{\{A_{T_0}\geq\overline{A},A^i_{T_1}\geq\Phi^H,A^i_{T_2}\geq D_2^H\}}] + \mathbb{E}_0[A^i_{T_2}\mathbf{1}_{\{A_{T_0}\geq\overline{A},A^i_{T_1}\geq\Phi^H,A^i_{T_2}<D_2^H\}}]\Big) \\
&\quad - e^{-rT_0}K\mathbb{E}_0[\mathbf{1}_{\{A_{T_0}\geq\overline{A}\}}],
\end{aligned}
$$

where $\overline{A}$ is the unique value such that $S_{T_0}(\overline{A}) = K$ and we use the fact that $S_T(A)$ is increasing in A.

IA.9 Option pricing with finite number of index constituents

In the paper, we obtain analytical solutions to index options by letting the number of index constituents go to infinity. In actuality, indexes are composed of a finite number of constituents (125 in case of CDX and 500 in case of SPX). In this section, we conduct a simulation exercise to verify that the number of index constituents is sufficiently high that index option prices are well approximated by our analytical formulas. We use the same parameter values as in Section IA.8.1. We consider 3-month equity index put options that are ATM (strike equal to the forward SPX value, $K = 2259.6$) and roughly one standard deviation OTM ($K = 2071.0$). The analytical option prices are 67.72 and 23.36, respectively. We also consider 3-month credit index call options that are ATM (strike equal to the upfront value of the 5Y FEP forward-starting CDX, $K = -171.8$ bps) and roughly one standard deviation OTM ($K = -124.7$ bps). The analytical option prices are 15.25 and 6.12 bps, respectively.

Next, we use simulation to price the options for a finite number, N, of index constituents. We use $M = 50,000$ paths. The estimated equity index put option price is given by

$$e^{-rT_0} \frac{1}{M} \sum_{j=1}^{M} \max \left(K - \frac{1}{N} \sum_{j=1}^{N} S^i_{T_0}(A^{i,j}_{T_0}), 0 \right),$$

and the credit index call option price is given by

$$e^{-rT_0} \frac{1}{M} \sum_{j=1}^{M} \max \left(\frac{1}{N} \sum_{j=1}^{N} U^i_{T_0}(A^{i,j}_{T_0}) - K, 0 \right).$$

Figure IA11 shows index option prices as a function of N.[17] The left panels show CDX options, and the right panels shows SPX options. The top panels show ATM options, and the bottom panels show OTM options. The grey areas indicate 95% confidence intervals. The blue lines show the analytical option prices for $N \to \infty$.

Consider first the equity index options with $N = 500$. The ATM option has a simulated price of 67.69 with a 95% confidence interval of [66.51,68.87], and the OTM option has a simulated price of 23.15 with a 95% confidence interval of [22.43,23.87]. For both options, the analytical price is within the 95% confidence interval of the finite-N option price.

Consider next the credit index options with $N = 125$. The ATM option has a simulated price of 16.80 bps with a 95% confidence interval of [16.46,17.13] bps, and the OTM option has a simulated price of 6.60 bps with a 95% confidence interval of [6.37,6.83] bps. For both options, the analytical price lies outside of the 95% confidence interval of the finite-N option price. The finite-N option prices are 10.1% and 7.9%, respectively, higher than the analytical option prices.

The upshot is that while the analytical SPX option prices are very good approximations to the $N = 500$ index option prices, the analytical CDX option prices are downward-biased

[17] $N = 1$ corresponds to an option on a single-name CDS or single stock.

compared to the $N = 125$ index option prices.[18] However, the magnitudes of the biases are small relative to the size of the mispricing that we document in the paper.

Figure IA12 compares index distributions for finite N (estimated from the simulated data using a normal kernel function with optimal bandwidth) with the limiting distributions for $N \to \infty$ (obtained using the analytical option price formulas together with the Breeden-Litzenberger Theorem). The left panels show CDX options, and the right panels shows SPX options. The top panels show results for $N = 125$, and the bottom panels show results for $N = 500$. Visually, the distributions are very similar, with the distributions for finite N having only slightly more dispersion than the limiting distribution.

IA.10 Computation of asset return volatility

IA.10.1 Data

We build our sample for computing asset volatilities of CDX and SPX constituents from several databases. Daily stock price data come from the Center for Research in Security Prices' (CRSP's) US stock database. Quarterly company fundamentals come from the CRSP/Compustat Merged database. One- and five-year CDS spreads and expected recovery rates come from Markit. Finally, corporate actions and reference entity data come from Markit's Reference Entity Database (RED).

We use six-digit Committee on Uniform Security Identification Procedures (CUSIP) codes to identify companies that are present in both the CRSP and Markit data. Specifically, we associate with each RED code the CRSP permanent company identifier whose six-digit CUSIP—that is, the first six characters of CRSP's historic eight-character issue identifier

[18] Note that for $N = 500$, the analytical CDX option prices are within the 95% confidence intervals of the finite-N option prices. In this case, the ATM option has a simulated price of 15.54 bps with a 95% confidence interval of [15.21,15,86] bps, and the OTM option has a simulated price of 6.14 bps with a 95% confidence interval of [5.91,6.36] bps.

(the *NCUSIP* item)—corresponds to the six-digit CUSIP available in Markit RED data.[19]

Then, we incorporate corporate actions among reference entities, exclusively focusing on events in which a RED code was changed because the reference entity was renamed. We do not incorporate other corporate action types, such as mergers and acquisitions, directly; i.e., via the corresponding events in the RED database. Instead, we incorporate them indirectly whenever there are two RED codes with the same CRSP permanent company identifier that have not yet been linked. This ensures that mergers are consistent across the two data sets in that the surviving company is identical in both CRSP and Markit data.

Finally, we use CRSP's permanent company identifier to obtain company fundamentals from the CRSP/Compustat Merged database. In case of companies with multiple share classes, we drop the share class that is less liquid in terms of trading volume over the 2012–2019 sample period.

IA.10.2 Asset returns

We compute asset returns as the leverage-weighted average of equity and synthetic short- and long-term bond returns; that is,

$$r_t^{A^i} = (1 - lev_1^i - lev_2^i) r_t^{S^i} + lev_1^i r_t^{B_1^i} + lev_2^i r_t^{B_2^i},$$

where $r_t^{S^i}$ denotes firm i's daily equity return from CRSP for date t (CRSP's RET item), and $r_t^{B_1^i}$ and $r_t^{B_2^i}$ denote synthetic short- and long-term bond returns based on firm i's one- and five-year Markit CDS spreads, respectively, for the same period.[20] The leverage ratios, lev_1^i and lev_2^i, are computed as described in Section IA.6.

The synthetic bond return computation is based on no-arbitrage arguments. As shown in Duffie (1999), selling CDS protection on firm i and buying a risk-free floating rate note

[19]The RED code is the primary identifier of a credit default swap's reference entity.

[20]CRSP's return computation takes into account all distributions to shareholders, such as dividend payments.

produces the same cash flow stream as a floating rate note with matching payment dates issued by the same firm. In the same spirit, the cash flow stream of a fixed-rate bullet bond approximately equals selling CDS protection, buying a risk-free floating rate note, and swapping the risk-free floating rate payments to a fixed rate via an interest rate swap (IRS). In this case, the excess return on the fixed-rate bullet bond can be decomposed into

$$r_t^{B_j^i} = r_t^{CDS_j^i} + r_t^{IRS_j},$$

where $r_t^{CDS_j^i}$ denotes firm i's one- (if $j = 1$) or five-year (if $j = 2$) CDS return and $r_t^{IRS_j}$ denotes the return on a one- (if $j = 1$) or five-year (if $j = 2$) IRS.

Specifically, the CDS return over the period from date s to date t is

$$r_t^{CDS_j^i} = -\big(C_{j,t}^i - C_{j,s}^i\big) PVBP_t\big(C_{j,t}^i, R_t^i\big) + C_{j,s}^i \frac{t-s}{360},$$

where $C_{j,t}^i$ denotes firm i's one- (if $j = 1$) or five-year (if $j = 2$) par spread on date t and R_t^i denotes firm i's expected recovery rate.[21] The risky present value of a basis point for a given par spread and recovery rate, $PVBP_t(C, R)$, is obtained via the ISDA CDS Standard Model and using locked-in LIBOR rates from Markit.[22] For additional details concerning the CDS return computation, see Junge and Trolle (2015).

[21] If there is a credit event between dates s and t, then the return is

$$r_t^{B_j^i} = -\big(1 - R_{\tau_i}^i\big) + C_{j,s}^i \frac{\tau_{\tau_i} - s}{360},$$

where R_τ^i is the realized recovery rate and τ_i is the credit event date. There are no credit events among CDX and SPX constituents during our sample period.

[22] The ISDA CDS Standard Model is the market standard for marking to market CDSs based on a term structure of par spreads. The simplified version of the model that we use to compute the risky present values actually assumes that the term structure of risk free rates is piecewise constant, and that both the default intensity and the recovery rate are constant. Given a par spread and recovery rate, the model finds that value of the default intensity that makes a par CDS's present value equal to zero.

Similarly, the IRS return is

$$r_t^{IRS_j} = -(S_{j,t} - S_{j,s})PVBP_t$$

where $S_{j,t}$ denotes the date-t fixed rate on a one- (if $j = 1$) or five-year (if $j = 2$) IRS referencing three-month LIBOR. The present value of a basis point, $PVBP_t$, is computed using zero-rates bootstrapped from deposit and swap rates. Specifically, the short-end of the interest rate curve is composed of rates on LIBOR deposit with less than three months to maturity, and the remainder of the curve comprises swap rates.[23]

We compute asset returns both for companies for which we can establish a CRSP/Markit link and for zero-leverage companies for which we cannot expect to find Markit data. In total, we can compute asset returns for 135 companies that were a CDX constituent at some point between 2012 and 2019 and for 430 companies that were at some point a SPX constituent. Panels A of Figure IA13 shows that for roughly 50% of the CDX constituents for which we can compute asset returns, we are able to do so throughout the sample period. For SPX constituents that share is a little lower at roughly 40%, see Panel B of Figure IA13. The varying number of observations for the remaining companies is due to both missing data and index inclusions/exclusions. In our analysis, we disregard a few companies with very few observations by requiring that we have at least one month of data (i.e., 21 observations) for each quarter for which we produce firm-quarter statistics. This leaves a total of 135 and 425 companies in case of CDX and SPX, respectively.

Panel A of Figures IA14 and IA15 show the distributions of asset returns for CDX and SPX constituents, respectively. Panels B, C, and D of the two figures show the distributions of the asset return's components; namely, the equity return (Panel B), and the synthetic

[23] The swaps are standard USD-denominated fixed for floating swaps. Floating-leg payments occur quarterly and reference three-month LIBOR, and fixed-leg payments occur semi-annually. The swaps have maturities of at least one year.

one- (Panel C) and five-year (Panel D) bond returns.

IA.10.3 Systematic asset volatility

We decompose asset returns into systematic and idiosyncratic components by assuming that the return of the common systematic component has the same structure as the returns of the individual companies; that is,

$$r_t^A = (1 - lev_1 - lev_2) r_t^S + lev_1 r_t^{B_1} + lev_2 r_t^{B_2},$$

where r_t^S denotes the return on aggregate equity, $r_t^{B_1^i}$ and $r_t^{B_2^i}$ denote returns on aggregate short- and long-term debt, and lev_1 and lev_2 denote aggregate short- and long-term leverage ratios.

In this case, a one-factor linear model

$$r_t^{A^i} = \alpha_i + \beta_i r_t^A + \epsilon_t^{A^i}$$

becomes

$$r_t^{A^i} = \alpha_i + \beta_i^S r_t^S + \beta_i^{B_1} r_t^{B_1} + \beta_i^{B_2} r_t^{B_2} + \epsilon_t^{A^i}, \tag{IA6}$$

where $\beta_i^S = \beta_i(1 - lev_1 - lev_2)$, $\beta_i^{B_1} = \beta_i lev_1$, and $\beta_i^{B_2} = \beta_i lev_2$. We use Equation (IA6) to estimate the systematic component of asset returns.[24] Specifically, r_t^S is given by the daily SPX return from CRSP (CRSP's *SPRTRN* item), and $r_t^{B_1}$ and $r_t^{B_2}$ are computed from CDX and IRS returns as

$$r_t^{B_j} = r_t^{CDX_j} + r_t^{IRS_j},$$

[24] We estimate Equation (IA6) for each firm and quarter, i.e., we do not impose the cross-equation restrictions implied by the explicit expressions for β_i^S, $\beta_i^{B_1}$, and $\beta_i^{B_1}$.

where the CDX return is given by

$$r_t^{CDX_j} = -(U_{j,t} - U_{j,s}) + C\frac{t-s}{360} - (L_t - L_s),$$

using the notation from Section IA.1 in the Internet Appendix.

While total asset volatility is estimated as the annualized standard deviation of $r_t^{A^i}$, systematic asset volatility is estimated as the annualized standard deviation of

$$\hat{r}_t^{A^i} = \hat{\alpha}_i + \hat{\beta}_i^S r_t^S + \hat{\beta}_i^{B_1} r_t^{B_1} + \hat{\beta}_i^{B_2} r_t^{B_2}, \tag{IA7}$$

where $\hat{\alpha}_i$, $\hat{\beta}_i^S$, $\hat{\beta}_i^{B_1}$, and $\hat{\beta}_i^{B_2}$ denote OLS estimates of α_i, β_i^S, $\beta_i^{B_1}$, and $\beta_i^{B_2}$, respectively.

IA.11 Option pricing with stochastic bankruptcy costs

Here we show how to extend the model to allow for stochastic bankruptcy costs that follow a continuous Markov chain $\alpha_t = \sum_{i=1}^n \alpha_i \mathbf{1}_{\{s_t=i\}}$, where $s_t \in \{1, 2, \ldots, n\}$ follows a continuous time Markov chain with constant transition intensities q_{ij} and where α_i are constant bankruptcy cost parameters. We assume the jumps in s_t are independent of all other sources of risk. Further, we define the transition matrix Q with off-diagonal element $Q_{ij} = q_{ij}\ \forall i \neq j$ and with diagonal element $Q_{ii} = -\sum_{j\neq i} q_{ij}$. Note that equity prices and thus SPX and SPX option prices are not affected by bankruptcy costs. Thus they are unchanged. Instead, the bankruptcy cost process enters the bond and CDS payoffs, and thus also affects CDX and CDX option values. Further, since α_t is independent of A_t and A_t^i, the bond and CDS prices will depend only on the conditional expectation of α_t, $\overline{\alpha}(s_0, t) = E[\alpha_t \mid s_0]$. Instead, the CDX option will also depend on the volatility of α_t, which has the potential to increase CDX option prices relative to those implied by SPX options.

IA.11.1 CDS value

Consider a CDS contract from T_0 to T_2 with unit notional and with a coupon rate of C. Following the same approach as in the main text, the upfront amount of the CDS contract is

$$
\begin{aligned}
U_2^i(T_0) &= \mathrm{Prot}_2^i(T_0) - C \times \mathcal{A}_2^i(T_0) \\
&= e^{-r(T_1-T_0)}\mathbb{E}_{T_0}[(1 - \frac{\alpha_{T_1} A_{T_1}^i}{D_1 + D_2} + C_1)\mathbf{1}_{\{A_{T_1}^i < \Phi\}}] \\
&\quad + e^{-r(T_2-T_0)}\mathbb{E}_{T_0}[(1 - \frac{\alpha_{T_2} A_{T_2}^i}{D_2})\mathbf{1}_{\{A_{T_1}^i \geq \Phi, A_{T_2}^i < D_2\}}] - C_0 - C_1 e^{-r(T_1-T_0)},
\end{aligned}
$$

where C_0, C_1 are as defined in the main text.

Since the Markov Chain process is independent of A^i, A we can rewrite this as:

$$
\begin{aligned}
U_2^i(T_0) = e^{-r(T_1-T_0)}&\mathbb{E}_{T_0}[(1 - \frac{\overline{\alpha}(s_{T_0}, T_1 - T_0) A_{T_1}^i}{D_1 + D_2} + C_1)\mathbf{1}_{\{A_{T_1}^i < \Phi\}}] \\
&+ e^{-r(T_2-T_0)}\mathbb{E}_{T_0}[(1 - \frac{\overline{\alpha}(s_{T_0}, T_2 - T_0) A_{T_2}^i}{D_2})\mathbf{1}_{\{A_{T_1}^i \geq \Phi, A_{T_2}^i < D_2\}}] - C_0 - C_1 e^{-r(T_1-T_0)},
\end{aligned}
$$

where we define the expected bankruptcy cost $\tau \geq 0$:

$$
\overline{\alpha}(s, \tau) = E[\alpha_\tau \mid s_0 = s] \tag{IA8}
$$

$$
= \sum_{i=1}^{n} \alpha_i P[s_\tau = i \mid s_0 = s] \tag{IA9}
$$

Define the (n, n) matrix $P(t)$ with element $p_{ij}(t) = P[s_t = j \mid s_0 = i]$. Clearly, it satisfies for $j \neq i$:

$$
p_{ij}(t + dt) = \sum_{k \neq j} p_{ik}(t) q_{kj} dt + p_{ij}(t)(1 - \sum_{k \neq j} q_{jk} dt)
$$

from which it follows that

$$p_{ij}(t)' = \sum_k p_{ik}(t)Q_{kj}$$

In matrix form:

$$P(t)' = P(t)Q$$

which admits the matrix solution $P(t) = \exp(tQ)$, where $\exp(M) = \sum_k \frac{1}{k!}M^k$.

We can also compute the conditional variance of the bankruptcy cost as

$$V[\alpha_\tau \mid s_0 = s] = E[\alpha_\tau^2 \mid s_0 = s] - \overline{\alpha}(s,\tau)^2,$$

where

$$E[\alpha_\tau^2 \mid s_0 = s] = \sum_{i=1}^n \alpha_i^2 p_{si}(\tau).$$

IA.11.2 CDX value

We value the CDX at time T_0. Like in the main text we will use the LHP model to derive the expression. The new feature is that there are now two common factors A_{T_0}, s_{T_0}. The index upfront amount, conditional on the common factors A_{T_0}, s_{T_0}, is given by:

$$\begin{aligned}
U_{T_0}(A_{T_0}, s_{T_0}) = &\lim_{N\to\infty} \frac{1}{N}\sum_{i=1}^N U_2^i(T_0) \\
&= \mathbb{E}[U_2^i(T_0)|A_{T_0}, s_{T_0}] \\
&= e^{-r(T_1-T_0)}\Big((1+C_1)\mathbb{E}[\mathbf{1}_{\{A_{T_1}^i<\Phi\}} \mid A_{T_0}] - \frac{\overline{\alpha}(s_{T_0}, T_1-T_0)}{D_1+D_2}\mathbb{E}[A_{T_1}^i\mathbf{1}_{\{A_{T_1}^i<\Phi\}} \mid A_{T_0}]\Big) \\
&\quad + e^{-r(T_2-T_0)}\Big(\mathbb{E}[\mathbf{1}_{\{A_{T_1}^i\geq\Phi, A_{T_2}^i<D_2\}} \mid A_{T_0}] - \frac{\overline{\alpha}(s_{T_0}, T_2-T_0)}{D_2}\mathbb{E}[A_{T_2}^i\mathbf{1}_{\{A_{T_1}^i\geq\Phi, A_{T_2}^i<D_2\}} \mid A_{T_0}]\Big) \\
&\quad - C_0 - C_1e^{-r(T_1-T_0)}.
\end{aligned}$$

IA.11.3 CDX options

The time-0 value of a CDX call option with strike K and expiration at T_0 is:

$$
\begin{aligned}
C_0^{CDX} &= e^{-rT_0}\mathbb{E}_0[\max(U_{T_0}(A_{T_0}, s_{T_0}) - K, 0)] \\
&= e^{-rT_0}\sum_{i=1}^{n} P[s_{T_0} = i \,|\, s_0]\, \mathbb{E}_0[\max(U_{T_0}(A_{T_0}, i) - K, 0)]
\end{aligned}
$$

It remains to evaluate $\mathbb{E}_0[\max(U_{T_0}(A_{T_0}, i) - K, 0)]$ $\forall i = 1, \ldots, n$. But this is similar to the expression in the main text. Indeed:

$$
\begin{aligned}
& e^{-rT_0}\mathbb{E}_0[\max(U_{T_0}(A_{T_0}, i) - K, 0)] \\
&\quad = e^{-rT_0}\mathbb{E}_0\Bigg[\Bigg(e^{-r(T_1-T_0)}\Big((1+C_1)\mathbb{E}[\mathbf{1}_{\{A^i_{T_1}<\Phi\}} \,|\, A_{T_0}] - \frac{\overline{\alpha}(i, T_1 - T_0)}{D_1 + D_2}\mathbb{E}[A^i_{T_1}\mathbf{1}_{\{A^i_{T_1}<\Phi\}} \,|\, A_{T_0}]\Big) \\
&\qquad + e^{-r(T_2-T_0)}\Big(\mathbb{E}[\mathbf{1}_{\{A^i_{T_1}\geq\Phi, A^i_{T_2}<D_2\}} \,|\, A_{T_0}] - \frac{\overline{\alpha}(i, T_2 - T_0)}{D_2}\mathbb{E}[A^i_{T_2}\mathbf{1}_{\{A^i_{T_1}\geq\Phi, A^i_{T_2}<D_2\}} \,|\, A_{T_0}]\Big)\Bigg)\mathbf{1}_{\{A_{T_0}<\overline{A}\}}\Bigg] \\
&\qquad - e^{-rT_0}\tilde{K}\mathbb{E}_0[\mathbf{1}_{\{A_{T_0}<\overline{A}\}}] \\
&\quad = e^{-rT_1}\Big((1+C_1)\mathbb{E}_0[\mathbf{1}_{\{A_{T_0}<\overline{A}, A^i_{T_1}<\Phi\}}] - \frac{\overline{\alpha}(i, T_1 - T_0)}{D_1 + D_2}\mathbb{E}_0[A^i_{T_1}\mathbf{1}_{\{A_{T_0}<\overline{A}, A^i_{T_1}<\Phi\}}]\Big) \\
&\qquad + e^{-rT_2}\Big(\mathbb{E}_0[\mathbf{1}_{\{A_{T_0}<\overline{A}, A^i_{T_1}\geq\Phi, A^i_{T_2}<D_2\}}] - \frac{\overline{\alpha}(i, T_2 - T_0)}{D_2}\mathbb{E}_0[A^i_{T_2}\mathbf{1}_{\{A_{T_0}<\overline{A}, A^i_{T_1}\geq\Phi, A^i_{T_2}<D_2\}}]\Big) \\
&\qquad - e^{-rT_0}\tilde{K}\mathbb{E}_0[\mathbf{1}_{\{A_{T_0}<\overline{A}\}}],
\end{aligned}
$$

where

$$\tilde{K} = K + C_0 + C_1 e^{-r(T_1-T_0)}$$

and $\overline{A}$ is the unique value such that $U_{T_0}(\overline{A}, i) = K$ and we use the fact that $U_T(A, i)$ is decreasing in A. Note in particular, that the endogenous threshold $\overline{A}$ depends on the state i and so will be different across different bankruptcy cost states.

IA.12 Details on trading strategies

As described in the paper, in addition to holding the option premium in a margin account, we assume that an initial amount of capital is required when selling options. Let P_t denote the straddle price at time t and X_t the required capital. Assuming that capital in the margin account earns the risk-free rate, the excess return from selling the straddle is

$$R^e_{t+1} = \frac{-P_{t+1} + P_t(1 + r_t)}{X_t}.$$

In the paper, we assume that X_t is proportional to the option premium, $X_t = cP_t$, and adjust c to achieve a 10% unconditional annualized volatility of realized excess returns within each option maturity.

As a robustness check, here we explore an alternative assumption that X_t is constant over time, and again adjust the required amount to achieve a 10% unconditional annualized excess return volatility. Table IA.3 and Figure IA17 are the counterparts to Table 7 and Figure 12 in the paper. Under the alternative assumption about capital, selling CDX volatility is even more attractive relative to selling SPX volatility. For instance, for the full sample, trading the EW portfolios against each other generates an annualized Sharpe ratio of 1.143 (vs. 0.877 with the original assumption about capital).

Note, however, that the return distributions are much more leptokurtic. This is also evident from Figure IA18, which shows daily excess returns for each of the EW strategies assuming constant capital (in the top row) and proportional capital (in the bottom row). Clearly, constant capital leads to extreme return volatility during the Covid-19 crisis, which is not the case with proportional capital.

References (Internet Appendix)

Duffie, Darrell, 1999, Credit swap valuation, *Financial Analysts Journal* 55, 73–87.

Gatheral, Jim, 2006, *The Volatility Surface* (Wiley, Hoboken, New Jersey).

Junge, Benjamin, and Anders B. Trolle, 2015, Liquidity risk in credit default swap markets, Working paper, Swiss Finance Institute.

Morini, Massimo, and Damiano Brigo, 2011, No-armageddon measure for arbitrage-free pricing of index options in a credit crisis, *Mathematical Finance* 21, 573–593.

Pedersen, Claus M., 2003, Valuation of portfolio credit default swaptions, Lehman Brothers Fixed Income Quantitative Credit Research

White, Richard, 2014, Forward CDS, indices and options, OpenGamma Quantitative Research.

	Data	Model
Panel A: Full sample		
$\Delta log(CDX), \Delta\beta_0^{SPX}$	0.710	0.754
	[0.659,0.754]	[0.709,0.792]
$\Delta log(CDX), \Delta\beta_1^{SPX}$	-0.685	-0.708
	[-0.733,-0.631]	[-0.752,-0.657]
$\Delta\beta_0^{CDX}, \Delta log(SPX)$	-0.701	-0.634
	[-0.746,-0.649]	[-0.687,-0.573]
$\Delta\beta_0^{CDX}, \Delta\beta_1^{SPX}$	-0.637	-0.759
	[-0.690,-0.577]	[-0.796,-0.715]
$\Delta\beta_1^{CDX}, \Delta log(SPX)$	-0.285	-0.211
	[-0.370,-0.196]	[-0.300,-0.118]
$\Delta\beta_1^{CDX}, \Delta\beta_0^{SPX}$	0.286	0.320
	[0.196,0.371]	[0.231,0.402]
Panel B: Ex-Covid-19 sample		
$\Delta log(CDX), \Delta\beta_0^{SPX}$	0.698	0.674
	[0.644,0.744]	[0.618,0.724]
$\Delta log(CDX), \Delta\beta_1^{SPX}$	-0.613	-0.600
	[-0.670,-0.549]	[-0.658,-0.534]
$\Delta\beta_0^{CDX}, \Delta log(SPX)$	-0.621	-0.724
	[-0.677,-0.558]	[-0.767,-0.675]
$\Delta\beta_0^{CDX}, \Delta\beta_1^{SPX}$	-0.585	-0.831
	[-0.645,-0.517]	[-0.859,-0.798]
$\Delta\beta_1^{CDX}, \Delta log(SPX)$	-0.307	-0.165
	[-0.393,-0.217]	[-0.258,-0.069]
$\Delta\beta_1^{CDX}, \Delta\beta_0^{SPX}$	0.346	0.315
	[0.258,0.429]	[0.225,0.400]

Table IA.1: Remaining cross-market correlations

Each panel shows the six cross-market correlations that were not reported in Table 4 of the paper. Correlations to the left ("Data") are computed from the data. Correlations to the right ("Model") are computed from the fitted data using the benchmark specification of the model in Section 4. 95% confidence intervals are given in brackets. The full sample period is February 29, 2012 to April 29, 2020 (426 weekly observations). The ex-Covid-19 sample period is February 29, 2012 to December 31, 2019 (409 weekly observations).

	CDX options			SPX options		
Diffusion	✓	✓	✓	✓	✓	✓
Systematic jumps		✓	✓		✓	✓
Idiosyncratic jumps			✓			✓
A_0	4351.6	4351.5	4350.8	4351.6	4351.5	4350.9
D_1/A_0	0.0373	0.0373	0.0373	0.0373	0.0373	0.0373
D_2/A_0	0.2450	0.2450	0.2450	0.2450	0.2450	0.2450
δ	0.0129	0.0129	0.0129	0.0129	0.0129	0.0129
σ	0.3318	0.3116	0.2978	0.3318	0.3181	0.3080
ρ	0.2101	0.1298	0.1683	0.0628	0.0243	0.0260
λ		0.5044	0.5396		1.4668	1.4625
m		-0.1259	-0.1279		-0.0567	-0.0567
v		0.0085	0.0097		0.0027	0.0027
λ_i			0.0013			0.0013
IV RMSE	0.1862	0.0128	0.0121	0.0531	0.0022	0.0022
1Y CDX (bps)	0.9	0.9	8.3	0.9	0.9	8.3

Table IA.2: Parameters, in-sample analysis

The table shows the calibrated parameters for the in-sample analysis in Section 4.6. All specifications have $m_i = -2$, $v_i = 0$ and $\alpha = 0.8$.

	CDX options				SPX options				CDX vs. SPX options			
	M1	M2	M3	EW	M1	M2	M3	EW	M1	M2	M3	EW
Panel A: Full sample												
Mean	0.104	0.115	0.154	0.124	0.008	0.012	0.007	0.009	0.048	0.051	0.073	0.058
t-stat	2.676	2.782	3.698	3.187	0.223	0.335	0.203	0.258	2.579	2.900	4.175	3.412
Std.dev.	0.100	0.100	0.100	0.093	0.100	0.100	0.100	0.098	0.055	0.054	0.055	0.050
SR	1.042	1.147	1.538	1.337	0.079	0.120	0.073	0.092	0.874	0.959	1.322	1.143
Skewness	-5.265	-7.510	-6.063	-7.458	-4.116	-4.612	-4.286	-4.494	2.223	1.154	-0.280	1.742
Kurt	91.258	145.518	114.268	145.778	47.126	72.070	89.650	63.181	36.730	44.154	57.470	43.983
Panel B: Ex-Covid-19 sample												
Mean	0.186	0.231	0.267	0.228	0.082	0.112	0.119	0.104	0.052	0.060	0.074	0.062
t-stat	4.907	5.827	6.728	6.347	2.584	3.498	3.653	3.314	2.579	2.895	3.569	3.285
Std.dev.	0.100	0.100	0.100	0.087	0.100	0.100	0.100	0.099	0.060	0.060	0.059	0.054
SR	1.860	2.312	2.665	2.605	0.816	1.120	1.186	1.055	0.872	0.998	1.246	1.146
Skewness	-1.138	-2.223	-1.206	-1.901	-2.618	-2.408	-2.256	-2.460	-0.047	-0.183	0.194	0.065
Kurt	18.228	20.375	18.449	16.692	26.397	26.304	24.886	26.227	13.047	12.375	11.958	11.874

Table IA.3: Summary statistics of trading strategies, constant required capital

In each market and for each option maturity category, the strategy sells closest-to-ATM straddles each trading day with a holding period of one day. We assume that the strategy requires an initial amount of capital, which we assume is constant over time and which we adjust to achieve a 10% unconditional annualized volatility of realized excess returns for each option maturity. "EW" denotes an equally weighted portfolio of the three option maturities. "CDX vs. SPX options" denotes a short-long strategy then allocates 50% of funds to selling CDX straddles and 50% to buying SPX straddles. Means, standard deviations, and Sharpe ratios ("SR") are annualized. t-statistics are corrected for heteroscedasticity and serial correlation up to four lags using the approach of The full sample consists of 1881 daily returns between February 28, 2012 and April 30, 2020. The ex-Covid-19 sample consists of 1801 daily returns between February 28, 2012 and December 31, 2019.

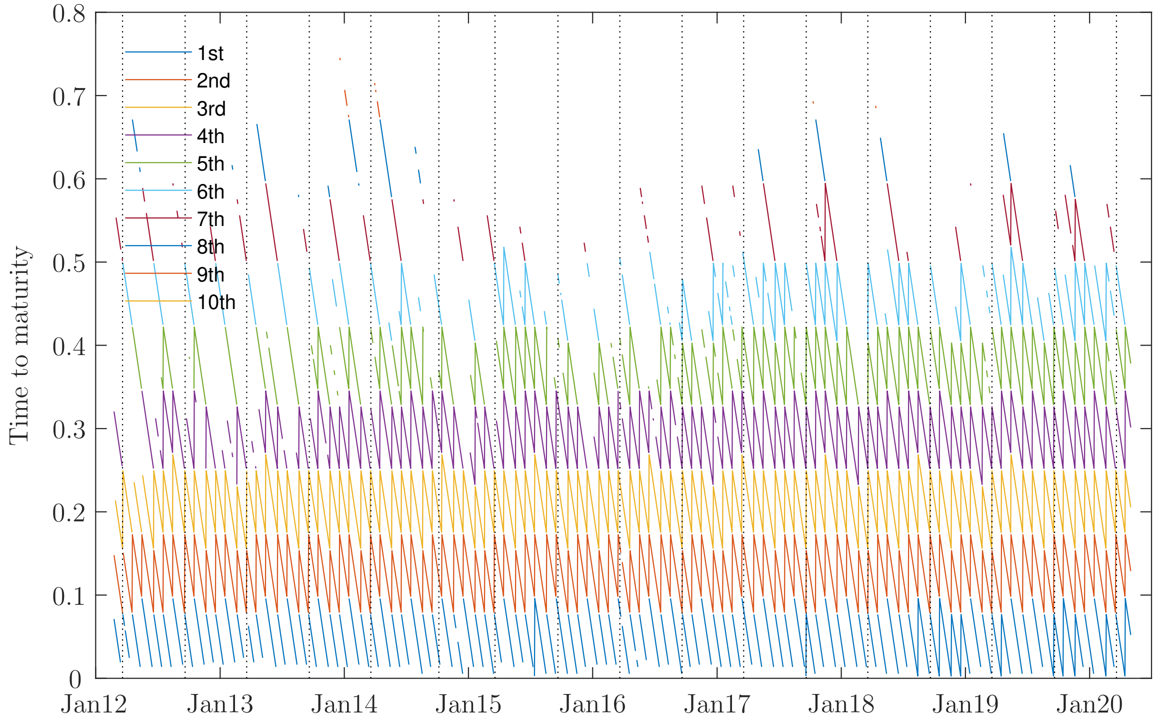

Figure IA1: Time series of quoted CDX option maturities

Option expiries are 3rd Wednesday of the month. Vertical dotted lines mark roll dates. Daily data from February 24, 2012 until April 30, 2020.

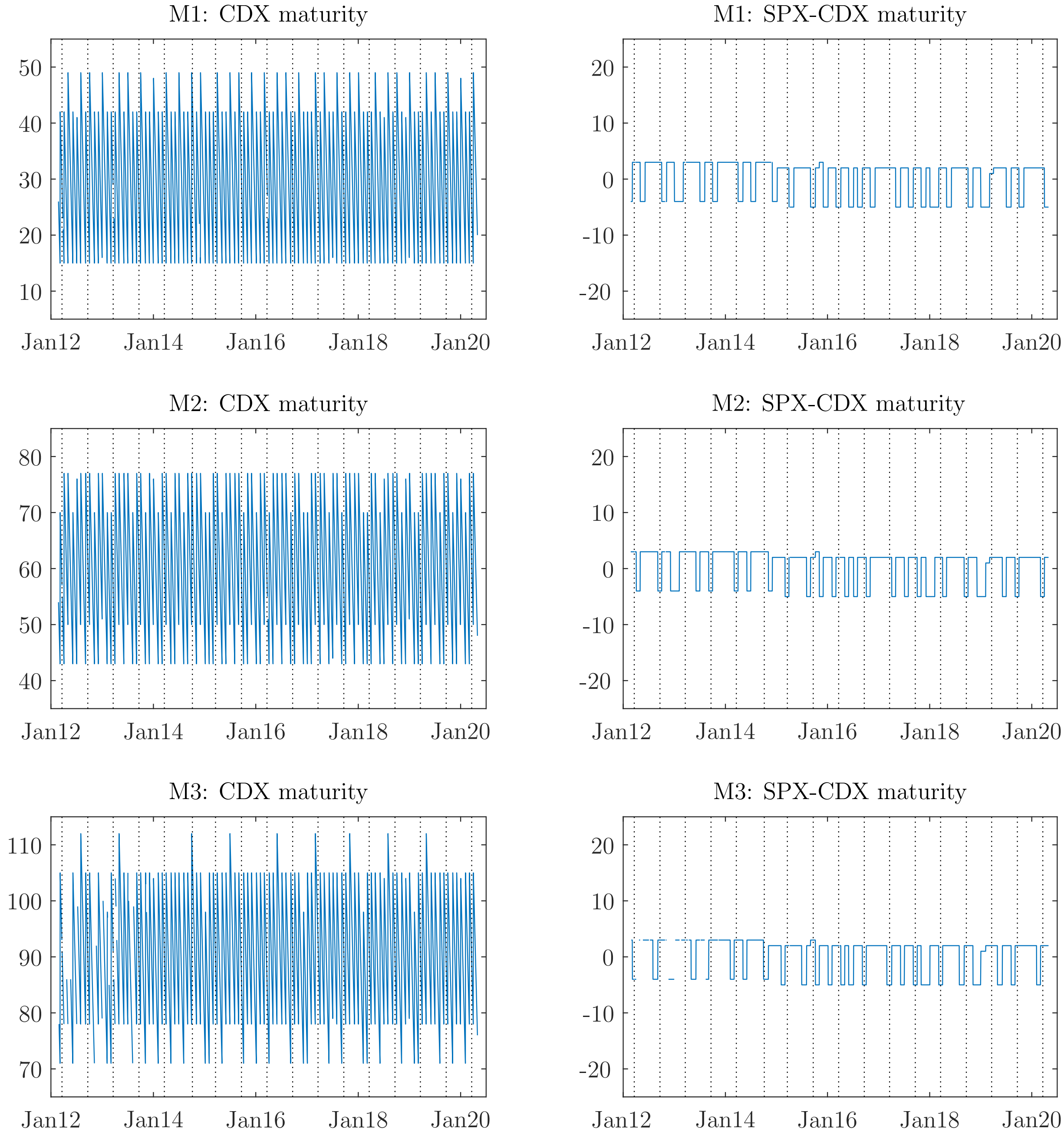

Figure IA2: Maturities of M1, M2, and M3 options

The left panels show CDX option maturities in calendar days. The right panels show the difference between SPX and CDX option maturities in calendar days. Vertical dotted lines mark CDX roll dates. Daily data from February 24, 2012 until April 30, 2020.

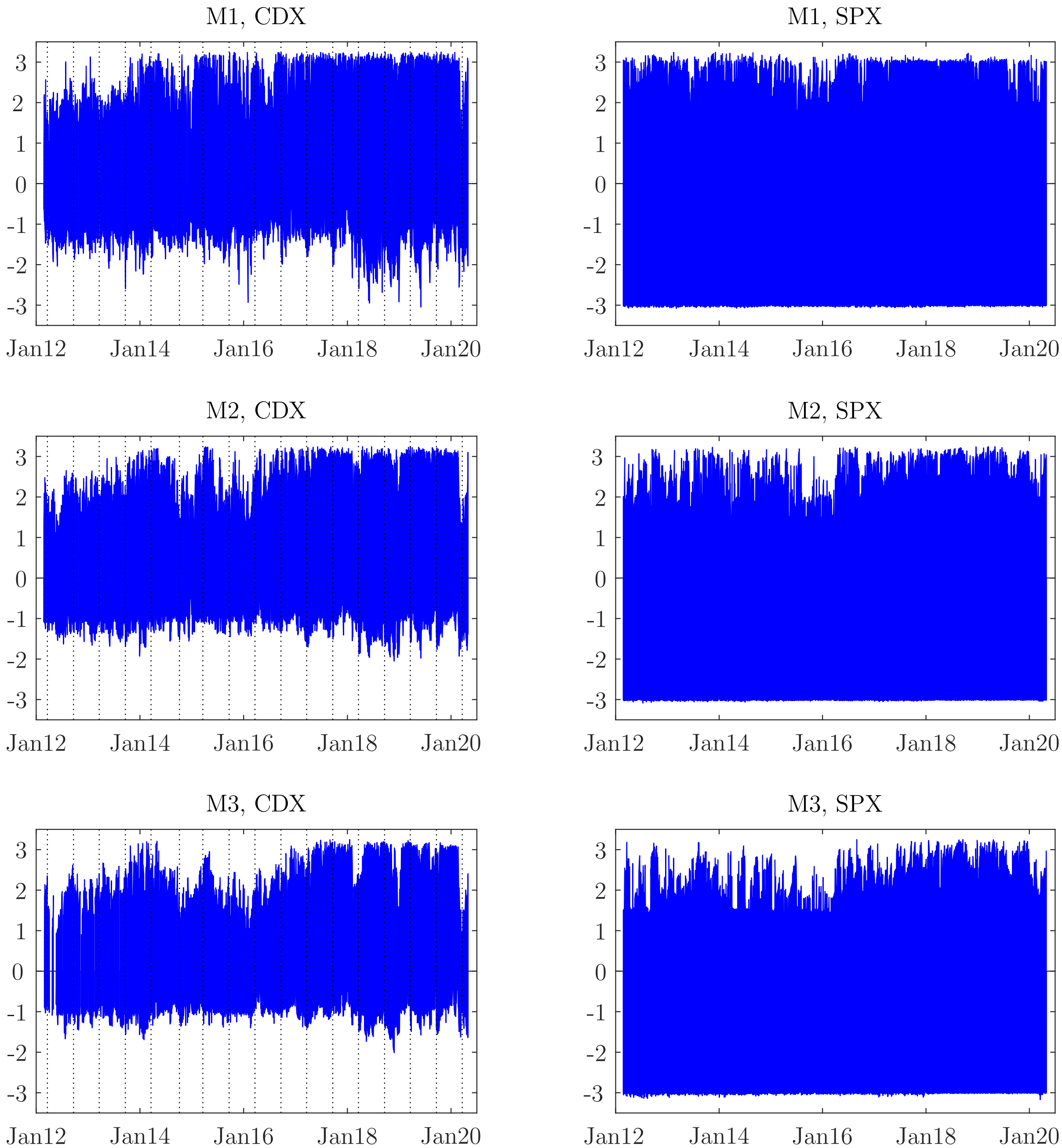

Figure IA3: Moneyness-range of M1, M2, and M3 option

The left (right) panels show the range of moneyness spanned by CDX (SPX) options. Moneyness is defined as $m = \log(K/F(\tau))/(\sigma\sqrt{\tau})$, where K is the strike, $F(\tau)$ is the forward (the front-end-protected spread in case of CDX options and the forward price in case of SPX options), σ is the at-the-money implied volatility, and τ is the maturity. Vertical dotted lines mark CDX roll dates. Daily data from February 24, 2012 until April 30, 2020.

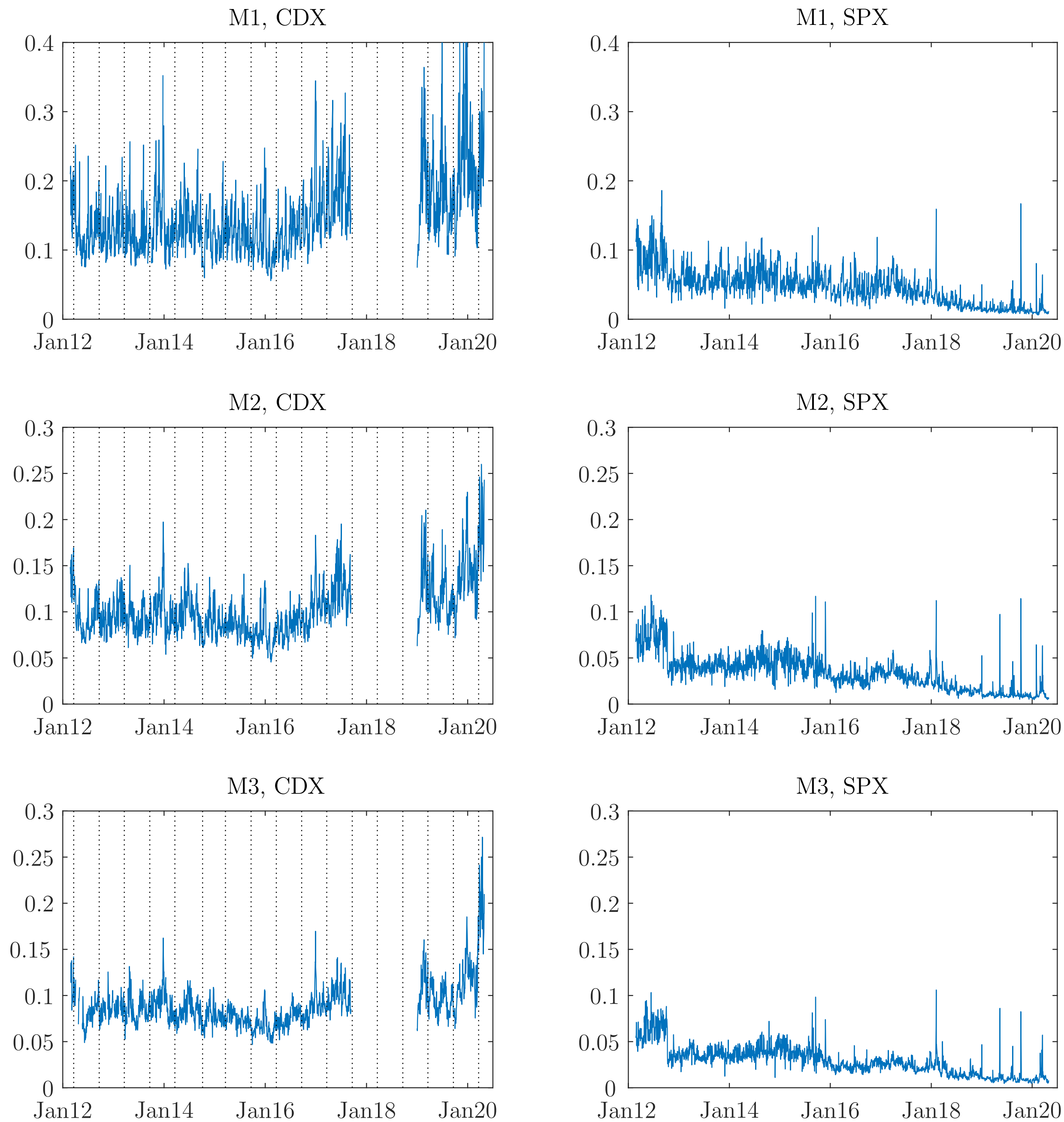

Figure IA4: Relative bid-ask spreads of M1, M2, and M3 at-the-money option

The left (right) panels show the relative bid-ask spreads of at-the-money CDX (SPX) options. Relative bid-ask spreads are defined as $\frac{P_t^{ask} - P_t^{bid}}{P_t^{mid}}$. Vertical dotted lines mark CDX roll dates. Daily data from February 24, 2012 until April 30, 2020.

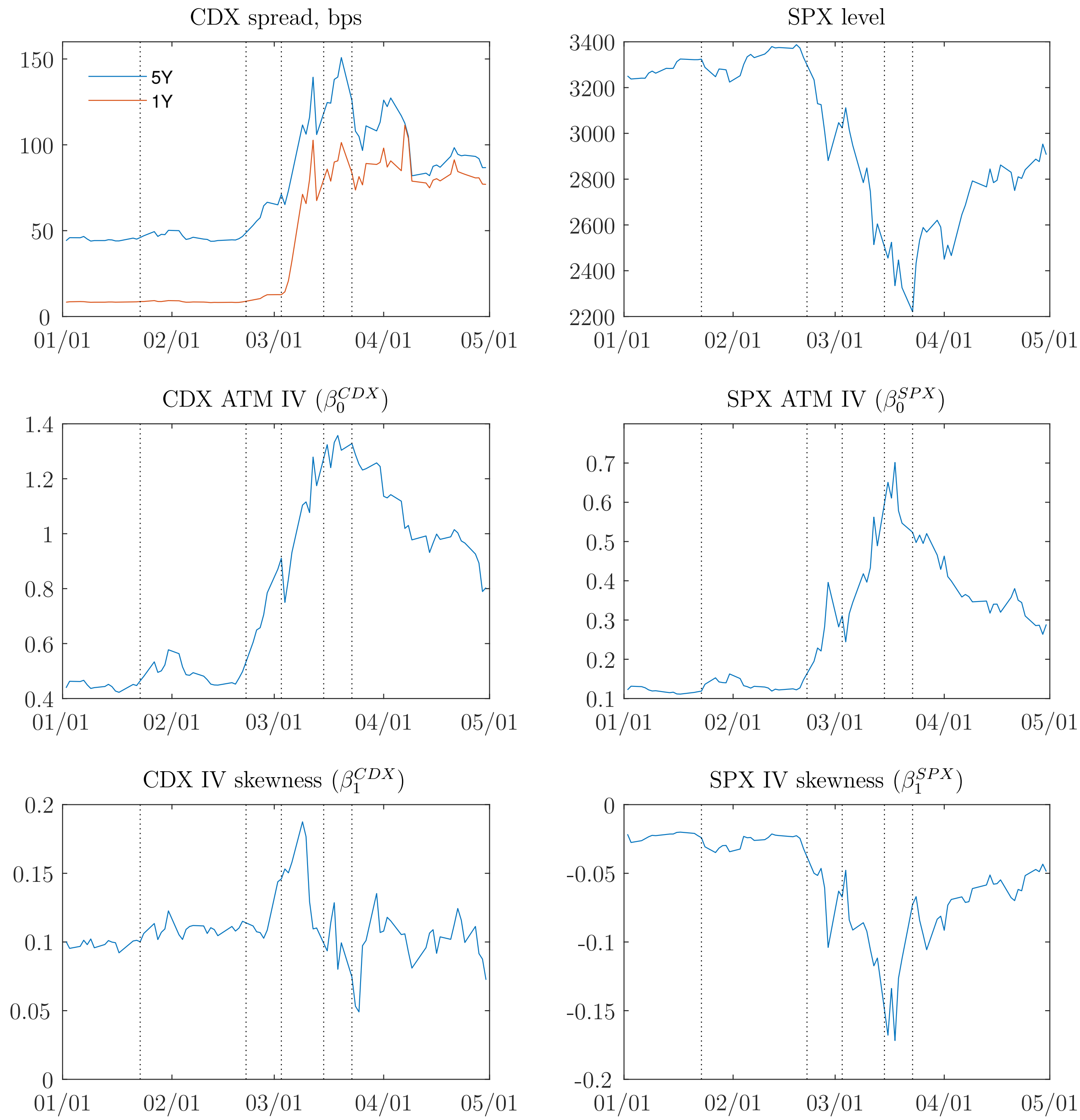

Figure IA5: Summary of CDX and SPX options markets during Covid-19 crisis

The top left (right) panel shows time series of the CDX spread (SPX level). The middle left (right) panel shows time series of the at-the-money CDX (SPX) implied volatility proxied by β_0. The bottom left (right) panel shows time series of the skewness of the CDX (SPX) implied volatility smile proxied by β_1. The vertical dotted lines mark the Wuhan lockdown on January 23, the Italy quarantine on February 22, the 50 bps rate cut by the Federal Reserve on March 3, 2020, the 100 bps rate cut and credit market support by the Federal Reserve on March 15, 2020, and the expansion of credit market support by Federal Reserve on March 23, 2020. Daily data from January 2, 2020 until April 30, 2020.

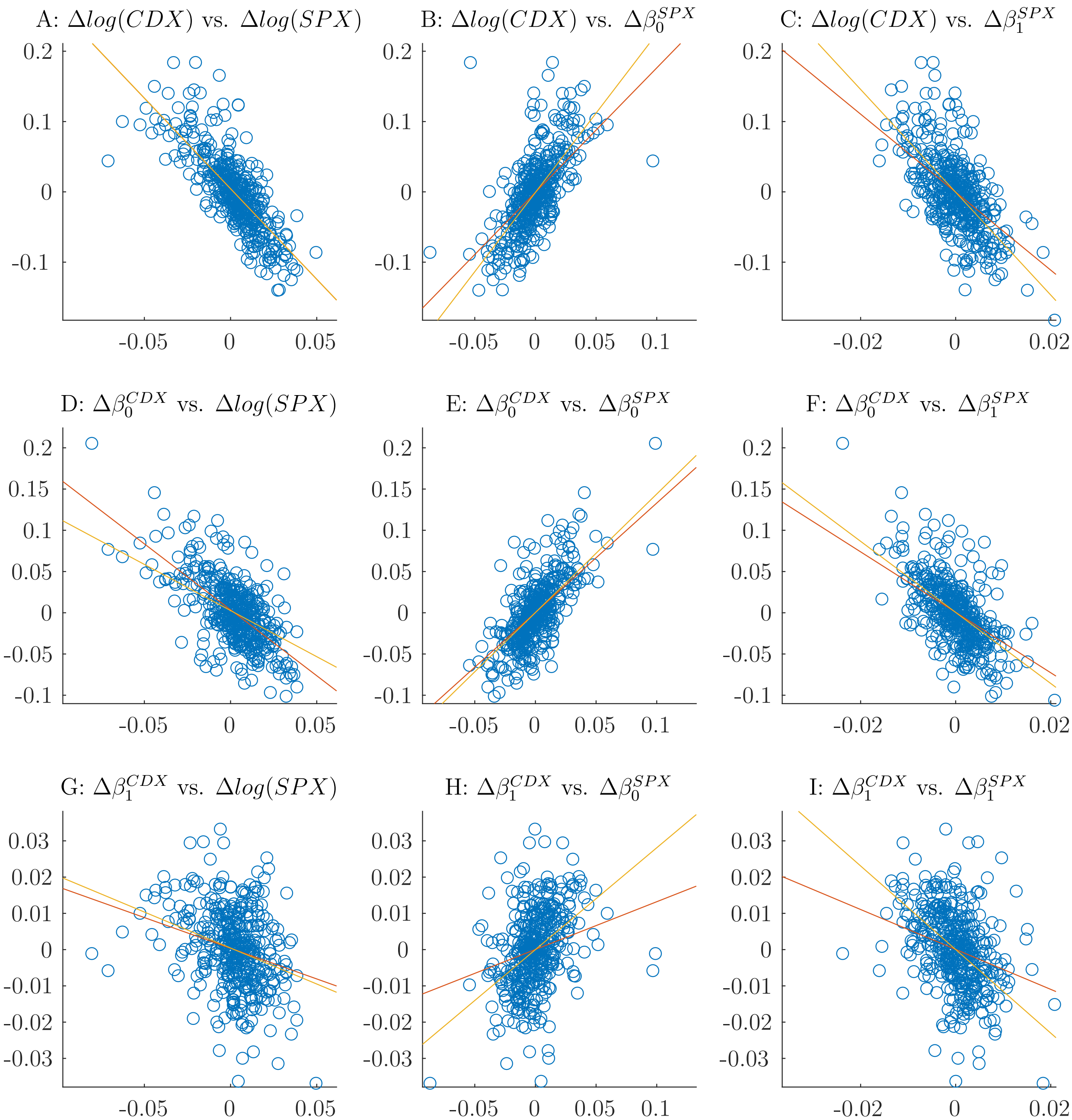

Figure IA6: All cross-market interactions

The figure shows all nine cross-market correlations. We only display observations that fall within the 0.5th and 99.5th percentile of the univariate distributions. The red (yellow) lines show the fits of linear regressions applied to the data (fitted data using the benchmark specification of the model in Section 4). The sample period is February 29, 2012 to April 29, 2020 (426 weekly observations).

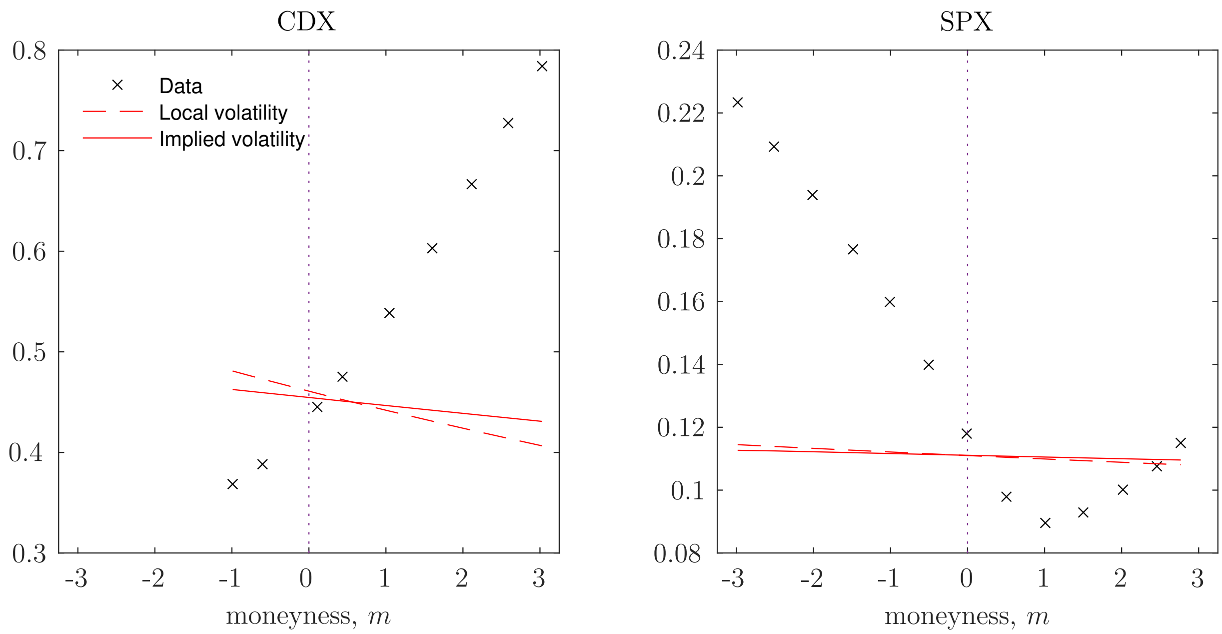

Figure IA7: Local and implied volatility smiles in the pure-diffusion version

The figure shows the local and implied volatility smiles for CDX and SPX on December 31, 2019. CDX data is displayed in the left panel and SPX data is displayed in the right panel. Moneyness is defined as $m = \log(K/F(\tau))/(\sigma\sqrt{\tau})$, where K is the strike, $F(\tau)$ is the forward (front-end-protected) spread in case of CDX options and the forward price in case of SPX options), σ is the at-the-money implied volatility, and τ is the option maturity. Crosses show data. The dashed red lines show the local volatility smiles in the pure-diffusion version of the model. The solid red lines show the two-month implied volatility smiles.

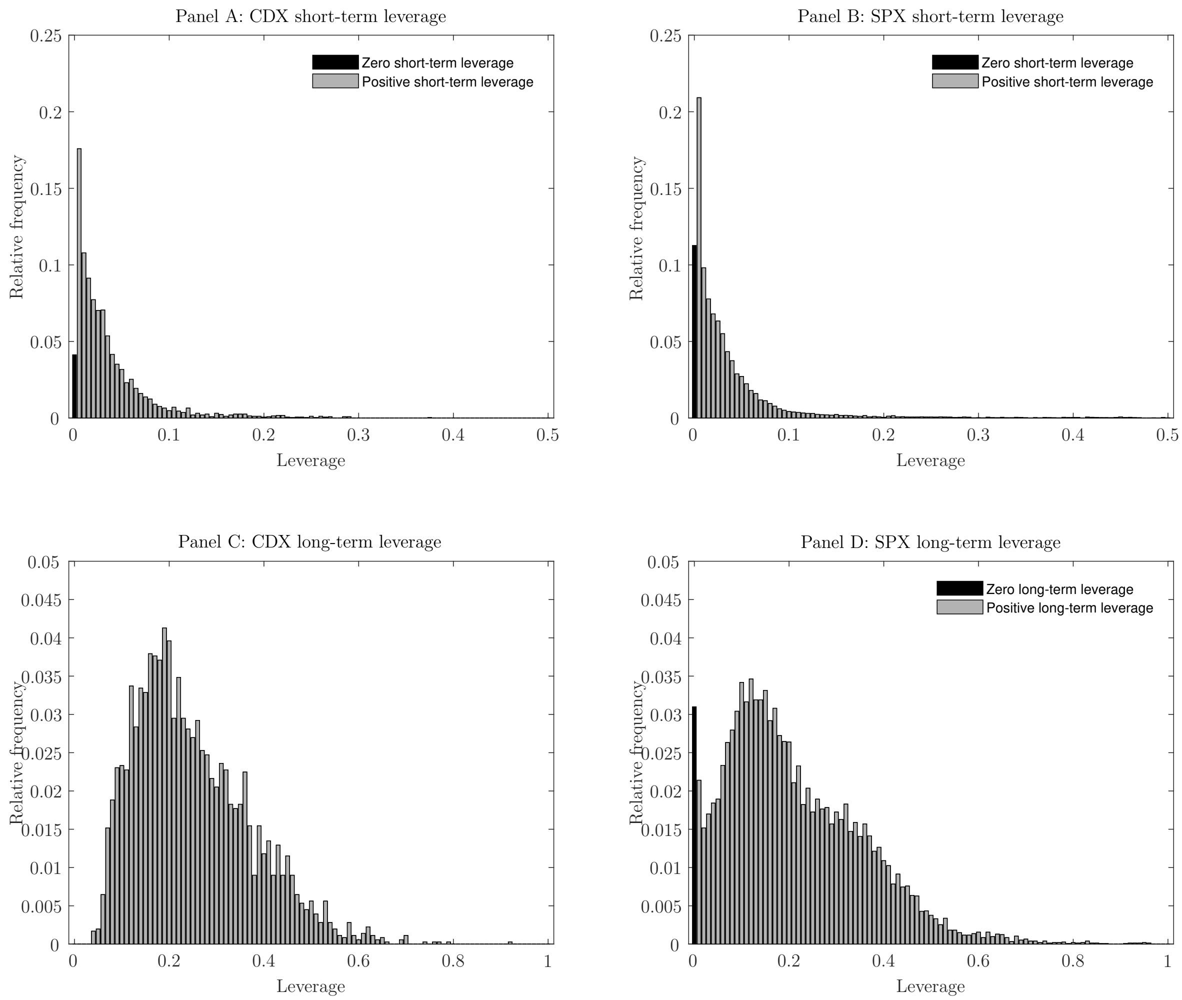

Figure IA8: Distributions of short- and long-term leverage across index constituents
Panels A and B (C and D) show the distribution of firm-quarter short-term (long-term) leverage observations for the constituents of the CDX and SPX, respectively. Short-term (long-term) leverage is defined as book value of short-term (long-term) debt relative to the sum of market value of equity and book value of total debt. The sample is from first quarter of 2012 until first quarter of 2020.

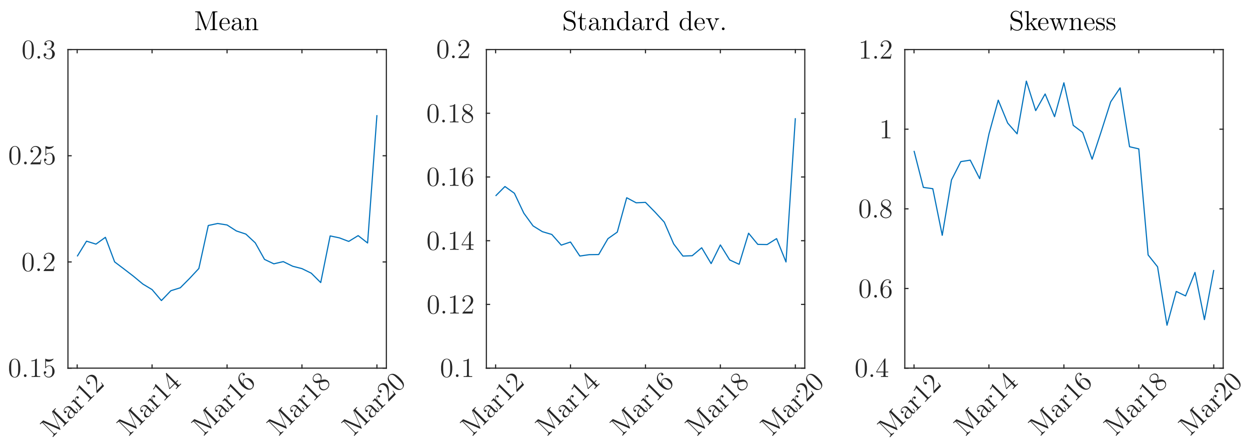

Figure IA9: Time series of moments of leverage distributions

The figure shows the time series of the mean, standard deviation, and skewness of the distribution of long-term leverage for SPX constituents.

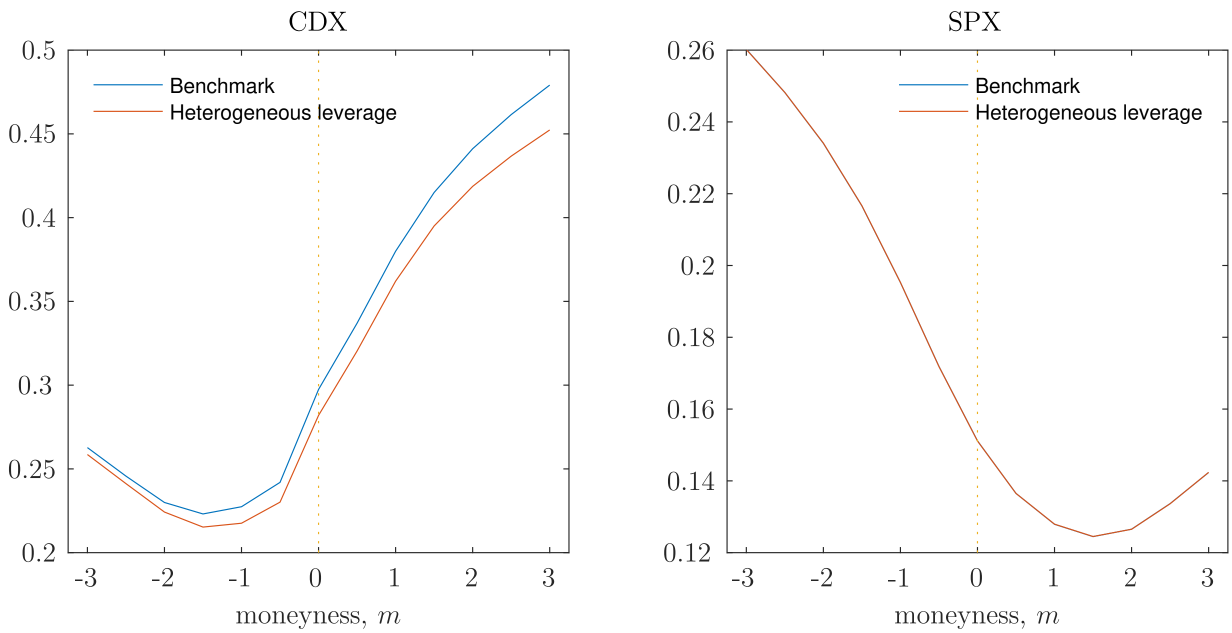

Figure IA10: Implied volatility smiles with heterogeneity in leverage

The figure shows the implied volatility smiles for CDX options (left panel) and SPX options (right panel) for the benchmark homogenous model (blue line) and the heterogeneous model (red line) fitted to the same set of SPX options.

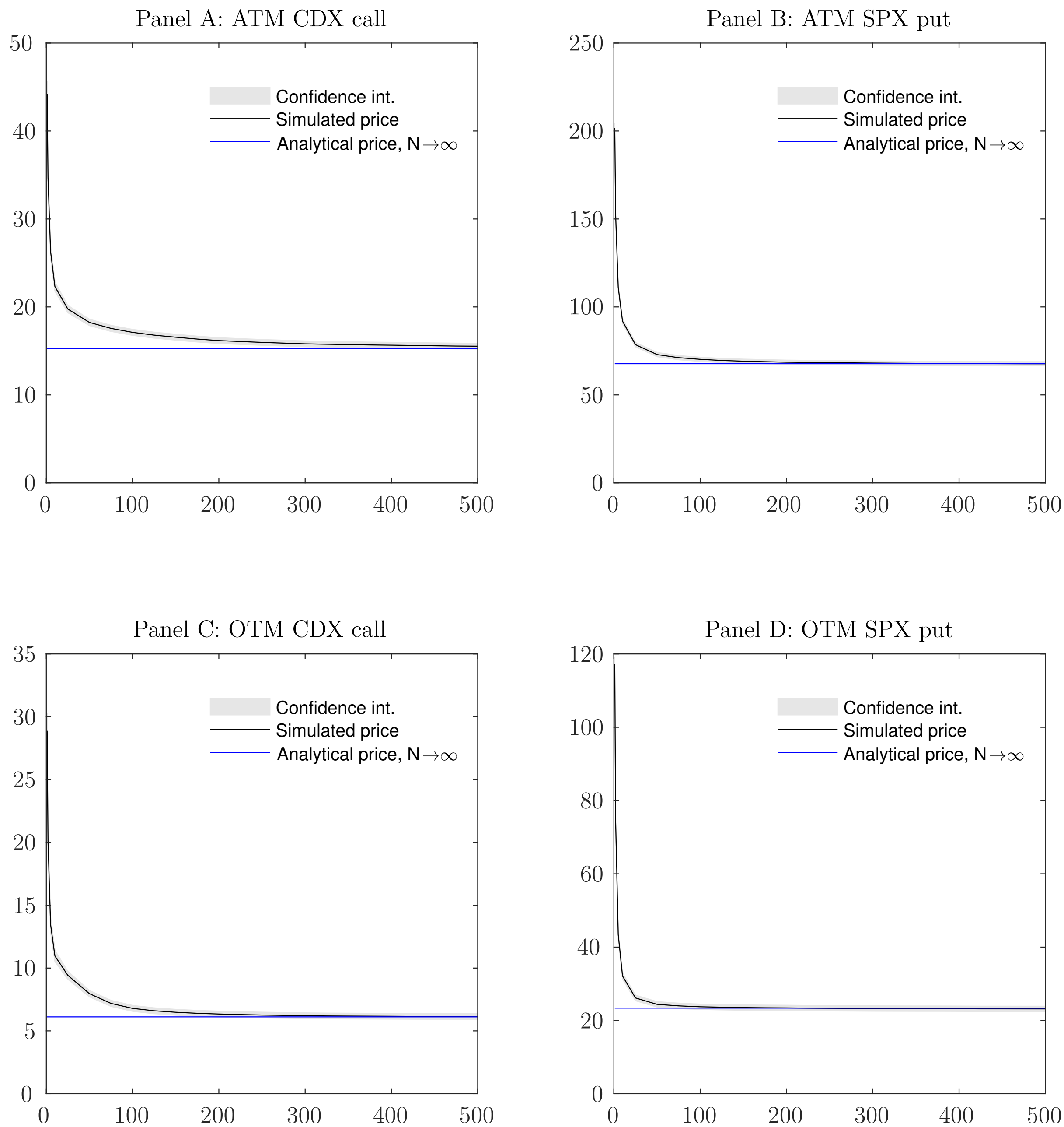

Figure IA11: Option pricing with a finite number of index constituents

The left panels show CDX option prices (in basis points), and the right panels shows SPX option prices. The top panels show ATM options, and the bottom panels show OTM options.

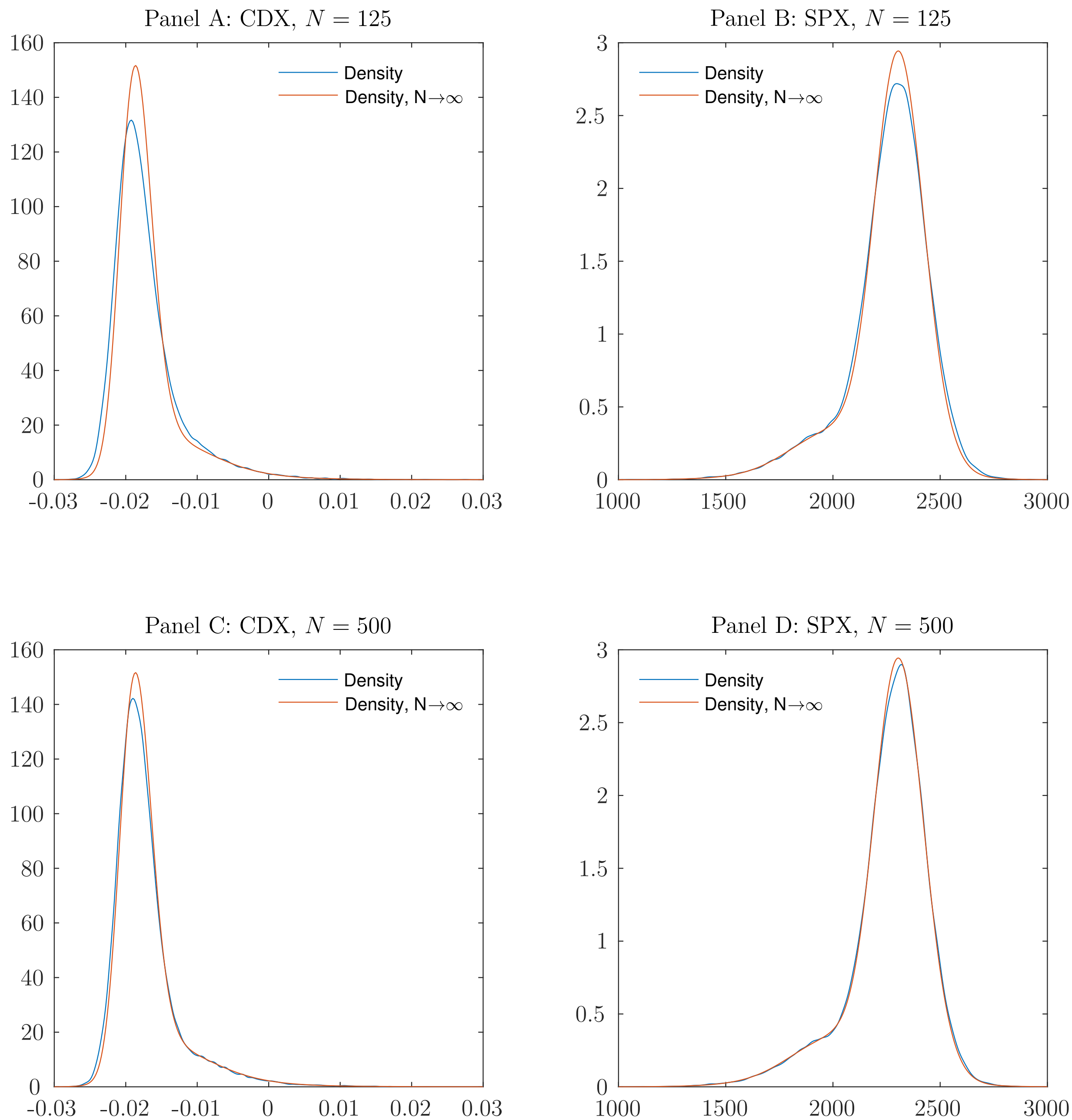

Figure IA12: Index distributions

The index distributions for finite N are estimated from the simulated data using a normal kernel function with optimal bandwidth. The limiting distributions for $N \to \infty$ are obtained using the analytical option price formulas together with the Breeden-Litzenberger Theorem. The left (right) panels show CDX (SPX) distributions (SPX distributions are multiplied by 10^3). The top (bottom) panels show results for $N = 125$ ($N = 500$).

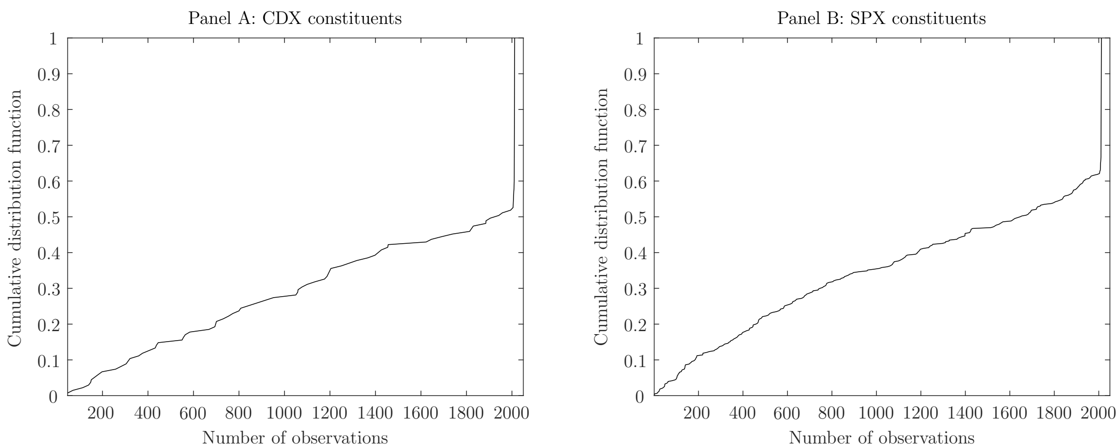

Figure IA13: Cumulative distribution function of asset return observations

Panels A and B show the cumulative distribution function of asset return observations for companies that were a CDX (Panel A) or SPX (Panel B) constituent at some point between 2012 and 2019. Daily data from January 3, 2012 until December 31, 2019.

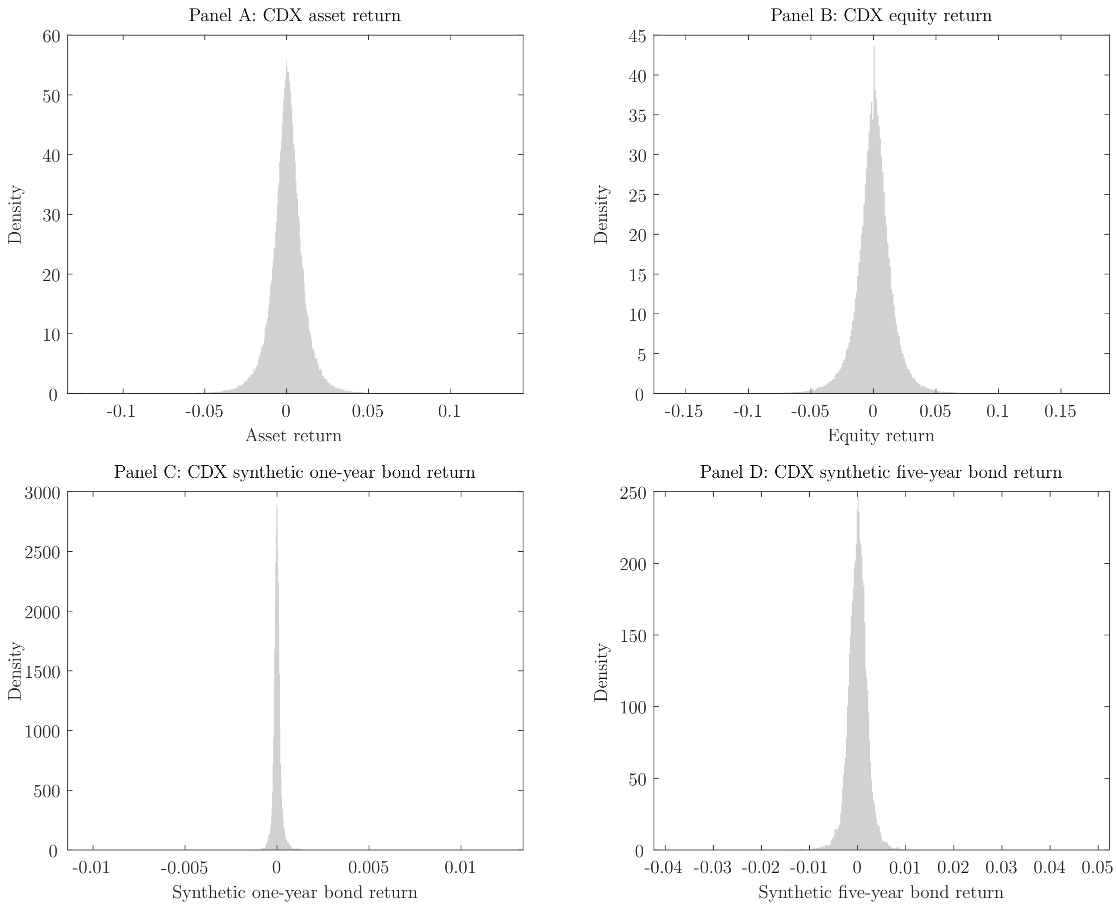

Figure IA14: Return distributions CDX constituents

Panel A shows the density of the asset return distribution for CDX constituents, and Panels B–D show the densities of the distributions of the asset return's components. Panel B shows the density of the equity return distribution, and Panels C and D show the density of the distributions of synthetic one- and five-year bond returns, respectively. Daily data from January 3, 2012 until December 31, 2019.

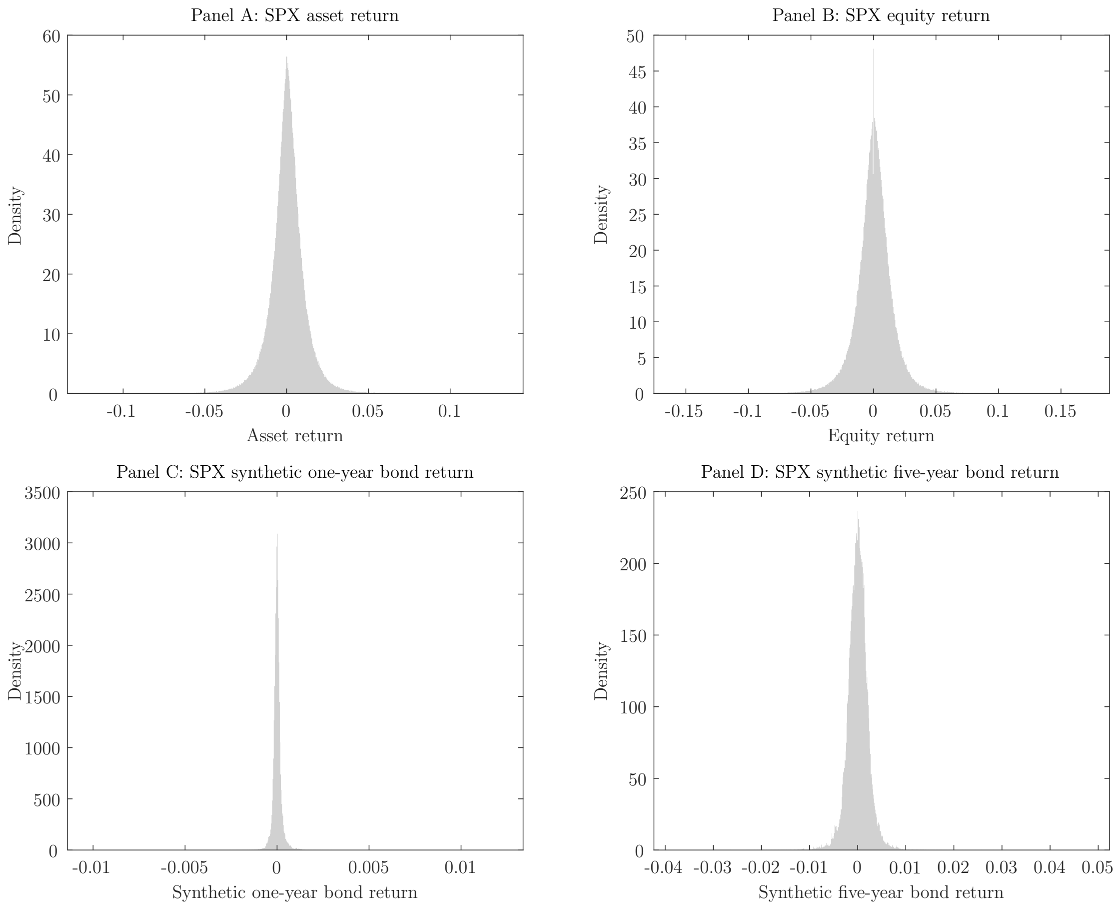

Figure IA15: Return distributions SPX constituents

Panel A shows the density of the asset return distribution for SPX constituents, and Panels B–D show the densities of the distributions of the asset return's components. Panel B shows the density of the equity return distribution, and Panels C and D show the density of the distributions of synthetic one- and five-year bond returns, respectively. Daily data from January 3, 2012 until December 31, 2019.

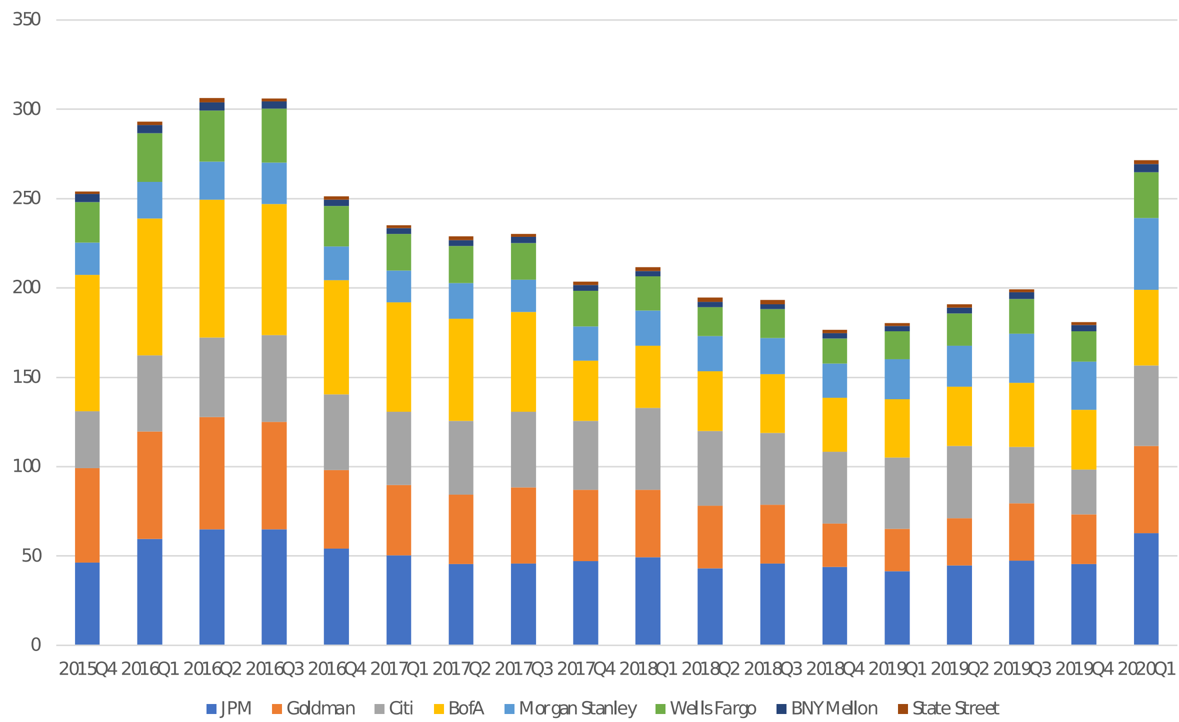

Figure IA16: Risk-weighted assets for CVA risk across the 8 US G-SIBs

The figure shows the risk-weighted assets (RWAs) for counterparty valuation adjustment (CVA) risk across the eight US global systemically important banks (G-SIBs). The data comes from the quarterly "Pillar 3 Regulatory Capital Disclosures". The sample period is Q4 2015 and Q1 2020 (prior to Q4 2015 not all banks reported RWAs specifically for CVA risk).

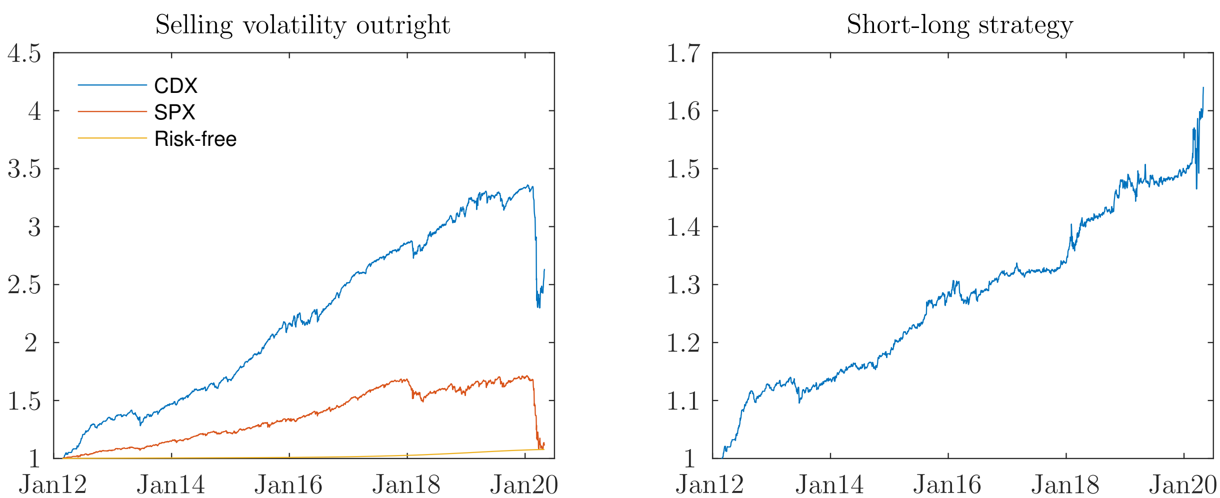

Figure IA17: Cumulative performance of trading strategies, constant required capital

The figure shows shows the evolution of one dollar invested in each of the EW strategies at the beginning of the sample (see Table IA.3 for details on the trading strategies). The left panel shows the performance of selling CDX and SPX straddles outright. The right panel shows the performance of the short-long strategy that allocates 50% of funds to selling CDX straddles and 50% to buying SPX straddles. On those trading days where options returns on unavailable, we invest at the risk-free rate. The sample period is from February 24, 2012 to April 30, 2020 (2042 daily observations).

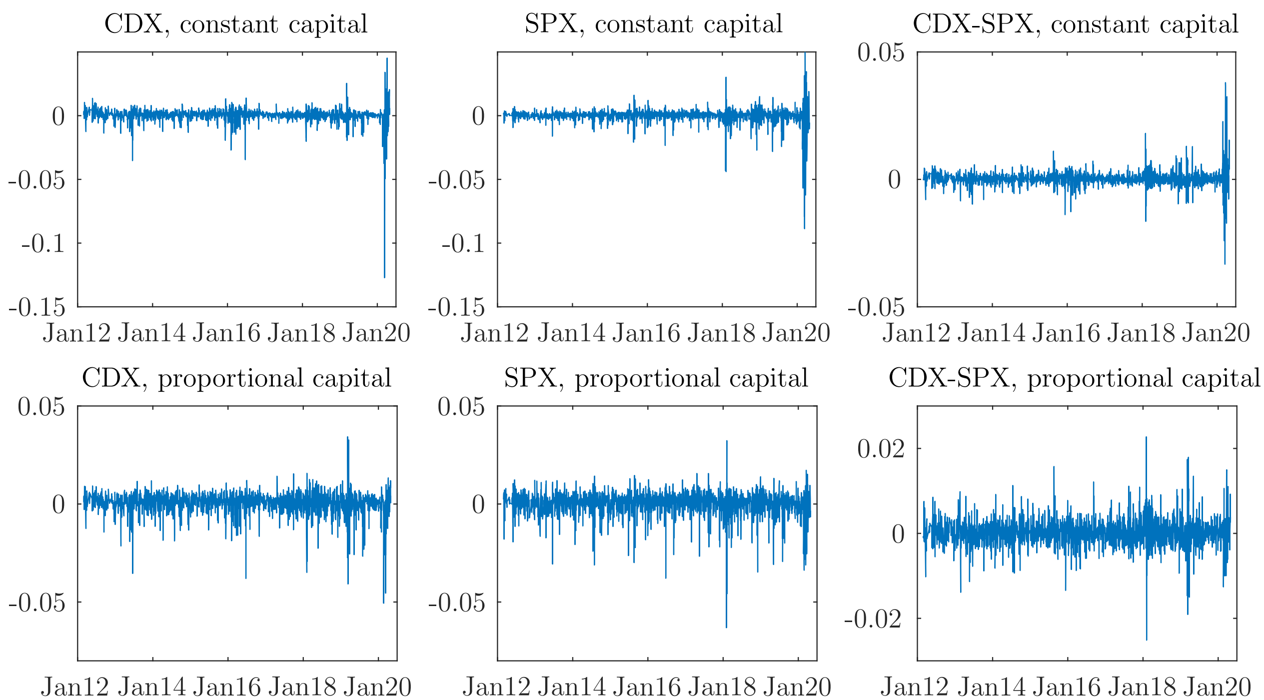

Figure IA18: Daily excess returns

The figure shows daily excess returns for each of the EW strategies. "CDX-SPX" denotes the short-long strategy that allocates 50% of funds to selling CDX straddles and 50% to buying SPX straddles. The top row shows excess returns when the required amount of capital is constant over time. The bottom row shows excess returns when the required amount of capital is proportional to the option premium. Each sample consists of 1881 daily returns between February 28, 2012 and April 30, 2020.